I. THE RATE OF RECOMBINATION OF IODINE ATOMS

II. SOME STUDIES OF THE TRACE QUANTITIES OF LEAD, URANIUM, AND THORIUM IN MARINE CARBONATE SKELETONS

Thesis by

Royal R. Marshall

In Partial Fulfillment of the

Requirements

for the Degree of

Doctor of Philosophy

California Institute of Technology

Pasadena, California

1955

Acknowledgments

I wish to express my appreciation to Drs. Norman Davidson, Claire Patterson, and Harrison Brown for the valuable ideas, encouragement, and constructive criticism they have furnished during the preparation of this thesis.

ABSTRACT

PART I

The rate constants for the homogeneous recombination of iodine atoms in the gas phase, $I + I + M \longrightarrow I_2 + M$, $d[I_2]/dt = k[I]^2[M]$, have been measured for the gases M = A, neo-C_5H_{12} and n-C_5H_{12} at room temperature. The rate constants are 4.2 ($\pm$ 0.4) x 10^9, 58 ($\pm$ 4) x 10^9, and 65 ($\pm$ 6) x 10^9 liter^{2}mole^{-2}sec^{-1}, respectively. In these experiments and those with iodine solutions, a short, intense pulse of light from a flash lamp dissociated 1-10% of the iodine molecules in a reaction cell. The photoelectric cell response to a light signal modulated with the change in the iodine atom concentration was amplified and used as the vertical deflection input of an oscilloscope. The oscilloscope trace, a direct indication of the subsequent recombination observed during periods from 0.0002 sec after the flash to as long as 0.01 sec, was recorded photographically.

The rate constants for the recombination of iodine atoms in the liquids CCl_4 and n-C_7H_{16}, $d[I_2]/dt = k[I]^2$, were found to be at room temperature 0.72 ($\pm$ 0.11) x 10^{10} and 2.2 ($\pm$ 0.4) x 10^{10} liter mole^{-1} sec^{-1}, respectively. The primary quantum yields in the solutions were found to be 0.19 ($\pm$ 0.05) and 0.41 ($\pm$ 0.26), respectively.

PART II

A procedure is described for the chemical isolation from carbonates of microgram quantities of lead, uranium, and thorium suitable for mass spectrometric analyses. The concentration of lead in a Jurassic belemnite as well as a Mississippian Spirifer has been found to be less than 1 ppm while for Strombus gigas, a living species of gastropod, the value

0.19 ± 0.04 ppm was found. The uranium concentration in this gastropod was determined as 0.036 ± 0.002 ppm. The isotopic composition of the lead from the Strombus gigas has also been determined and is compared to other analyses of "common" lead.

TABLE OF CONTENTS

TABLE OF CONTENTS

TABLE OF CONTENTS

LIST OF TABLES

LIST OF FIGURES

LIST OF FIGURES

LIST OF FIGURES

PART I

The Rate of Recombination of Iodine Atoms

Reprinted from THE JOURNAL OF CHEMICAL PHYSICS, Vol. 21, No. 4, 659-664, April, 1953
Printed in U. S. A.

THE JOURNAL OF CHEMICAL PHYSICS VOLUME 21, NUMBER 4 APRIL, 1953

Photoelectric Observation of the Rate of Recombination of Iodine Atoms*†

ROYAL MARSHALL AND NORMAN DAVIDSON
Gates and Crellin Laboratories of Chemistry, California Institute of Technology, Pasadena, California

(Received October 7, 1952)

The rate of the homogeneous three-body recombination of iodine atoms, $I+I+M \rightarrow I_2+M$, $d[I_2]/dt = k[I]^2[M]$, is measured. A short intense pulse of light from a flash lamp dissociates 1–9 percent of the *ca* 10^{18} iodine molecules in a 200-cc cell, and the subsequent recombination of iodine atoms is followed by fast photoelectric techniques.

The measured values of k at room temperature are $4.2(\pm 0.4)\times 10^9$ liter^2 moles^{-2} sec^{-1} (argon), $58(\pm 4)\times 10^9$ (neopentane), $65(\pm 6)\times 10^9$ (pentane). The value for neopentane is the same at 200°C.

The large values of the recombination rate constants indicate that an important recombining process consists of a "sticky" collision between an I atom and an M molecule or atom, leading to the formation of a complex IM, which reacts with a second I atom. The lifetimes of the collision complexes are estimated.

The rates of the reverse process, the dissociation of I_2 by collision with M, are calculated; the pre-exponential factors are extraordinarily large.

The extinction coefficients of gaseous iodine have been remeasured.

A SHORT, intense pulse of light from a flash lamp can be used to produce an appreciable concentration of atoms, free radicals, or other photolysis products. If the flash time is comparable to or shorter than, the lifetime of these reactive species, it may be possible to detect them and to measure their rates of reaction by flash spectroscopy or photoelectric spectrophotometry. Norrish and Porter,[1] Ramsey and Herzberg,[2] and the authors[3] have independently introduced the use of flash lamps for the study of photochemical problems.

In the experiment described here, the pulse of light from the flash lamp, *FL* (Fig. 1), passes through the filter *G* and dissociates some (1–9 percent) of the *ca* 10^{18} iodine molecules in cell *C*. In the presence of an inert gas M, the iodine atoms thus formed subsequently recombine by the homogeneous three-body reaction

$$I+I+M \rightarrow I_2+M, \quad d[I_2]/dt = k[I]^2[M]. \qquad (1)$$

The iodine molecule concentration as a function of time is measured photoelectrically with the aid of the constant light beam *L* (wavelength selected by the filter *F*) and displayed as the vertical coordinate on the screen of an oscilloscope. A single sweep shows a large spike due to scattered light from the flash lamp. When this has decayed (point indicated by arrow), the photocurrent is greater than before the flash because of the decreased I_2 concentration. It returns to its steady value as reaction (1) occurs.

It should be recalled that the first reliable determinations of the rates of recombination of halogen atoms were made by observing spectrophotometrically the change in the steady-state concentration of halogen molecules when a system is illuminated by a constant light beam of large and known intensity.[4] This method is applicable when the quantum yield for photodissociation is known. An apparently less accurate determination of the recombination rate for bromine atoms is based on the comparison of the rates of thermal and photochemical bromination of hydrogen.[5]

EXPERIMENTAL

Chemistry

Linde argon, stated by the supplier to be better than 99.8 percent pure; Phillips Petroleum Company pure grade normal pentane, purity greater than 99 mole percent; a NBS standard sample of neopentane, 99.96 mole percent pure; and cp resublimed iodine were used. Iodine from the solid at 18–25° was vaporized into the cell through two stopcocks lubricated with Dow Corning silicone high vacuum grease. Iodine concentrations were of the order of $1-1.8\times 10^{-5}$ mole/liter. The other gas was then added to a measured pressure and, in the case of hydrocarbons, frozen down, and the cell sealed.

Electronics

The flash tube is of quartz, 4 mm i.d., 15 cm long, and filled with xenon at *ca* 12 cm pressure; it is similar to

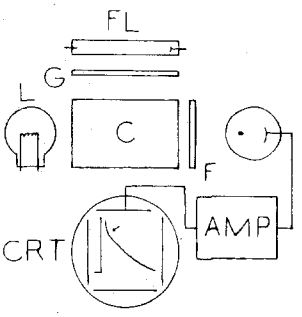

FIG. 1. Schematic diagram of the apparatus; *FL*, flash lamp; *C*, reaction cell; *L*, constant light source; *G* and *F*, filters; *CRT*, cathode-ray tube; *AMP*, amplifier.

* This research has been supported by the U. S. Office of Naval Research, under Contract Nonr-220 (01).
† Contribution No. 1741.

[1] R. G. W. Norrish and G. Porter, Nature **164**, 658 (1949); G. Porter, Proc. Roy. Soc. (London) **A200**, 284 (1950).

[2] G. Herzberg and D. A. Ramsey, Disc. Faraday Soc., No. 9, 80 (1950).

[3] Davidson, Marshall, Larsh, and Carrington, J. Chem. Phys. **19**, 1311 (1951).

[4] E. Rabinowitch and H. L. Lehmann, Trans. Faraday Soc. **31**, 689 (1935); E. Rabinowitch and W. C. Wood, *ibid.* **32**, 907 (1936); J. Chem. Phys. **4**, 497 (1936).

[5] K. Hilferding and W. Steiner, Z. physik. Chem. **B30**, 399 (1935).

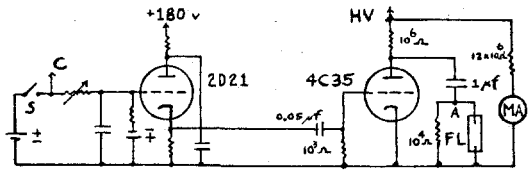

FIG. 2. Flash lamp firing circuit; S, firing switch; C, sweep trigger terminal on oscilloscope; HV, high voltage source; FL, flash lamp; MA, milliammeter.

the General Electric FT-127 tube. Fifty to seventy joules, stored at 10–12 kv in a 1 μf capacitor, can be discharged through the tube in about 10 μsec. Closing the switch S (Fig. 2) triggers a single sweep of the oscilloscope and also fires the 2D21 thyratron after a selected RC delay. The 90-v pulse across the cathode resistor of this tube fires the 4C35 hydrogen thyratron. This changes the potential at A from zero to minus 10–12 kv, and the flash lamp breaks down.

The lamp is mounted along the axis of an MgO coated parabolic reflector directed downwards toward a similar reflector in which the cell, a 10 cm long by 5 cm diameter Pyrex cylinder with Corex windows, rests. The beam from the constant light L, a 4-in. automobile spotlight run at 8 v from a storage battery, is limited by a circular aperture to a beam 2 cm in diameter through the center of the cell.

The photocurrent from a 929 vacuum phototube develops a voltage across a 10^6 ohm resistor. The resistance coupled ac amplifier with a gain of 100 consists of a cathode follower and a single stage of amplification, both using 6AK5 tubes. The amplified signal is fed into the amplifier of a Du Mont 304-H oscilloscope. The exponential rise and decay times of the amplifier-oscilloscope combination are 10 μsec and 0.12 sec. This system, of course, measures only the changes in the photocurrent and not its steady value.

The theoretical rms noise to signal ratio, due to statistical fluctuations of the photocurrent, is approximately $(e/it_r)^{\frac{1}{2}}$, i = dc photocurrent, e = electronic charge, t_r = rise time of amplifier. In a typical case, with $i = 2\times10^{-6}$ amp, this is 10^{-4}. The observed noise to signal ratio is just about equal to this. This is the order of magnitude of the minimum fractional change in photocurrent that can be detected. Amplifier noise is several times smaller than the photocell shot noise. Low frequency fluctuations (120 cycles or less) of *ca* 2×10^{-4} of the dc photocurrent are present and are presumably due to fluctuations in the light output of L. It is worthy of emphasis that in light modulation-spectrophotometric experiments of this nature, sensitivity is typically limited by the intensity and constancy of the light source.

Blocking of the amplifiers due to the large pulse of scattered light from the flash lamp was a serious problem that was, in part, overcome by the following measures. (1) The photocell collecting voltage was kept small, 14 volts. This is large enough so that the photocell sensitivity for small signals is not very dependent on voltage. The voltage pulse due to the flash was 7–14 volts when no filter, G, was used. When G was a Corning 3486 filter, cutting out light of wavelength shorter than 510 mμ, and F was a 487 mμ interference filter, the flash pulse was about 0.3 volt. The initial degree of dissociation of the iodine was cut down about two-thirds by the 3486 filter. (2) The oscilloscope amplifier is a dc amplifier which does not block. Nevertheless, the blocked time is about 150 and 400 μsec with and without the 3486 filter. This at present is the limitation of our apparatus for measuring very fast reactions.

In each series of experiments, gain and time calibrations were accomplished with the light from a 6-v flashlight bulb chopped at 600 cycles/sec. The photocurrents produced by this lamp (*ca* 10^{-8} amp) and by L were measured with a 10^4 ohm standard resistor, a type K Leeds and Northrup potentiometer, and a galvanometer of sensitivity 10^4 mm/μamp. These data and the amplitude of the 600-cycle square wave on the oscilloscope screen permit one to convert deflection on the screen into fractional change of photocurrent. The decrease in deflection sensitivity of about 3 percent, due to illumination by the constant light L with a concomitant change in photocell collecting voltage of 1–2 volts, was directly measured in each experiment.

Spectrophotometry

Two different defined "extinction coefficients" are of importance here. The extinction coefficient that is commonly used in spectrophotometry we shall call the integral extinction coefficient ϵ; $\epsilon = D/(l[I_2])$; D = decadic optical density, l = path length, $[I_2]$ = iodine concentration in moles/liter. The partial molar extinction coefficient $\bar{\epsilon}$ is defined by $\bar{\epsilon}l = \partial D/\partial[I_2]$. In the flash photolysis experiment, small fractional changes in photocurrent are observed from which the corresponding small fractional changes in iodine concentration are computed.

For wavelengths below 499.5 mμ, the convergence limit of the banded spectrum, ϵ and $\bar{\epsilon}$ should be equal, independent of inert gas concentration [M], and iodine concentration. In the region of discrete absorption $\bar{\epsilon}$, in general, will be a function of $[I_2]$ and [M], and typically $\partial\bar{\epsilon}/\partial[M] > 0$, $\partial\bar{\epsilon}/\partial[I_2] < 0$; ϵ will also be a function of $[I_2]$ and [M] and $\epsilon > \bar{\epsilon}$.

Some values of ϵ, the integral extinction coefficient, measured with a 10-cm cell in a Beckman spectrophotometer, are listed in Table I. Concordant values ($\pm$2 percent) for ϵ at 490 and 498 mμ were found in two experiments. In one, a cell with 71.8 mm of pentane and excess solid iodine was at a temperature of 22.8° in the spectrophotometer, corresponding to a vapor pressure of 0.256 mm, $[I_2] = 1.39\times10^{-5}$ molar.[6] In the second experiment an evacuated cell at 24° was satu-

[6] L. J. Gillespie and L. H. D. Fraser, J. Am. Chem. Soc. 58, 2260 (1934).

rated with solid iodine at 22.2°, $p=0.244$ mm, and then sealed off.

Extinction coefficients at other wavelengths were measured relative to that at 498 mμ in cells with 80–760 mm argon and iodine concentrations of $1.0-1.7\times10^{-5}$ molar. Because of the low absorption, the data were not expecially accurate. It was observed, however, that, in the banded region of the spectrum, ϵ did fall off at argon pressures below 300 mm, especially at the higher iodine concentrations. Thus, at 90 mm of argon, with $[I_2]=0.9$ and 1.7×10^{-5} molar, ϵ at 546 mμ was 94 percent and 84 percent of the high pressure value. The effect on $\bar{\epsilon}$ is, of course, still greater.

Our data in Table I differ somewhat from those given by Rabinowitch and Wood.[7] Our observations confirm their result that ϵ is independent of pressure of air, argon, or helium, above 500 mm. Our results are in qualitative agreement with the more precise observations of Luck on the effect of iodine and inert gas pressures on the absorption of the 546 mμ mercury line by iodine at 210°C and at higher iodine concentrations than used here.[8] He observed a limiting ϵ of 637 at high inert gas pressures and low $[I_2]$, the same as the value measured by us at room temperature.

Most of the data for the recombination rate were obtained using as the filter F a Bausch and Lomb interference filter with a measured maximum transmission of 36 percent at 487 mμ, a half-width of 8 mμ, and a transmission of the order of $\frac{1}{2}$–1 percent through the rest of the spectrum. Some of the argon runs were made with a Baird Associates 546 mμ multilayer interference filter (plus a yellow filter to eliminate blue light) with a half-width of 5 mμ and a maximum transmission of 70 percent. In the 487 mμ range, $\bar{\epsilon}=\epsilon$; but the band width of the filter is different from that of the spectrophotometer used for the data in Table I. By direct transmission measurement in the experimental arrangement used in the rate runs, an effective ϵ of 383 was found for this filter; this value has been used for ϵ in the interpretation of data. With the 546-mμ filter, the measured value of ϵ of 640 was taken for $\bar{\epsilon}$ except for some low pressure runs, where a value of 600 was used.

Interpretation of Data

The integrated form of the rate equation (1) is $1/[I]-1/[I]_0=2k[M]t$, where $[I]_0$ is the concentration of iodine atoms just after the flash. Since the degree of dissociation of iodine molecules by the flash is small, the change in transmitted light intensity J is given by $dJ/J_\infty=2.303\bar{\epsilon}l\times[I]/2$. The oscilloscope deflection S, due to the change in the photocurrent i, is then given by

$$\frac{1}{S}-\frac{1}{S_0}=\frac{4k[M]t}{i_\infty g\times2.303\bar{\epsilon}l}(1+t_{\frac{1}{2}}/RC), \qquad (2)$$

where g is the gain of the photocell-amplifier-oscilloscope combination in units of deflection per ampere change in photocurrent.

The last factor is a small approximate correction for the decay of the signal because of clipping by the ac amplifier; $t_{\frac{1}{2}}$ is the time at which $[I]=[I]_0/2$ and RC is the exponential decay time of the amplifier-oscilloscope combination. A small correction to S is made for the deflection due to the pulse of light from the flash lamp and for the subsequent negative overshoot.

TABLE I. Extinction coefficients of iodine.

(mμ)	478	487	490	498	510	520	546	560	580	600
ϵ[a]	···	440	478	580	700	751	640	490	280	145
ϵ[b]	400	540	600	740	810	822	670	550	300	140

[a] This research.
[b] Reference 7.

RESULTS AND DISCUSSION

Results

Figure 3 exhibits a typical trace from an experiment. The plots of $1/S$ *vs* t gave reasonably good straight lines from which k was calculated by Eq. (2). The results of the runs at room temperature are summarized in Table II.

One set of measurements was made at 200(±10)°C on a cell containing 1.20×10^{-5} mole/liter of iodine and 2.17×10^{-3} mole/liter of neopentane. The absorption coefficient of iodine at 487 mμ was the same to ±10 percent at this temperature as at room temperature, and the measured rate constant for recombination of 59×10^9 is the same as that obtained at room temperature.

Consideration of Possible Errors

Absorption of 0.0047 calorie (5×10^{16} quanta of $\lambda=500$ mμ) in a 200-cc cell containing a little iodine and argon at 206 mm (the lowest pressure used) corresponds to a temperature rise of 0.7°. Provided the energy was uniformly absorbed throughout the cell, this would have no effect on the measurements.

Rabinowitch[9] has estimated 0.16 cm² sec⁻¹ for the diffusion coefficient D of iodine atoms into argon at one atmos pressure. On the basis of the densities of the solids, we estimate a diameter of 6.2A for pentane and neopentane, and 0.10 for the diffusion coefficient of iodine atoms into either of these gases at one atmos

[7] E. Rabinowitch and W. C. Wood, Trans. Faraday Soc. **32**, 540 (1936). These authors ran the absorption spectrum of a cell which they state contained 0.158 mm of I_2, obtained by saturating the cell at "about 19°C." According to the data they used (Baxter, Hickey, and Holmes, J. Am. Chem. Soc. **29**, 127 (1907); the results in this reference agree essentially with that of reference 6), the vapor pressure of iodine at 19° is 0.178 mm, not 0.158 mm, and at 17° it is 0.155 mm. If one assumes that Rabinowitch and Wood were actually working at 0.178 mm pressure of iodine, the agreement between the two sets of data would be better at 498 mμ and poorer at 546 mμ.

[8] W. Luck, Z. Naturforsch. **6A**, 313 (1951).

[9] E. Rabinowitch, Trans. Faraday Soc. **32**, 917 (1936).

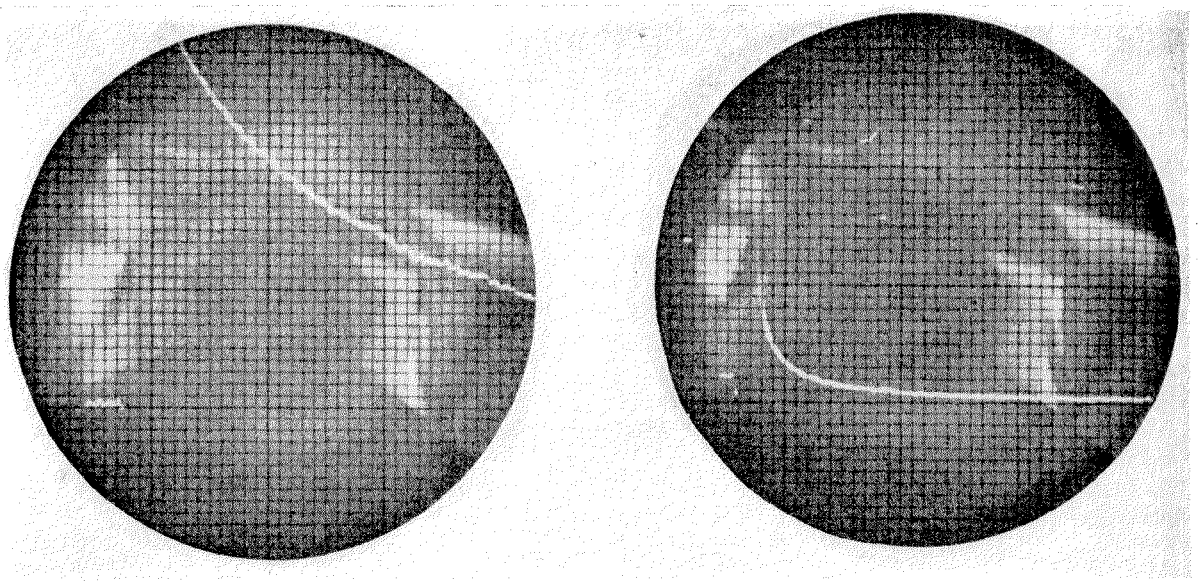

FIG. 3. On the left is the pattern displayed on oscilloscope as iodine atoms recombine: p (argon) = 740-mm Hg; time scale = 0.159×10^{-3} sec/smallest grid division (= 0.1 inch); $i_\infty = 2.66$ μamp; $g = 2.25 \times 10^3$ smallest grid divisions/μamp; $t_{\frac{1}{2}} = 1.8 \times 10^{-3}$ sec; $[I_2] = 9.0 \times 10^{-6}$ mole liter^{-1}; $[I]_0 = 1.6 \times 10^{-6}$ mole liter^{-1} (an especially high energy flash). On the right is the signal resulting from scattered light from flash lamp and negative overshoot from ac amplification when the constant light L is off.

pressure. According to Eq. (1), the time for three-fourths of the iodine atoms to recombine is $t_{3/4} = 3/(2k[M][I]_0)$. The mean distance diffused in this time is $(2Dt_{3/4})^{\frac{1}{2}}$. The lowest values of argon and pentane pressure studied were 0.25 and 0.05 atmos, with $t_{3/4}$ of 0.02 sec in each case; the corresponding diffusion distances are 0.16 and 0.28 cm. Thus heterogeneous recombination on the walls did not significantly affect the results.

Non-uniform creation of iodine atoms in the cell would make the calculated rate constant greater than the true value. The minimum light transmission parallel to the axis of the cell was of the order of 85 percent; it is unlikely that internal filter effects were significant. No satisfactory way of investigating whether the light intensity from different parts of the flash lamp was the same was developed. One lamp, a commercial FT-127, seemed to emit a greater intensity from the anode region. Rate constants measured with this lamp were 100 percent higher than those reported in Table II with one orientation of the lamp and 50 percent higher when the lamp was rotated through 180°. No such effects were noted with the lamp used for the measurements of Table II. In view of this and the effect of the MgO reflectors in diffusing the light, it is probable that the illumination was sufficiently uniform.

The average deviation from the mean of the results in Table II is about 10 percent. This variability is probably due to errors of measurement of the oscillograph traces, to fluctuations in the gain of the amplifier, and to errors in the measurement of the small current of *ca* 10^{-8} amp. involved in the measurement, with chopped light, of amplifier gain.

In view of the discrepancies between the two sets of measurements of the extinction coefficient of iodine in Table I, it must be pointed out that any error here results in a corresponding error in the rate constants.

Discussion

The value of k for argon measured by the photostationary state technique[4] is 6.9×10^9 liter^2 mole^{-2} sec^{-1}. The value reported here is 4.2×10^9 and an independent measurement of this quantity by Norrish, Porter, and collaborators at Cambridge,[10] gave $4.39(\pm 0.11) \times 10^9$. We believe that further experience with flash lamp measurements is needed before a confident estimate of their reliability can be made. The concordance of the two flash lamp determinations plus the consideration of errors in the preceding section indicates, we believe, that the flash lamp determinations are more accurate than the photostationary state measurement. It should be noted that any correction for a possible lack of uniformity in the luminosity of the flash lamp, considered in the previous section, would increase the difference between the two values.

In a recent study of the thermal and photochemical bromination of neopentane, it was concluded that at 197°C the ratio of k's for the reaction $Br + Br + M \rightarrow Br_2 + M$ for neopentane and hydrogen as third bodies is 174.[11] Since recombination rate constants are not very dependent on temperature, the values of k for iodine atom recombination in the presence of neopentane and argon measured in the present research, taken in con-

[10] Private communication.

[11] F. R. Schweitzer and E. R. Van Artsdalen, J. Chem. Phys. 19, 1028 (1951).

junction with Rabinowitch's results that $k_A/k_{H_2}=0.95$ and 0.59 for iodine atom and bromine atom recombinations, respectively, strongly suggest that the ratio of efficiencies of neopentane and hydrogen as third bodies for halogen atom recombinations is 8–14, not 174. Other aspects of this investigation[11] of the bromination of neopentane have recently been criticized.[12]

Rabinowitch[13] has discussed the homogeneous recombination process, $I+I+M\rightarrow I_2+M$, in terms of two kinds of triple collisions:

$$(I+I)+M, \tag{3a}$$

$$(I+M)+I. \tag{3b}$$

For case (a), the first double collision is between two iodine atoms; for case (b), the first double collision is between an iodine atom and an M molecule or atom. The important parameter which enters into the elementary kinetic theory calculation of the number of triple collisions, but not into the calculation of number of double collisions, is the duration of a double collision. The recombination rate constant k (in units of cc^2 $molecules^{-2}$ sec^{-1}) is given by Rabinowitch as

$$k=8\pi\sigma_{MI}^2\sigma_I^2RT\left(\frac{M_M+M_I}{2M_I^2M_M}\right)^{\frac{1}{2}}(2\tau_{II}+\tau_{MI})\beta. \tag{4}$$

The σ's are collision diameters, $\sigma_{MI}=0.5(\sigma_I+\sigma_M)$; τ_{II} and τ_{MI} are the durations of the double collisions between two iodine atoms and between an iodine atom and M, and β is the probability that a triple collision results in recombination.

From a chemical kinetic point of view, one may view the recombination process in the way outlined by Eqs. (5):

$$\begin{aligned} &I+I\rightleftharpoons I_2^*,\\ &I_2^*+M\rightarrow I_2+M, \end{aligned} \tag{5a}$$

$$\begin{aligned} &I+M\rightleftharpoons IM^*,\\ &IM^*+I\rightarrow I_2+M. \end{aligned} \tag{5b}$$

I_2^* and IM^* are excited molecules; the former loses vibrational energy and is stabilized by collision with M, the latter can react with a free iodine atom in a two-body process. The rate constants for dissociation of I_2^* and IM^* are $(1/\tau_{II})$ and $(1/\tau_{IM})$ of Eq. (4). An equation which is the same as (4) except for small numerical factors can be derived from the reaction schemes, (5), by the standard stationary state argument.

Using Eq. (4), the results in Table II, and collision diameters of 5.2, 3.6, and 6.2A for iodine atoms, argon atoms, and pentane or neopentane molecules, the calculated values of $(\tau_{II}+0.5\tau_{IM})\beta$ are 1.5×10^{-13} sec (argon), 1.6×10^{-12} sec (neopentane), and 1.8×10^{-12} sec (pentane).

For comparison, the values obtained by Rabinowitch for several third bodies are 2.5×10^{-13} (argon), 3.6×10^{-13} (nitrogen), 1.0×10^{-12} (carbon dioxide), and 4.2×10^{-12} sec (benzene). Assuming, purely for the sake of intercomparison of results, that all Rabinowitch's results are too high by a factor of 2.5/1.5, his value for benzene should be decreased to 2.5×10^{-12} sec. This value is not much larger than those found by us for the pentanes, so that one need not assume a special interaction between iodine atoms and the aromatic ring.

Two iodine atoms in the ground state ($^2P_{\frac{3}{2}}$) can interact to form molecules in the $^1\Sigma_g^+$, $^1\Pi_u$, and $^3\Pi_{2u,1u}$ states, which have potential energy curves with a minimum. (These curves are illustrated in reference 13, Fig. 1.) Herzberg[14] gives the fundamental vibration periods in the $^1\Sigma_g^+$ and $^3\Pi_{1u}$ states as 1.6×10^{-13} and 7.8×10^{-13} sec. The vibration periods of the $^1\Pi_u$ and $^3\Pi_{2u}$ states are presumably intermediate between these two values. In the approximation in which the potential curves are considered harmonic and centrifugal effects are neglected, the lifetime τ_{II} of I_2^* is a properly weighted average of the vibration periods listed above. The much larger τ-values calculated from benzene and the pentanes can be interpreted as indicating a very large cross section for vibrational deactivation of I_2^* by these molecules. A more plausible interpretation has been suggested by Rabinowitch, i.e., that the processes of type (b), "sticky" collisions between M and an I atom, are important and account for the large values of τ and their variation from substance to substance. When M is a polyatomic molecule, τ_{IM}, the lifetime of the collision complex, can be much longer than a single vibration period, because the small energy of attraction can be distributed among the various "soft" vibrational degrees of freedom of the molecule.

Finally, it is of interest to consider the inverse process, the dissociation of iodine molecules by collision with

TABLE II. Rate of recombination of iodine atoms at room temperature.

Argon								
p (M) (mm Hg)				206[a]	206[a]	380[b]	627[b]	
$k\times10^{-9}$ (liter^2 mole^{-2} sec^{-1})				4.9	5.1	4.3	4.3	
p (M)	703[b]	740[b]	1580[b]	740	740	740	740	740
$k\times10^{-9}$	4.0	3.6	3.7	3.7	4.2	3.9	4.6	4.2
k (av) $=4.2(\pm0.4)\times10^9$ liter^2 moles^{-2} sec^{-1}								
Neopentane								
p (M)	38.5		38.5		77		77	77
$k\times10^{-9}$	56		56		60		66	50
k (av) $=58(\pm4)\times10^9$ liter^2 moles^{-2} sec^{-1}								
Pentane								
p (M)	48.6	73.5	73.5	65.5[c]	65.5[c]	71.8[c]		
$k\times10^{-9}$	78	66	70	60	52	64		
k (av) $=65(\pm6)\times10^9$ liter^2 moles^{-2} sec^{-1}								

[a] 546 mμ filter, $\bar{\epsilon}$ taken as 600.
[b] 546 mμ filter, $\bar{\epsilon}$ taken as 640; all other measurements were made with the 487 mμ interference filter.
[c] For these measurements, the pentane vapor was dried over calcium chloride.

[12] S. W. Benson and H. Graff, J. Chem. Phys. **20**, 1182 (1952).
[13] E. Rabinowitch, Trans. Faraday Soc. **33**, 283 (1937).
[14] G. Herzberg, *Spectra of Diatomic Molecules* (D. Van Nostrand Company, Inc., New York, 1950), second edition, p. 540.

gas molecules M:

$$I_2+M\rightarrow I+I+M, \quad -d[I_2]/dt=k_D[I_2][M]. \quad (6)$$

For k_D, the rate constant for dissociation, $k_D=kK_c$, where K_c is the equilibrium constant for the dissociation of iodine, 3.80×10^{-23} mole liter^{-1} at 300°K.[15] Since k is not strongly dependent on temperature, $k_D=A\exp(-\Delta E/RT)$, where $\Delta E=35\,500$ cal. Then A is 1.1×10^{13} liter mole^{-1} sec^{-1} for argon, 1.6×10^{14} for neopentane, and 1.8×10^{14} for pentane. These are exceptionally large values for the pre-exponential factor in a bimolecular reaction. Rice[16] has noticed this in analyzing the results of Rabinowitch and Wood, and has suggested possible interpretations.

[15] "Selected values of chemical thermodynamic properties," National Bureau of Standards, Washington, D. C., Series III, June 30, 1948.

ACKNOWLEDGMENT

It is a pleasure to acknowledge the unfailing courtesy of Mr. Haskell Shapiro of the Hydrodynamics Laboratory in giving us both advice and material assistance with flash lamp problems.

[16] O. K. Rice, J. Chem. Phys. 9, 258 (1941).

B. The Recombination of Iodine Atoms in Liquids

1. Introduction

A major problem in chemical kinetics is the determination of the rates of the elementary reactions postulated as individual stages in an observed overall reaction. These elementary reactions typically involve unstable particles such as atoms and radicals. The instability of these isolated particles is reflected in the rapidity of their reactions and the measurement of the large rate constants is generally a formidable task. Indeed, the direct determination of rate constants for individual steps in chain reactions is rarely attempted. An important chain-terminating process in halogenation is the recombination of halogen atoms in liquids and gases. To augment the present knowledge of this elementary reaction, solutions of iodine in inert solvents have been investigated photochemically. The following paragraphs discuss the data obtained in terms of the recombination of iodine atoms in liquids.

The photochemical dissociation of iodine molecules (I_2) in solution and the subsequent recombination of the iodine atoms (I) may be represented by the following two equations:

$$I_2 + h\nu \rightarrow 2I \qquad (1)$$

and

$$I + I \rightarrow I_2 \qquad (2).$$

The rates of these two reactions may be written as

$$d[I]/dt = 2\phi q_a \qquad (3)$$

and

$$-d[I]/dt = 2k[I]^2 \qquad (4),$$

respectively, where ϕ is the primary quantum yield or the number of quanta absorbed by the iodine molecules divided by the number of molecules which dissociate, q_a is the number of quanta absorbed per liter, and k is the recombination constant in $mole^{-1}liter\ sec^{-1}$.

In the photostationary state the rate of formation of iodine atoms equals their rate of recombination and by equating equations (3) and (4),

$$k = \phi q_a / [I]_s^2 \qquad (5)$$

where $[I]_s$ is the photostationary state concentration of iodine atoms. The factor $[I]_s^2/q_a$ was determined for CCl_4 and $n\text{-}C_6H_{14}$ solutions by Rabinowitch and Wood (1), but without the values for the primary quantum yields, the recombination constants could not be evaluated.

Zimmerman and Noyes (2) have deduced the value of the primary quantum yield at 436 mμ and 578 mμ for the dissociation of iodine molecules in illuminated hexane solutions from their measured mean lifetimes of iodine atoms and the data of Rabinowitch and Wood. In addition, Zimmerman and Noyes calculated the value of k in C_6H_{14} at 25°C by combining the data from these two investigations.

The techniques applied to the study of the kinetics of recombination of iodine atoms in the presence of a relatively large number of third-body gas molecules (Part I, A), i.e., flash lamp photolysis and photoelectric spectrophotometry, can be used to observe directly the recombination in liquids. The rates observed are independent of the actual values of the primary quantum yield and the rate constants can be calculated directly. The rates of recombination are a few orders of magnitude faster in liquids than in argon at 1 atm. The experiments

in liquids are more difficult because of these greater velocities and the data obtained are less precise than those for the gases. In the succeeding sections experiments with solutions of I_2 in CCl_4 and $\underline{n}$-C_7H_{16} are described and the data obtained are considered to be the first values directly determined for the recombination rates of iodine atoms in these solvents.

2. Derivation of the Recombination Expression

This section contains the derivation of the mathematical expressions relating the iodine atom concentration to the experimentally observed parameters. The fundamental rate equation is solved for the iodine atom concentration at time $\underline{t}$ in terms of the reduced molecular iodine concentration since the reaction was observed by means of the amount of visible light absorbed by the solution which varied with the number of iodine molecules. The photoelectric current is related to the iodine molecule concentration through Beer's law and the amplified photoelectric signal is, in turn, related to the vertical deflection of the oscilloscope trace. A correction for the decay of the photoelectric cell in the ac circuits is derived and included in the final equation (equation (33)) which is an explicit expression for the rate constant in terms of the directly measured quantities.

a. The Integrated Rate Expression

Equation (4) is the fundamental rate expression for the recombination of iodine atoms in liquids. This equation differs from that for recombination in the gas phase only by being independent of the concentration of a third body; the third body in the liquid phase is

actually the solvent molecule whose concentration in all cases is so high that collisions involving these molecules and two iodine atoms are always imminent relative to the time for the two iodine atoms to meet.

Upon integration, equation (4) becomes

$$1/[I] - 1/[I]_o = 2kt \qquad (6)$$

where $[I]_o$ is the iodine atom concentration at t=o. If $\underline{Q}$ is defined as the difference between the iodine molecule concentration at any time after the very short, dissociating flash (t=o) and the concentration a hundred or so mean lifetimes afterward ($[I]_\infty$) or

$$Q \equiv [I_2] - [I_2]_\infty \qquad (7),$$

then

$$[I] = -2Q \qquad (8)$$

and

$$1/Q_o - 1/Q = 4kt \qquad (9)$$

where $\underline{Q_o}$ is the negative of one-half the initial iodine atom concentration.

b. Application of Beer's Law

The course of the reaction was followed spectrophotometrically* and the changes in light transmission through the reaction cell are related to the changes in the iodine molecule concentration. The relationship is assumed to be Beer's law or, in integrated form,

$$K = K_i \exp(-\alpha[I_2]) \qquad (10)$$

---

* The experimental details are discussed in the subsequent section entitled Experimental Procedure.

where $\underline{K}$ is the intensity of the transmitted light and $\underline{K_i}$ that of the incident light while $\underline{\alpha}$ is 2.30 times the molar extinction coefficient for iodine in solution times the length of solution traversed by the light. This equation may be rewritten as

$$K = K_i \exp\left(-\alpha\left(Q + [I_2]_\infty\right)\right) = K_\infty \exp\left(-\alpha Q\right) \quad (11)$$

where $\underline{K_\infty}$ is the transmitted light a few hundred mean lifetimes of the reaction after the flash. Since $\alpha Q \ll 1$ equation (11) may be expanded to

$$K = K_\infty (1 - \alpha Q) = K_\infty + dK \quad (12)$$

or

$$dK/K_\infty = -\alpha Q \quad (13).$$

Beer's law is a satisfactory relation to use for a narrow band of wave lengths since neither the incident light intensity nor the extinction coefficients in solution vary rapidly.

c. Light Intensity and Photoelectric Current

The transmitted light is observed by a photoelectric cell. The photoelectric current, $\underline{i}$, is assumed to be proportional to the light intensity and a function of the photoelectric cell voltage or

$$i = Kf\,(V - iR) \quad (14)$$

where $\underline{V}$ is the applied voltage and $\underline{R}$, the load resistance across which is developed the signal to be amplified. Equation (14) may be differentiated to give

$$di = f\,(V - iR)\,dK - KRf'\,(V - iR)di \quad (15)$$

which, after rearrangement and the introduction of the original expression, becomes

$$\frac{di}{i}\left[1+iR\,\frac{f'(V-iR)}{f(V-iR)}\right]=\frac{dK}{K} \qquad (16)$$

where $iR\,\dfrac{f'(V-iR)}{f(V-iR)}$ is a small correction term called β.

d. Deflection on the Oscilloscope Screen

The signal is amplified in an ac amplifier and displayed as a function of time upon an oscilloscope screen. The deflection on the screen is proportional to the photoelectric current change, and the constant of proportionality, g, the gain, is assumed constant during an experiment. The deflection, S, is briefly expressed as

$$S = g\,di \qquad (17).$$

When di from equation (17) is substituted in equation (16) and equation (13) is introduced, the relation between the iodine atom concentration expressed in Q and the experimentally evaluated terms is

$$Q = \frac{-S\left[1+iR\,\dfrac{f'(V-iR)}{f(V-iR)}\right]}{i_\infty g \alpha} = \frac{-S(1+\beta)}{i_\infty g \alpha} \qquad (18)$$

where i_∞ is the photoelectric current due to the light intensity K_∞. If the reciprocals of both sides of equation (18) are substracted from

$$\frac{1}{Q_o} = -\frac{i_\infty g \alpha}{S_o(1+\beta)} \qquad (19),$$

equation (9) can be rewritten as

$$4kt = (1/S - 1/S_o)\, i_\infty g\alpha/\,(1+\beta) \qquad (20)$$

or

$$k = \frac{i_\infty g \alpha}{4(1+\beta)}\left[\frac{1}{S}-\frac{1}{S_o}\right]\frac{1}{t} \qquad (21).$$

e. Correction for Signal Decay Due to AC Circuits

Equation (21) is an explicit expression for the recombination constant but a correction is necessary for the signal decay inherent in the ac amplifier and oscilloscope. A step-function input decays as if the electronic apparatus were simply a capacitor and a resistor in series with the output across the resistor. This differentiating circuit is illustrated in Fig. 1.

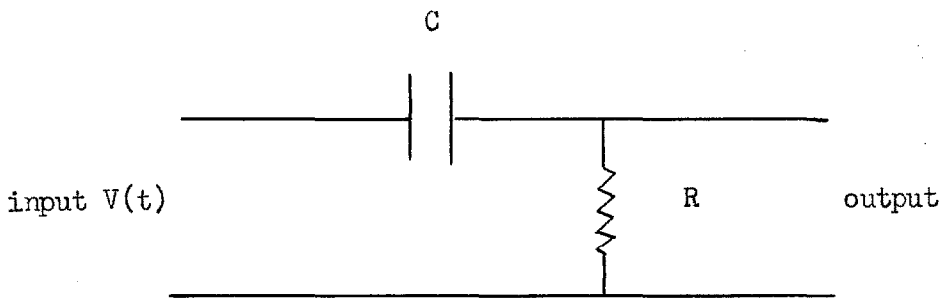

Fig. 1 Equivalent circuit in signal decay due to ac circuits.

To correct the reaction rate for the signal decay due to the ac circuits assume that the signal due to the second order chemical reaction may be approximated as an exponential,

$$V(t) = V_o \exp(-\gamma t) \qquad (22)$$

where γ is some constant determined by the reaction being studied, $V(t)$ is the input voltage at time t, and V_o is the initial input voltage. Since the correction is small, the fact that the signal is not exactly an exponential expression is not important. In the circuit of Fig. 1 the relation between the capacity, C, resistance, R, charge on the capacitor, P, and the input voltage is

$$RdP/dt + P/C = V_o \exp(-\gamma t) \quad (23).$$

The general solution to this equation is

$$P = A \exp(-\omega t) + \frac{V_o \exp(-\gamma t)}{R(\omega - \gamma)} \quad (24)$$

where

$$\omega = 1/RC \quad (25).$$

At $t = o$, the capacitor is uncharged and

$$A = \frac{V_o}{R(\gamma - \omega)} \quad (26).$$

Let V_m be the deflection voltage applied to the cathode ray tube. Then

$$V_m = RdP/dt = \frac{V_o}{\omega - \gamma}(\omega \exp(-\omega t) - \gamma \exp(-\gamma t)) \quad (27)$$

and

$$dV_m/dt = \frac{V_o}{\omega - \gamma}(\gamma^2 \exp(-\gamma t) - \omega^2 \exp(-\omega t)) \quad (28).$$

At $t = o$, $V_m = V_o$ and the observed initial logarithmic rate of change, $d \ln V_o/dt$, is $-(\omega+\gamma)$ while the initial logarithmic rate of change of the photoelectric current is $-\gamma$.

The initial logarithmic rate of change of the iodine atom concentration (equation (4)) is set equal to γ, therefore

$$\gamma = 2k[I]_o \quad (29).$$

The rate constant calculated from equation (21) includes the RC time of the ac circuits or

$$\gamma + \omega = 2k'[I]_o \quad (30)$$

where k' is this apparent rate constant. Now the mean lifetime of the iodine atoms, $t_{\frac{1}{2}}$, is the time at which

$$[I] = [I]_{o/2} \quad (31)$$

or

$$t_{\frac{1}{2}} = \frac{1}{2k'[I]_o} \tag{32}$$

since for this value, k' is sufficiently close to k. The ratio of k to k' is $\frac{1}{1+\omega/\gamma}$ but ω is $1/RC$ and γ is $1/t_{\frac{1}{2}}$ (equations (29) and 30)) so

$$k = \frac{i_\infty g \alpha}{4(1+\beta)\ (1+t_{\frac{1}{2}}/RC)} \left[\frac{1}{S} - \frac{1}{S_o}\right] \frac{1}{t} \tag{33}.$$

This is the complete explicit expression for the recombination constant. However, since the mean lifetimes of the iodine atoms in liquids were typically much less than a millisecond and the RC time was 12 x 10 milliseconds, this decay correction is negligible.

3. Experimental Procedure

a. Chemistry

The purity of the three chemicals, iodine, CCl_4, and n-C_7H_{16}, is of great importance in these experiments. For the solute, cp resublimed iodine was used. Eastman Kodak spectrophotometer grade CCl_4 was selected as one solvent and was found to be very satisfactory in contrast to cp CCl_4 which possessed an impurity with a large absorption peak at 320 mμ and which with iodine showed slowly decaying signals which could not be attributed to iodine atom recombination. Pure grade n-C_7H_{16} from Phillips Petroleum Company required purification before observations consistent with the recombination of iodine atoms could be made. The purification steps were the following:

1. Two washings with reagent grade, 30% fuming sulfuric acid, 10% by volume.
2. One washing with water.
3. One washing with 5% NaOH, 30% by volume.
4. Two washings with 5% $KMnO_4$, 30% by volume.
5. One washing with water.
6. Distillation over molten Na, 97.5 - 97.8°C distillation range.

The purified $\underline{n}$-C_7H_{16} was stored under Drierite until used to fill reaction cells. The reaction cells were stoppered with corks wrapped in tin-foil.

b. Outline of the Experimental Procedure

A triggering circuit started a sweep on an oscilloscope and pulsed a delay circuit which after a selected delay fired a high voltage circuit so that a large voltage was applied across the electrodes of a flash lamp which arced over producing a bright pulse of light, the iodine-molecule dissociating flash. The filtered flash-lamp light dissociated a few percent of the iodine molecules in a glass reaction cell through which a steady light source was shining. Filtered transmitted light from the steady source struck a photo-electric cell. The reduced optical density of the reaction cell after a flash due to dissociated iodine molecules led to increased photo-electric current. This positive signal was amplified in a two stage ac amplifier and fed into an oscilloscope. The signal on the screen was photographed.

c. The Flash Lamp

The flash lamp (Fig. 2) used in these experiments was a 37.5 cm long pyrex cylinder, 1.3 cm o.d. with 3 cm long, 40 mil tungsten leads sealed in at each end. Ca 1.5 cm in from each end on the tip of each tungsten electrode was silver soldered a small strip of nickel foil. This foil was bent to furnish a plane surface, the normal to which was along the axis of the flash tube. On each of these tabs was spot welded a small rectangular electron emitting plate kindly furnished by Mr. Haskell Shapiro of the Hydrodynamics Laboratory. A small side arm (9 cm long and with a standard taper (7/25), ground glass inner joint at the end) about 5 cm in from one end of the main cylinder was used for filling the flash lamp with 4.6 cm Hg pressure of Xe. At this pressure of inert gas the lamp was sealed off and mounted in an approximately cylindrically parabolic, MgO coated reflector. This reflector, enclosed on three sides, faced downward at two Corning no. 3486 filters.* Underneath these filters was another enclosure with a similar reflector facing upward. A 33.2 cm long, cylindrical, pyrex reaction cell with a 5.1 cm outside diameter and 2 filling arms laid in the trough of the bottom reflector. The ends of the cell consisted of 2 mm thick, corex filter plate windows. Light from the steady source passed through the cell via two 2 cm diameter holes at opposite ends of this bottom enclosure. The enclosure of the flash lamp and the

---

* Two 12 by 16.5 cm filters were required to match the length of the reaction cell; the transmission characteristics of one as measured against air in the Beckman model DU spectrophotometer are shown in Fig. 3.

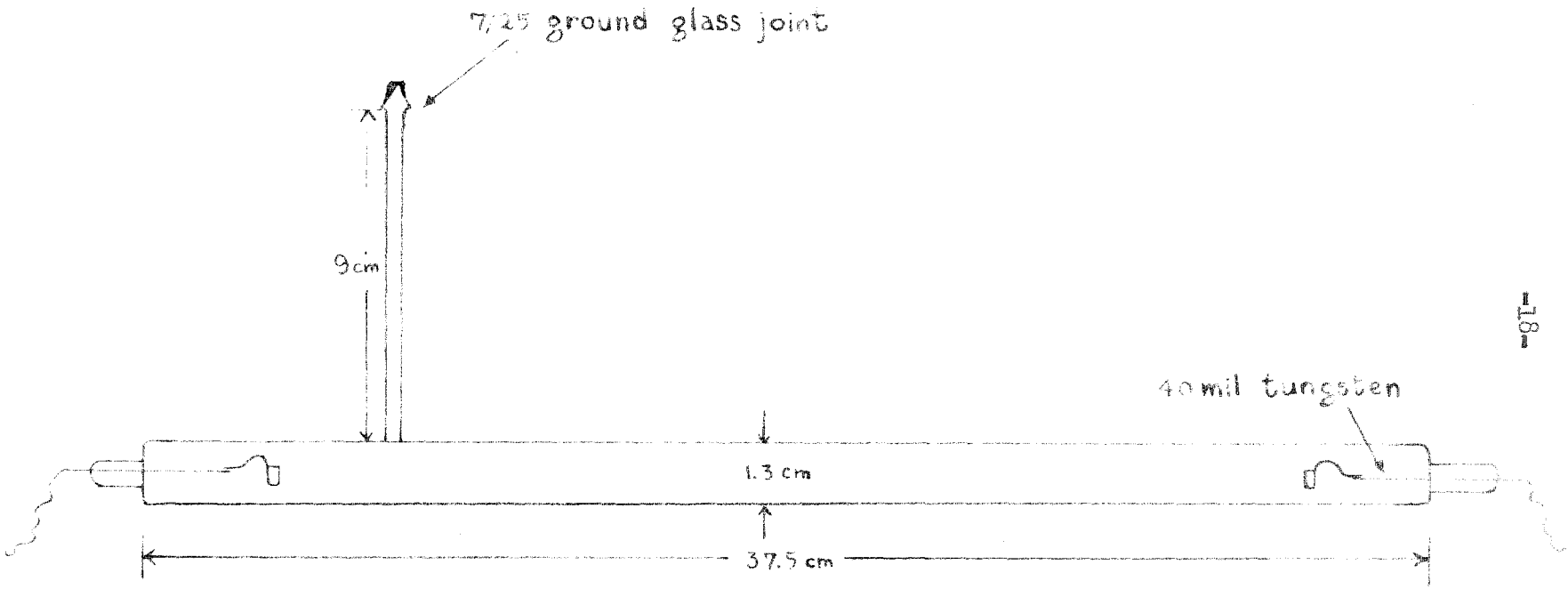

Fig. 2 The pyrex flash lamp.

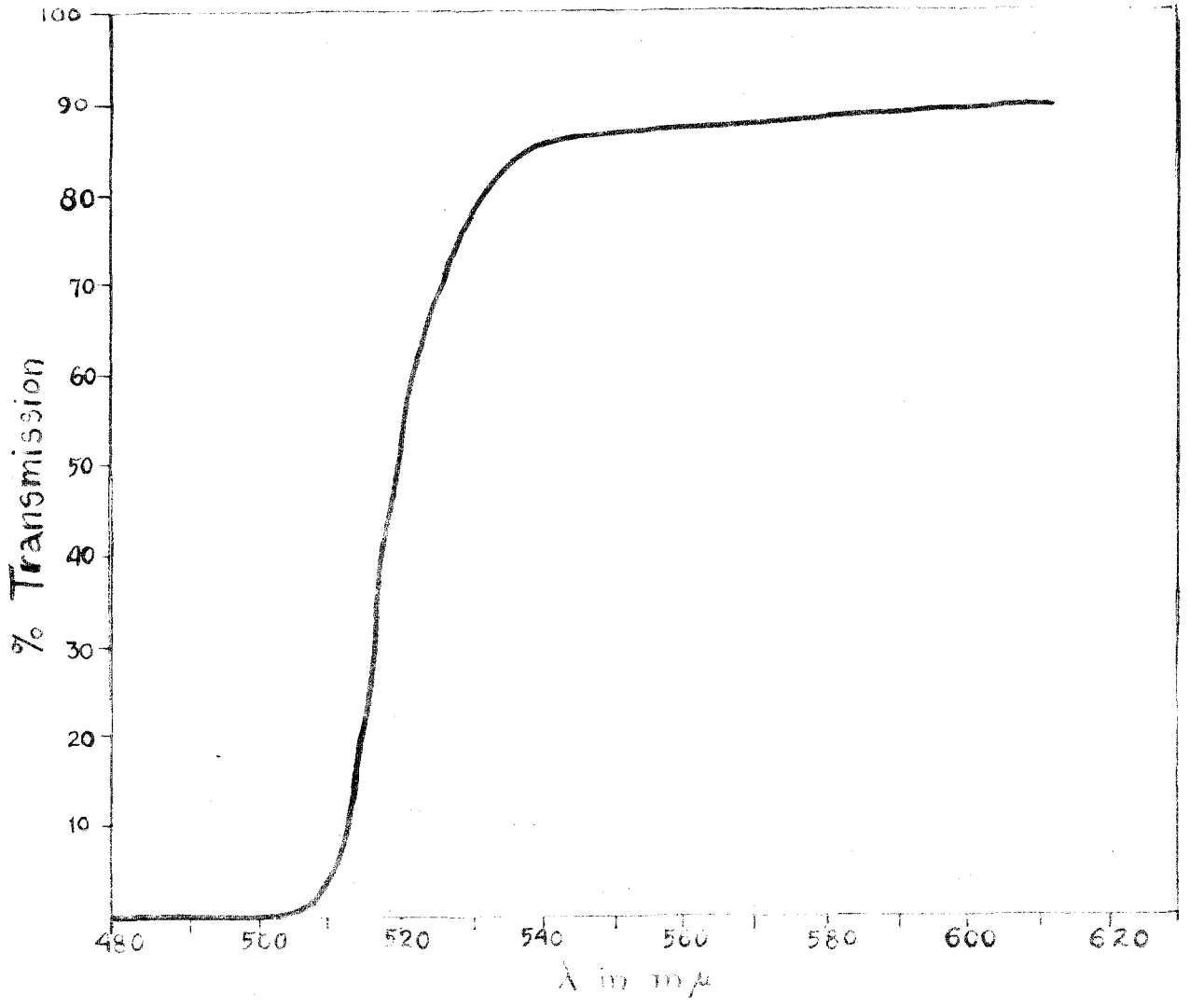

Fig. 3 Transmission curve for Corning No. 3486 cutoff filter.

reaction cell (except for the two small holes for the steady light) and the two filters (which eliminated most of the flash lamp light passed by the narrow band pass filter in front of the photoelectric cell) combined to keep the amount of scattered flash lamp light reaching the photoelectric cell low.

d. The Signal Detection Circuits

A 10v lead storage battery ran the steady source lamp, a sealed beam, 6-8v, 30w, parabolic reflector, automobile spotlight and a 6-8v, small panel light bulb (the calibration lamp). Light from the calibration light and the transmitted steady light reached the photoelectric cell by passing through a Bausch and Lomb interference filter with a measured maximum transmission of 36% at 487mμ, a half-width of 8mμ, and a transmission less than 1% throughout the rest of the spectrum (cf Fig. 4).

The photoelectric cell and the ac amplifier unit are schematically illustrated in Fig. 5. The ac signal developed across the 1 megohm resistor went to a cathode follower. The negative signal from this first stage went to the second 6AK5 where the positive signal, amplified nearly 100 times, was taken from across the plate load resistor and applied to the vertical deflection input terminal of a 304-H Du Mont Cathode-Ray Oscillograph.

The height of the signal due to an optical density change in the reaction cell is proportional to the gain of the circuits involved in the amplification and the presentation on the oscilloscope face. This gain is actually $g/(1+\beta)$ since g is a signal deflection to μamp ratio determined when only the calibration light is reaching

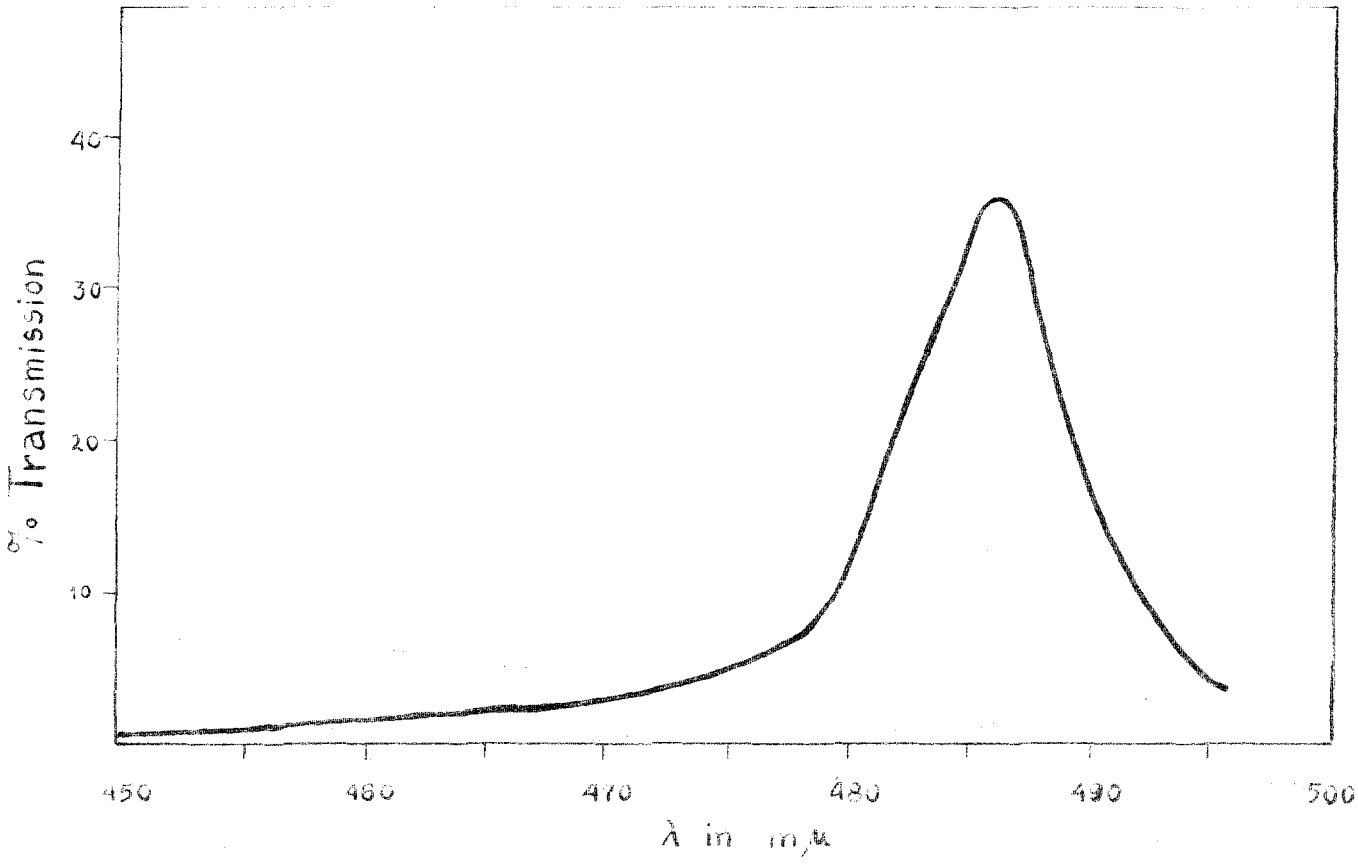

Fig. 4 Transmission curve for band-pass filter.

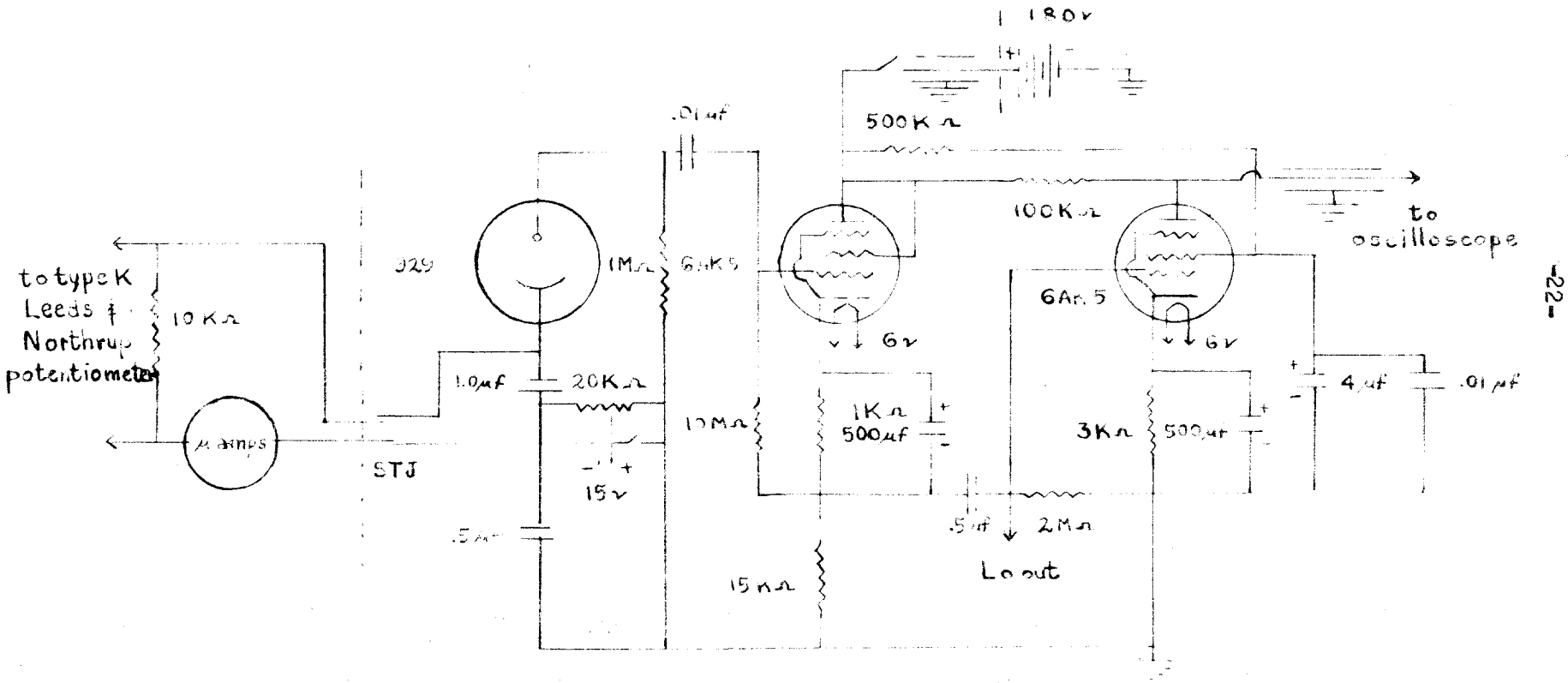

Fig. 5 Photoelectric cell and ac amplifier

the photoelectric cell. The decreased sensitivity of the photoelectric cell when the relatively extremely large amount of steady light is striking the photoelectric cell is corrected for by the factor $1/(1+\beta)$. The calibration lamp was behind a sector of 20 notches mounted on an 1800 rpm synchronous motor. Each complete square wave on the oscilloscope face was 1/600 sec. In addition to this time calibration for the sweep, the amplitude of the square wave divided by the photoelectric current for the unchopped calibration light furnishes β. The photoelectric current for the calibration and also for each recombination picture was measured with a 10,000 ohm precision registor (in series with the 1 megohm load resistor in the photoelectric cell circuit) and a type K Leeds and Northrup potentiometer. Typical calibration current was of the order of magnitude of 10^{-2} μamp while the steady light current during a recombination experiment was around 3 μamps.

The value of β may be found experimentally by comparing the square wave amplitude with and without the large steady light shining on the photoelectric cell. Let di_1 be the photoelectric current with just the calibration light striking the photoelectric cell and di_2, the current for the calibration signal with both light sources striking the photoelectric cell. These small currents may be written as

$$di_1 = K\, f(V) \tag{34a}$$

and

$$di_2 = K\, f(V-iR) \tag{34b}$$

If the first of these two equations is divided into the second and the law of the mean introduced,

$$di_2/di_1 = \frac{f(V) - iRf'(\xi)}{f(V)}, \quad (V-iR) < \xi < V \qquad (35).$$

With equation (17), equation (35) becomes

$$S_2/S_1 = 1 - iRf'(\xi)/f(V) \qquad (36)$$

and if the assumption

$$iRf'(\xi)/f(V) = iRf'(V-iR)/f(V-iR) \qquad (37)$$

is made,

$$\beta = \frac{S_1 - S_2}{S_1} \qquad (38).$$

e. The High-voltage Firing Circuit

Fig. 6 is a schematic of the triggering and delay circuits. When the switch in the triggering circuit was closed, a 15v positive pulse entered the sweep synchronization terminal of the oscilloscope and a sweep began. At the same time the pulse entered the delay circuit and after a delay determined by the selected RC value in the grid circuit of the 2D21 thyratron, this thyratron fired and a positive pulse was taken from across the cathode resistor and applied to the grid of the large thyratron, the 5C22 (cf Fig. 7) whose plate was highly positive, 10-15 kv. When this large thyratron fired, the positive side of four 1 μf, 20 kv, pyranol-filled (GE cat. no. 14F22) capacitors connected in parallel was suddenly discharged leaving the other side of the capacitors, ordinarily at ground potential, highly negative. This large negative voltage arced through the flash lamp in parallel with the 1000 ohm resistance to ground. From the plate of the thyratron four 20 megohm resistors (Sprague high-voltage, ferrule type) passed to

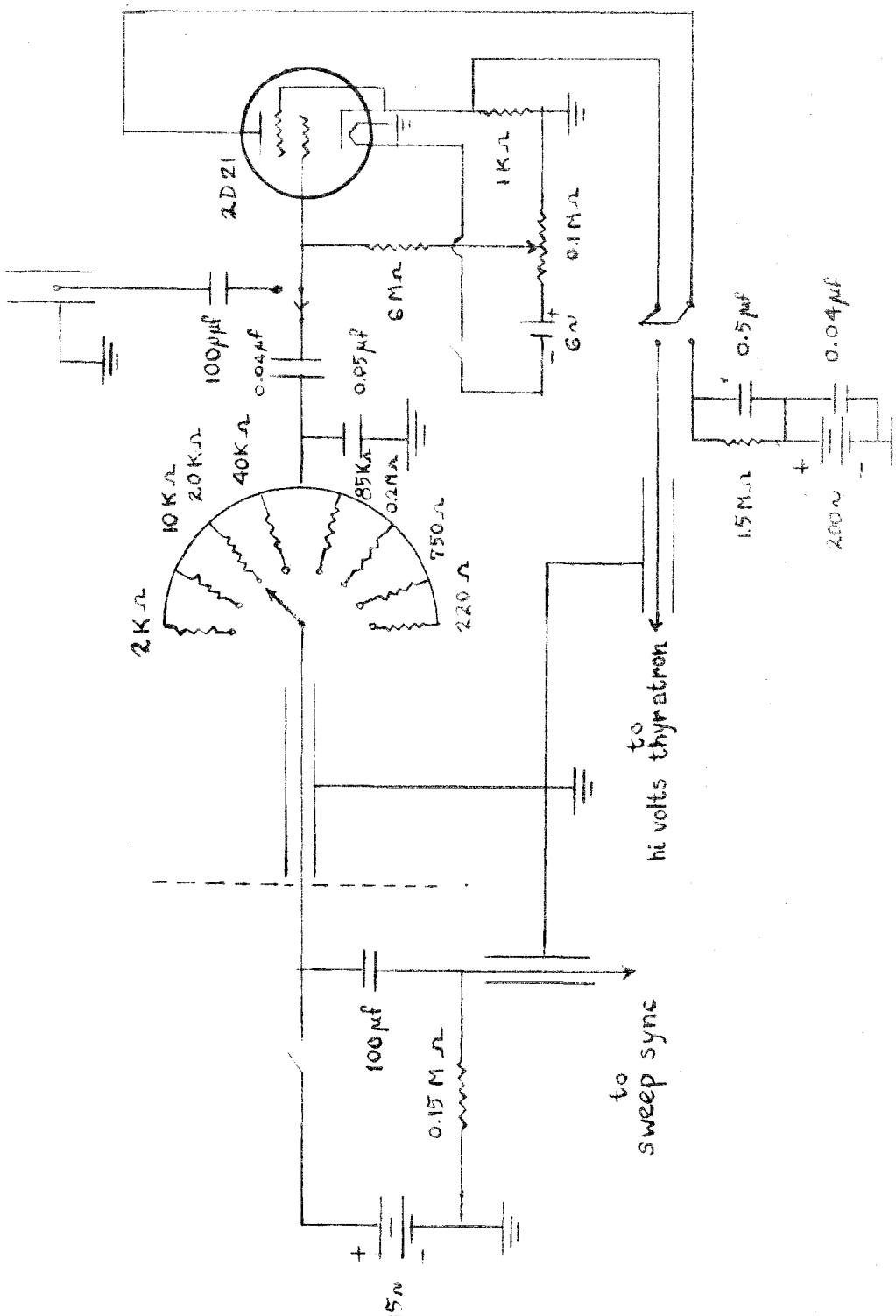

Fig. 6 Sweep trigger and delay circuits.

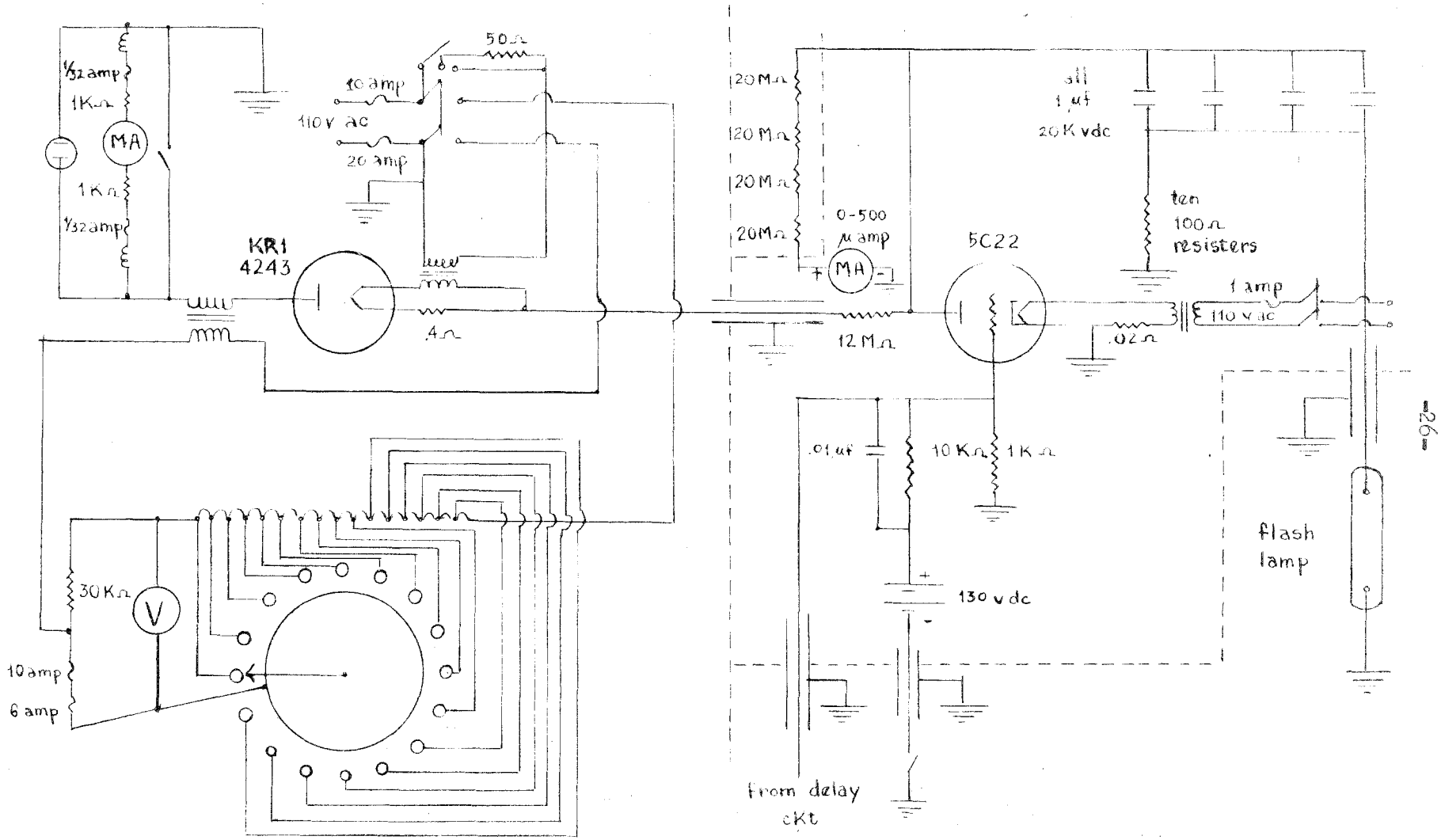

Fig. 7 High-voltage circuit for flash lamp.

ground through a 0-500 μ ammeter. The voltage at which the flash lamp was fired is used to compute the energy discharged through the lamp.

The high-voltage charging source (Fig.7) consisted of a vacuum diode (an old GE Kenotron, KR1, no. 4243) with the secondary of a high-voltage transformer in the plate circuit and the primary coil input regulated by an autotransformer. The maximum voltage obtainable with this power supply would be somewhat greater than 20 kv with 110 v ac input to the autotransformer. However, the 5C22 broke down spontaneously when the plate voltage became greater than 15-16 kv. This was not disturbing, however, since operation at 10-15 kv was perfectly satisfactory for the experiments.

f. Data Recording

A Mercury II 35 mm camera with a Universal f 2.7 Tricor lens with either Kodak Super XX or Linagraph Pan film was 25.5 cm* from the oscilloscope face. Just in front of the cathode ray tube is a celluloid disk bearing a grid whose squares were 0.1 inch on an edge (this 0.1 inch unit is subsequently called the s unit). The camera was operated on bulb for a few seconds and the picture of a blue trace** showing the scattered light and electrical

---

* The distance between the lens and the film was increased by means of a washer between the camera body and lens mount since the camera normally did not focus upon such a short objective distance.

** A P11 phosphor was used for maximum photographic sensitivity.

pickup from the flash alone, the recombination phenomenon, or the calibration square waves was taken (cf Figs. 8, 9, 18, 19, 23, 24, 25, and 26). Several pictures taken in succession of the calibration square waves with the photoelectric cell alternately shielded and unshielded from the steady light furnished the average amplitudes, S_1 and S_2, used in calculating β.

The negatives were studied in a microfilm reader. The trace of the sweep and the grid appeared on each negative so that in the analysis the signal heights and distances along the time axis from the end of the delay were conveniently recorded in terms of s units. The distances along the time axis were converted into seconds by the factor of 1/1200 divided by the average width of half a square wave from the calibration pictures. The reciprocals of the signal heights were plotted against time and the slope of the straight line through these points was calculated.

g. Limits of Observation and Errors

The theoretical rms noise to signal ratio, due to statistical fluctuations of the photoelectric current, is $(e/it_r)^{\frac{1}{2}}$ where e is the electronic charge; i, the photoelectric current (ca 3 μamps); and t_r, the rise time of the amplifier.* This ratio for these experiments was of the order of 10^{-4}. The observed noise to signal ratio agreed with this value. In addition, there was

---

* The rise time is considered to be $\frac{1}{2\pi n}$ where n is the high frequency cutoff, ca 25 kilocycles, at the half voltage point on the frequency response curve for the amplifier.

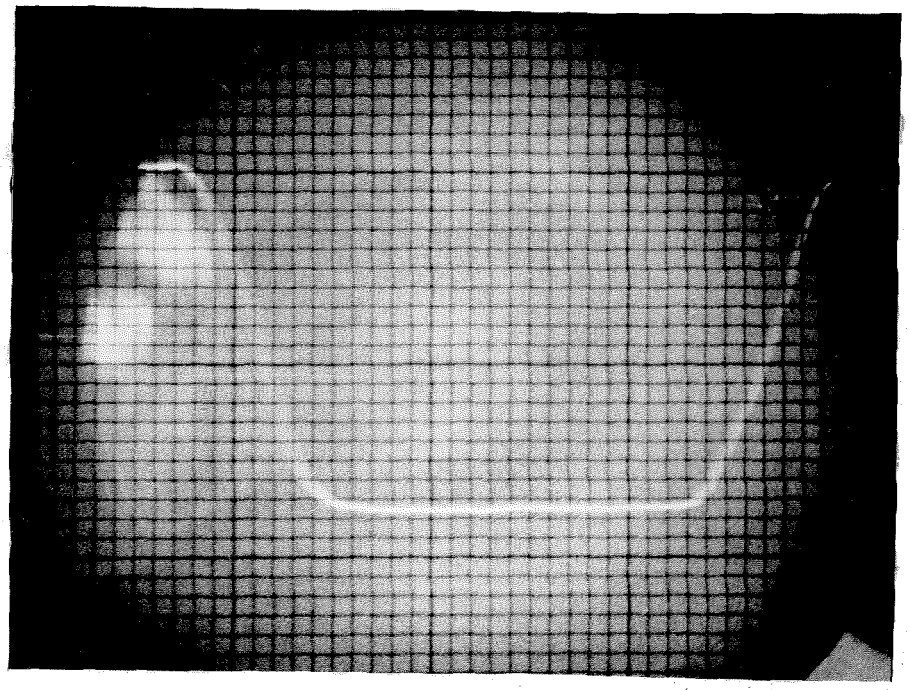

Fig. 8 Oscilloscope trace of one-half cycle of square wave used in time calibration (experiment of 7/16/53, writing rate = 0.0321 millisec/s-unit).

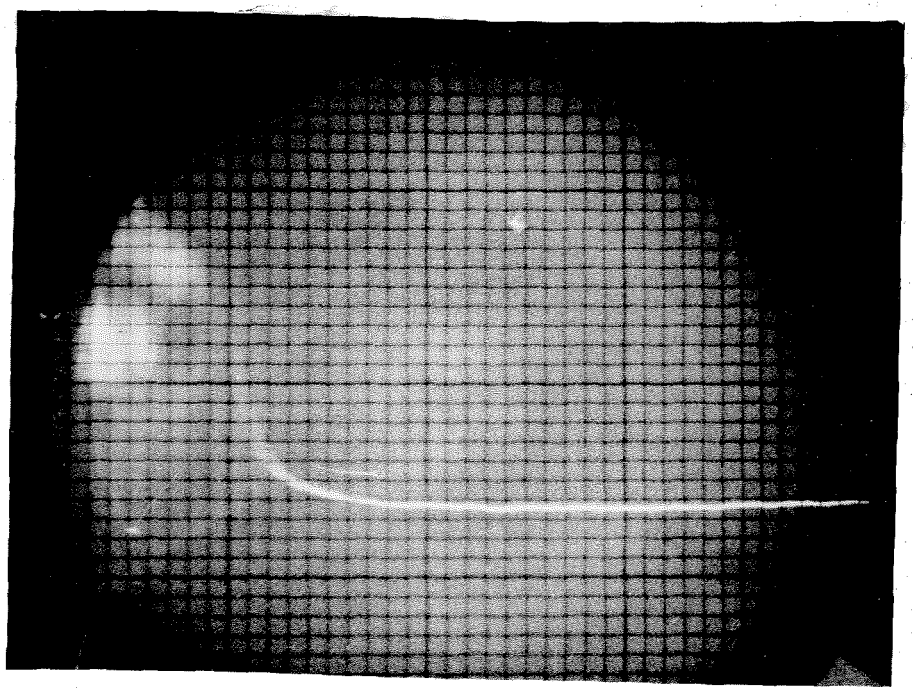

Fig. 9 Oscilloscope trace showing scattered light from flash lamp when steady light source is off (flash lamp energy=2.0×10^2 joules).

fluctuation of the steady light amounting to ca 2 x 10^{-4} of the dc photoelectric current of a low frequency (120 cycles or less) presumably due to mechanical vibration of the lamp. In other words the smallest signal that could be detected was of the order of one s unit or about 4 x 10^{-5} optical density units. The optimum size of signals from which to obtain kinetic data was about 10 times larger corresponding to an optical density change of 4 x 10^{-4}.

In Table 1 the errors (in percent) of the measured quantities used in calculating k are listed as well as the possible error in k due to the error in each measured quantity.

Table 1

Sources of Error

Measured Quantity		% Error (±)	% Error in k (±)
i		0.5	0.5
g	calibration current	4	4
	signal amplitude	1	1
α	extinction coefficient	5	5
	length of cell	0.3	0.3
β		50	2
S		2	4
t		2	2
$t_{\frac{1}{2}}$		20	0.1
RC		20	0.1
		Total	19

The likely error in the initial iodine atom concentration ranges from the neighborhood of ± 10% to over ± 100%. The

likely error depends upon the mean lifetime and the time at which the recombination is observed (the time at which the first measurement is made, t_1, is used in the error calculations).

An expression with which the error in the initial iodine atom concentration may be estimated can be obtained in the following way. Equation (6) can be rewritten as

$$t_{\frac{1}{2}} = \frac{1}{2k[I]_1} - t_1 \qquad (39).$$

When equation (39) is partially differentiated,

$$\partial t_{\frac{1}{2}} / \partial k = \frac{1}{2k^2 [I]_1} \qquad (40).$$

When equation (40) is divided through by $t_{\frac{1}{2}}$,

$$\partial \ln t_{\frac{1}{2}} / \partial k = \frac{1}{2k^2 [I]_1 \, t_{\frac{1}{2}}} \qquad (41)$$

and with the substitutions

$$t_{\frac{1}{2}} = \frac{1}{2k[I]_o} \qquad (42a)$$

and

$$1/[I]_1 = 2k(t_1 + t_{\frac{1}{2}}) \qquad (42b),$$

equation (41) becomes upon rearrangement

$$\frac{d[I]_o}{[I]_o} = \frac{t_1}{t_{\frac{1}{2}}} \frac{dk}{k} \qquad (43).$$

The term $\frac{t_1}{t_{\frac{1}{2}}} \frac{dk}{k}$ approximates the probable error in $[I]_o$. This fact is most conveniently verified by examining the values for ϕ in Tables 5 and 7. About half the values are outside the limits found from their per cent errors and the weighted average value (this value is assumed to be the true value). Equation (43) clearly indicates the weakness in extrapolation to the initial iodine atom concentration from observations at low iodine atom concentrations many half-lives after the dissociating flash.

In Table 2 values of t_1 and $t_1/t_{\frac{1}{2}}$ are given for each recombination picture for the 2.0×10^2 joule discharges. The ratios can be combined with the total possible error in k from Table 1 to find the errors in $[I]_o$.

Table 2

Factors for Determining the Error in $[I]_o$

A. CCl_4 solutions

1. 2.0×10^2 joule energy discharges

Date of Experiment	Picture No.	t_1 (millisec)	$t_1/t_{\frac{1}{2}}$
6/12/53	17	0.23	0.45
	18	0.23	0.48
	19	0.24	0.52
6/23/53	9	0.26	0.17
	16	0.46	3.1
	17	0.48	24
	18	0.47	12

Date of Experiment	Picture No.	t_1 (millisec)	$t_1/t_{\frac{1}{2}}$
7/1/53	28	0.19	0.39
	29	0.20	0.34
	30	0.19	0.33
	28	0.20	0.29
7/16/53	1	0.21	0.32
	3	0.22	0.29
	8	0.22	0.31
	9	0.23	0.42

2. 4.2×10^2 joule energy discharges

6/12/53	22	0.36	1.1
	23	0.41	1.4
	24	0.38	1.4
6/23/53	12	0.30	2.7
	13	0.29	2.6
	14	0.30	4.3
7/1/53	36	0.41	1.4
	37	0.41	1.3
	38	0.33	0.89

B. n - C_7H_{16} solutions

1. 2.0×10^2 joule energy discharges

Date of Experiment	Picture No.	t_1 (millisec)	$t_1/t_{\frac{1}{2}}$
4/1/53	12A	0.34	8.5
	13A	0.34	2.4
	16A	0.34	2.0

Date of Experiment	Picture No.	t_1 (millisec)	$t_1/t_{\frac{1}{2}}$
6/29/53	8	0.17	1.4
	9	0.17	1.9
	10	0.19	3.4
	13	0.18	1.9
	14	0.19	2.1
7/1/53	1	0.18	1.6
	2	0.19	7.6
	3	0.18	1.8
	6	0.16	4.6
	7	0.17	17
	41	0.20	1.2
	42	0.20	1.5
	43	0.23	1.6
	44	0.20	1.7
	45	0.20	3.3
2. 4.2×10^2 joule energy discharges			
4/1/53	2B	0.34	2.4
	3B	0.34	2.1
	8B	0.34	3.4
6/29/53	18	0.24	4.0
	19	0.20	20
	20	0.23	8.0
7/1/53	50	0.21	2.1
	51	0.20	5.7

Another source of possible error in the values of $[I]_o$ not included in equation (43) is that the flash lamp may not fire immediately after the 5C22 thyratron discharges. This would mean that extrapolation to the end of the delay for $\underline{t} = o$ is not valid. Actually the dependence of the intercept data for both gas and liquid reaction cells on the energy discharged through the flash lamp strongly suggests that delayed flash lamp firing occurs rarely if at all.

4. Data Obtained

a. I_2 in CCl_4 Solutions

The Recombination Signals

Upon illumination with the filtered* flash lamp light, a reaction cell containing only Eastman spectrophotometer grade CCl_4 exhibited a small negative change in the optical density with the filtered steady light. This small positive signal decaying to half-value in ca one millisecond represented an optical density change of the order of -2.6×10^{-5} for a 2.0×10^2 joule discharge and -5.2×10^{-5} for a 4.2×10^2 joule discharge; i.e., this small signal was approximately proportional to the flash lamp energy.

After I_2 was added to the CCl_4, a large positive signal was observed representing an optical density change of the order of -10^{-3}. The reciprocal height of the signal (corrected for the small positive signal observed before the addition of I_2**) plotted against

---

* Cf Fig. 3.

** Uncorrected signals when plotted also furnished reasonably straight lines with slopes about 9% lower than those of corrected signals.

time gave a reasonably straight line in agreement with equation (33) for the recombination of iodine atoms. Reciprocal signal heights versus time plots are shown in Figs. 10, 11, and 12. The points at the end of the sweep are high in practically all of the plots. The reason for this slight deviation toward the end of the reaction from the line for a second order rate expression is not known. Possibly a combination of effects tends to shift these points upward since at the edges of the oscilloscope face the signal is compressed along both the time and the amplitude directions (the cathode ray tube is curved at the edge). In addition, the small positive signal in the CCl_4 before I_2 was added was observed at higher monitor lamp currents (ca 5 μamps) than the phenomenon with I_2. Any slight over-correction would make the reciprocal values too high with the greatest error in the smallest signal. The compression in the time direction at the end of the sweep and the small positive-signal over-correction partially account for high reciprocal values but the small number of points actually affected in any plot and the incompleteness of the adjustment for these errors made replotting impractical.

The signals also furnish reasonably straight lines when plotted against time on semilogarithmic paper (cf Figs. 13, 14, and 15) and from these plots a first order reaction could be adduced.

Pictures representing the optical density change upon flash lamp illumination of I_2 in CCl_4 with a slow sweep (ca 0.017 second) at both 2.0×10^2 and 4.2×10^2 joules flash lamp discharges showed normal recovery of the optical density; i.e., the signal

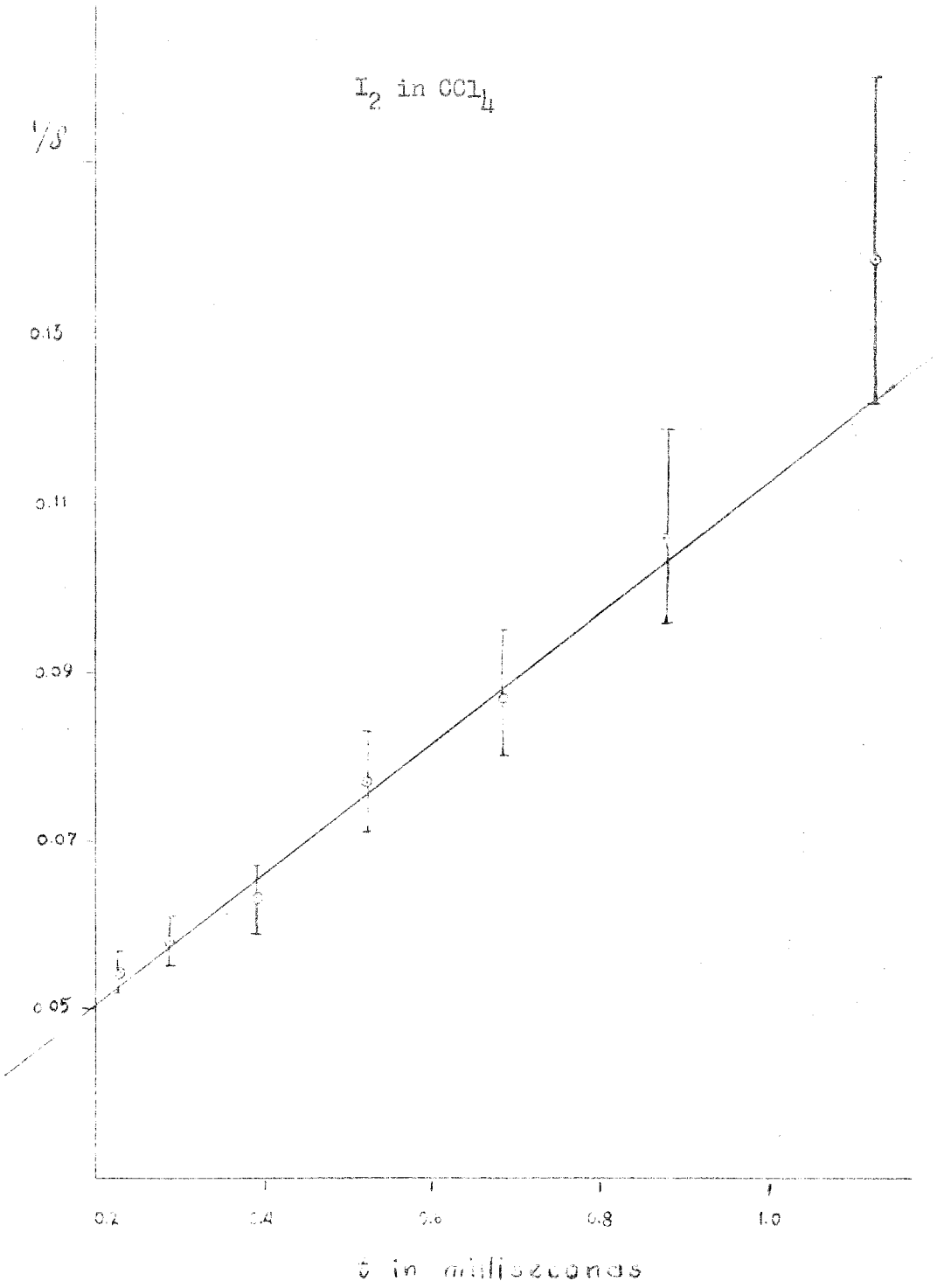

Fig.10 Reciprocal of signal deflection versus time (picture n. 18 6/12/56, error is ± 1 s-unit)

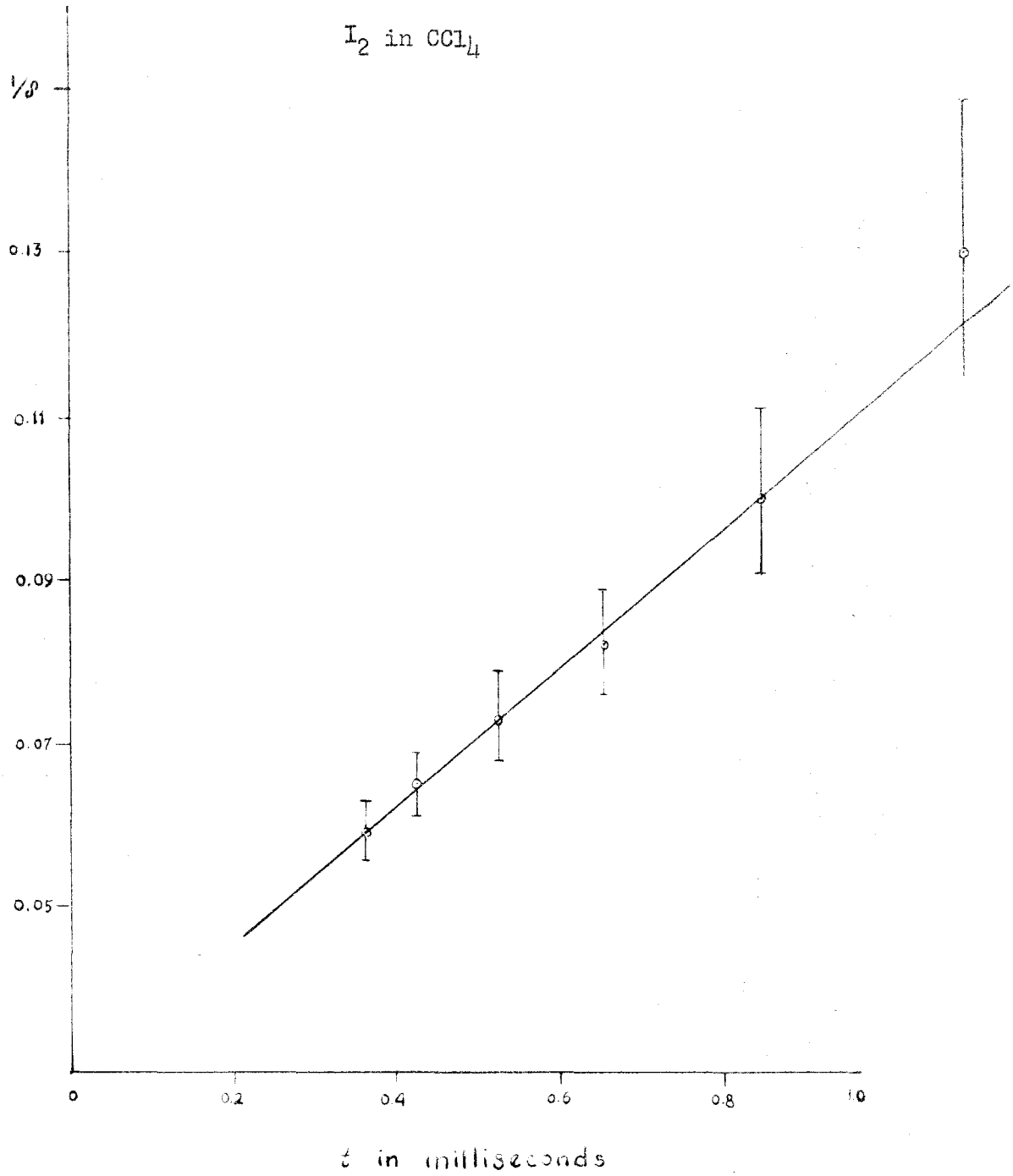

Fig. 11 Reciprocal of signal deflection versus time.
(picture no. 22, 6/12/53, error is ± 1 s-unit)

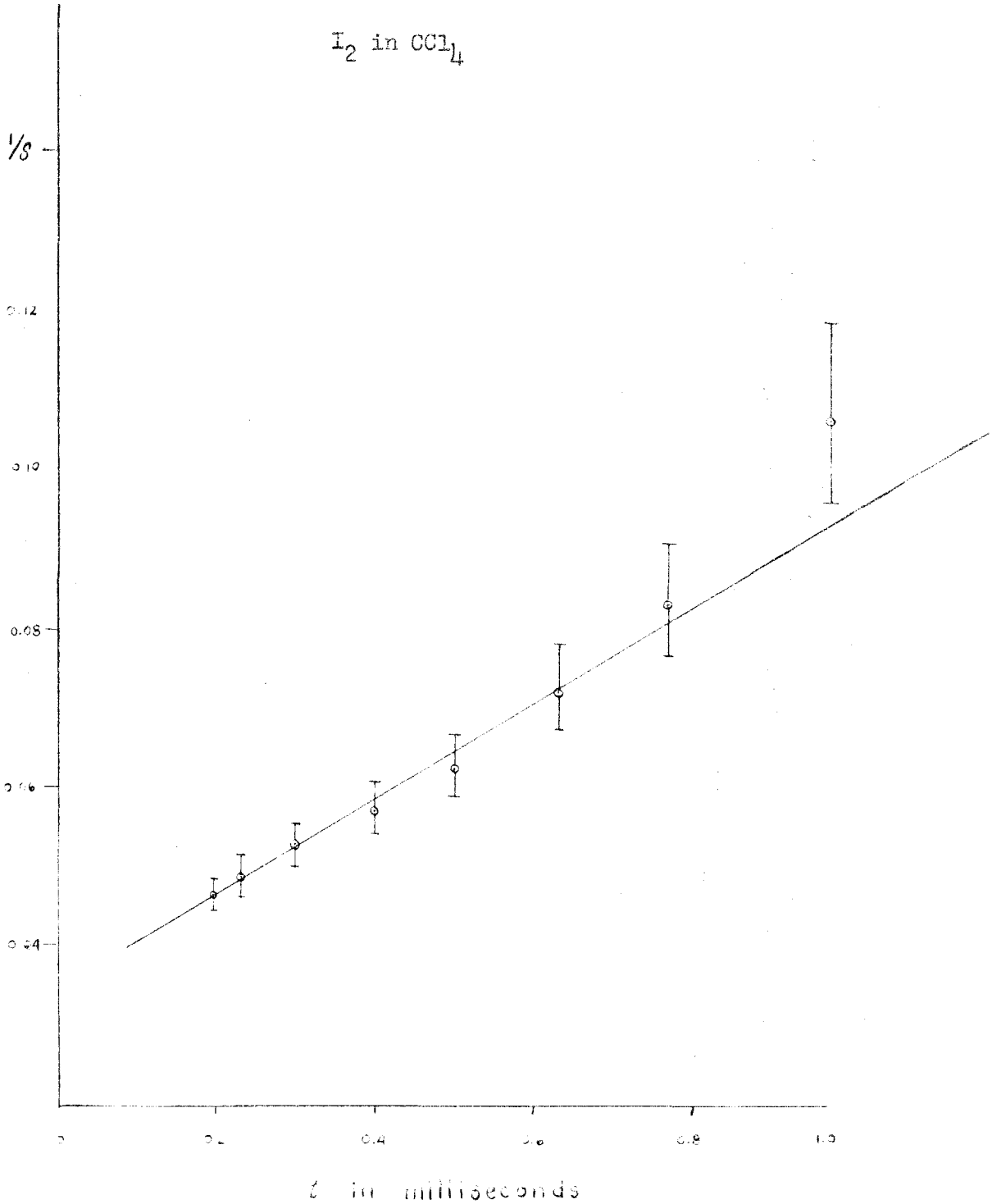

Fig 12 Reciprocal of signal deflection versus time
(Picture no. 28, 7/1/53, error is ± 1 s-unit)

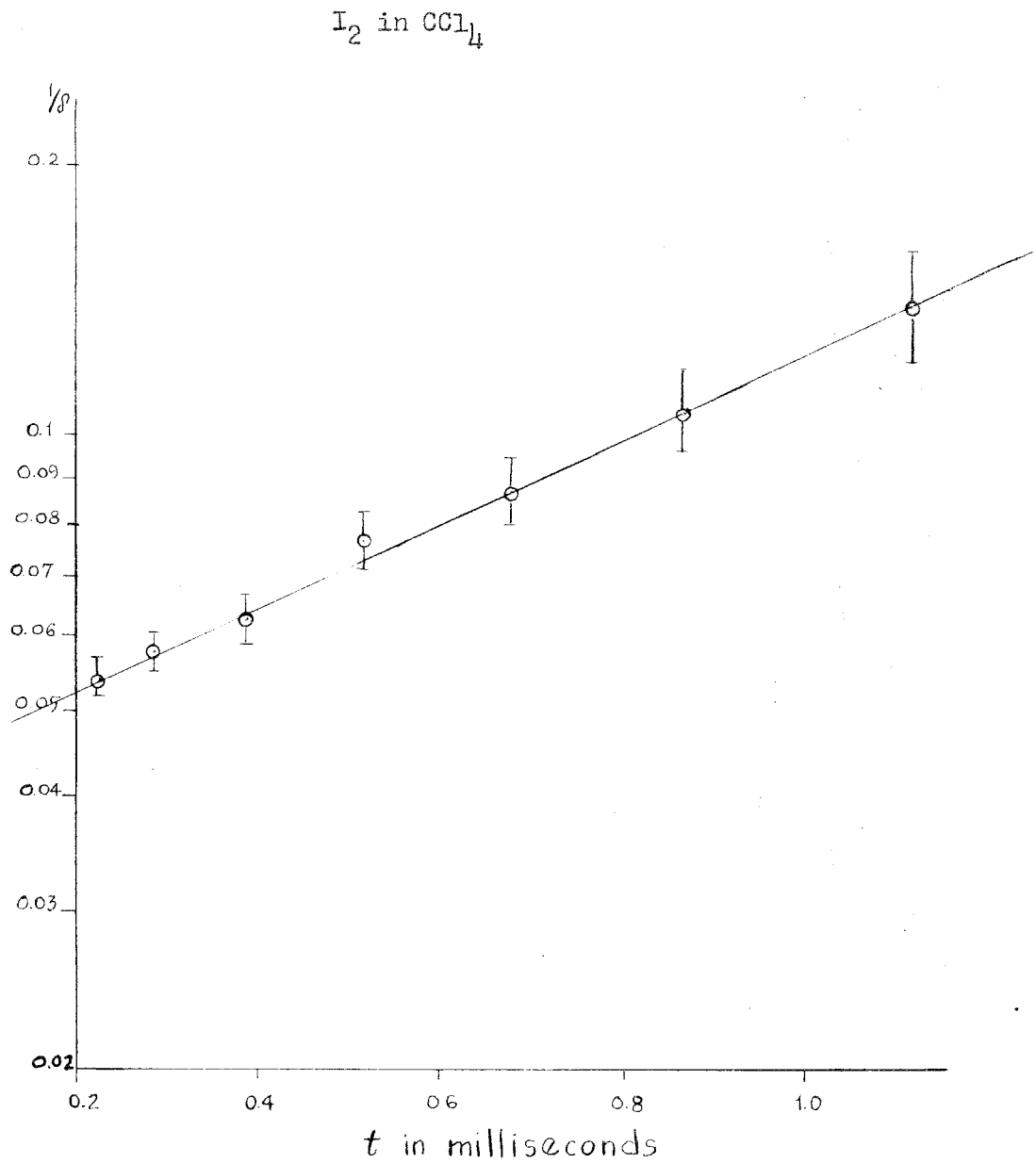

Fig. 13 Logarithm of reciprocal signal deflection versus time
(picture no. 18, 6/12/53, error is ± 1 δ-unit).

I_2 in CCl_4

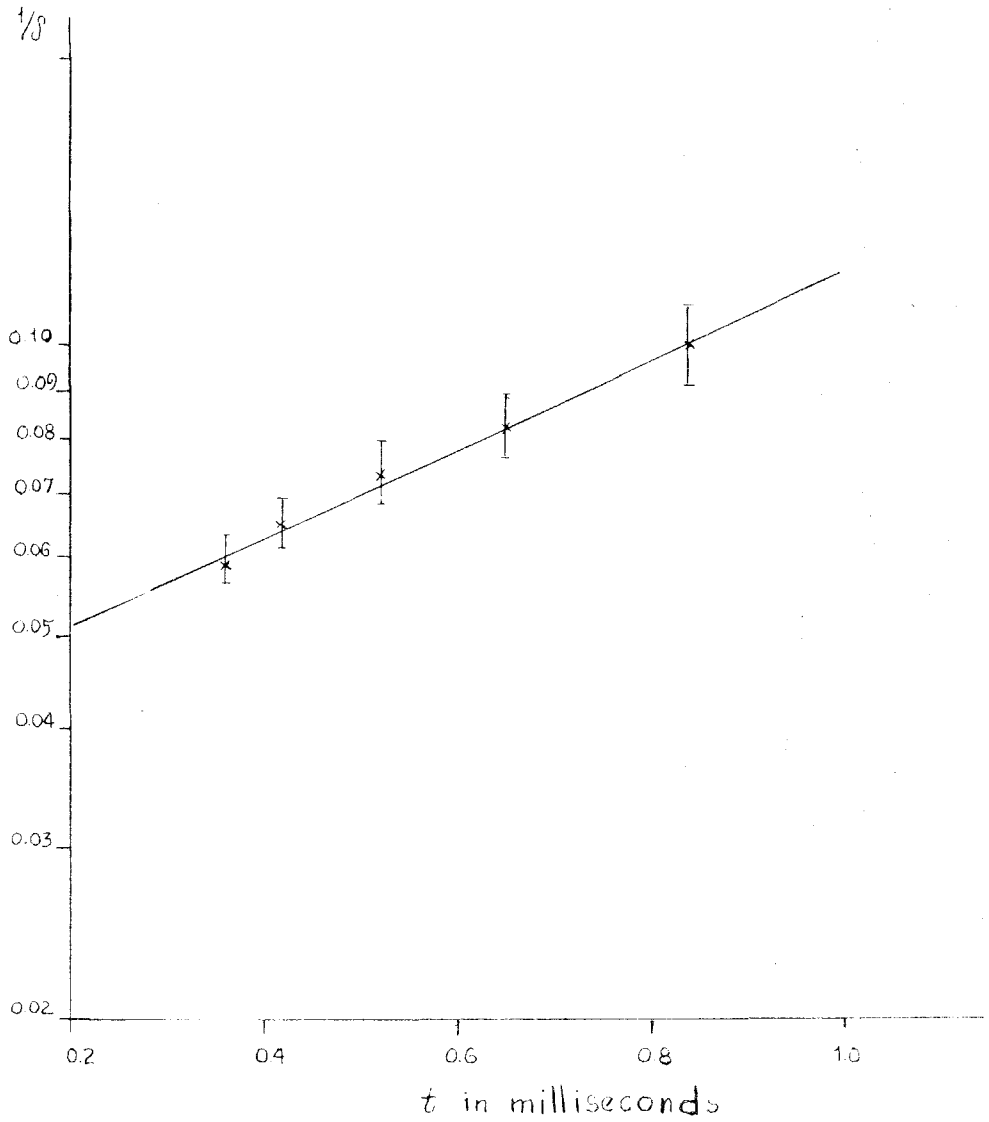

Fig. 14 Logarithm of reciprocal signal deflection versus time
(picture no. 22, 6/12/53, error is ± 1 s-unit).

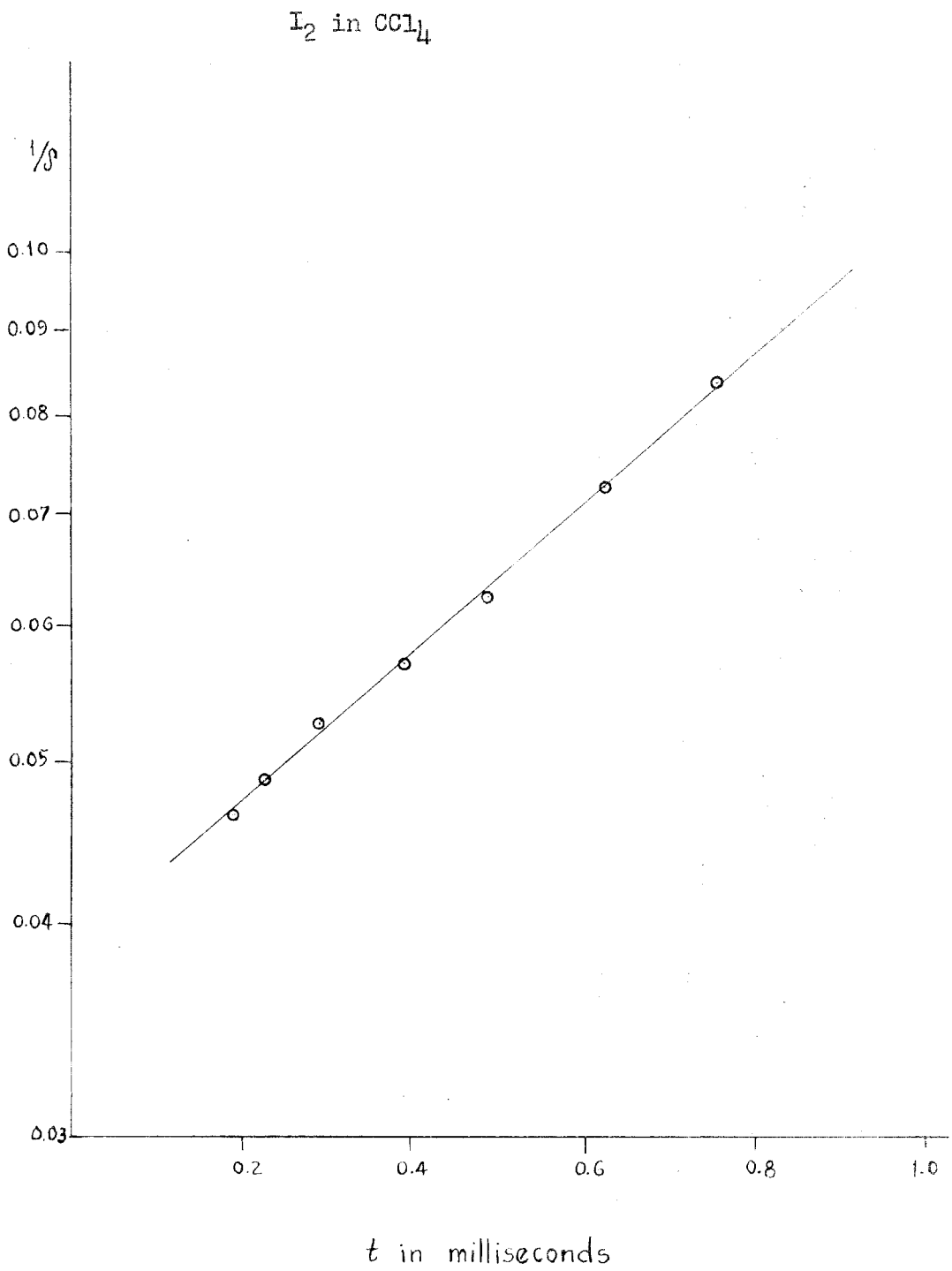

Fig. 15 Logarithm of reciprocal signal deflection versus time (picture no. 28, 7/1/53).

returned to the base line. Note that this normal recovery has been observed over a period ca 17 times as long as the actual period in which the data for the reported recombination values were obtained.

Determination of the Effective Extinction Coefficient

To determine the effective extinction coefficient for I_2 in CCl_4, the optical density for a reaction cell was measured with the same steady light, filter, and photoelectric cell as used in the recombination experiments and this solution used to fill a small 10 cm cell. The optical density of this small cell was measured at 517 mμ in the Beckman model DU spectrophotometer and after the blank correction was made, the concentration of iodine was calculated with the use of the reported (3) extinction coefficient of 930. With this concentration, the effective extinction coefficient was calculated. This procedure was repeated on the solution used in the experiment of 7/1/53. The data for the determination of the effective extinction coefficient are given in Table 4. The two values for the extinction coefficient found were 486 and 420 $mole^{-1}liter\ cm^{-1}$. Their average, 4.5×10^2, was used in computing the recombination constants in Table 5.

If the optical density for a reaction cell is taken to be $\log i_o/i_1$ where i_o is the photoelectric current due to the steady light with a reaction cell filled with H_2O* in the light path and i_1 is

---

* No difference between n - C_7H_{16} and H_2O blanks could be detected (cf Table 3) and the calculated differences between a CCl_4 blank and the other blanks are smaller than the experimental error.

Table 3

Steady Light Current Readings for n-C_7H_{16} and H_2O Cells

Cell	Steady light current (μamp)
H_2O	3.26
n-C_7H_{16}	3.23
H_2O	3.27
n-C_7H_{16}	3.26
H_2O	3.26
n-C_7H_{16}	3.26
n-C_7H_{16}	3.28
n-C_7H_{16}	3.61
n-C_7H_{16}	3.66
H_2O	3.72
n-C_7H_{16}	3.98
H_2O	3.69
n-C_7H_{16}	3.46
n-C_7H_{16}	3.44
H_2O	3.70
n-C_7H_{16}	3.62
H_2O	3.62
n-C_7H_{16}	3.66

the current for the case with the iodine solution in a reaction cell, then there is a 5-10% difference between optical densities determined when the steady light lamp is operated at 8 v and when it is operated at 6 v. At 6 v the steady light current for the solution and the blank was between 1 and 2 μamps and a higher optical density was measured than that determined at 8 v operation. At 8 v the steady light current was generally between 3 and 4 μamps and all the phenomenon pictures were taken with steady light current in the neighborhood of 3 μamps. The difference in optical density values with different steady light operating voltages is due to two effects:

a) photoelectric cell saturation

b) change in the energy distribution curve of the steady light.

The photoelectric cell current is not exactly proportional to the light intensity. The collecting voltage on the anode drops as the current increases and this decreases the sensitivity of the photoelectric cell somewhat. The photoelectric cell currents, i_o and i_1, may be written as

$$i_o = K_o f(V - i_o R) \qquad (44a)$$

and

$$i_1 = K_1 f(V - i_1 R) \qquad (44b)$$

Table 4

Optical Density Data Used in Calculating the Extinction Coefficient for I_2 in CCl_4 Under Conditions of the Recombination Experiments

A. First determination

1. Reaction cell (32.9 cm long) in steady light path

Cell	Steady light current (μamps)	Optical density ($\log i_o/i_1$)	Corrected O.D.
I_2 in CCl_4 / H_2O	2.51 / 4.16	0.218	0.228
I_2 in CCl_4 / H_2O	2.36 / 4.08	0.237	0.247
I_2 in CCl_4 / H_2O	2.45 / 4.05	0.217	0.227
I_2 in CCl_4 / H_2O	2.35 / 4.04	0.235	0.245
	Average and mean deviation		0.237 ± 0.009

2. Same solution in 10 cm cell in Beckman model DU spectrophotometer

Optical density of solution against H_2O at 517 mμ	$[I_2]$ (mole/liter)	ϵ $(\text{mole/liter})^{-1}\text{cm}^{-1}$
0.138	1.48×10^{-5}	486

B. Second determination

1. Reaction cell (32.9 cm long) in steady light path- - -see steady light current and optical density values in Table 5 for experiment of 7/1/53

2. Same solution in 10 cm cell in Beckman model DU spectrophotometer

Optical density of solution against H_2O at 517 mμ	$[I_2]$ (mole/liter)	ϵ $(\text{mole/liter})^{-1}\text{cm}^{-1}$
0.066	0.71×10^{-5}	420

C. Average value for $\epsilon = (4.5 \pm 0.2) \times 10^2$

The logarithm of both sides of the equation formed by dividing equation (44a) by equation (44b) becomes after the application of Taylor's expansion and rearrangement

$$\ln \frac{i_o}{i_1} = \ln \frac{K_o}{K_1} + \ln \frac{\left[1 - \frac{f'(V)}{f(V)} i_o R\right]}{\left[1 - \frac{f'(V)}{f(V)} i_1 R\right]} \qquad (45).$$

Since $f'(V) \ll f(V)$,

$$\ln \frac{i_o}{i_1} = \ln \frac{K_o}{K_1} + \ln \left[1 - \frac{f'(V)}{f(V)} \left(i_o R - i_1 R\right)\right] \qquad (46)$$

and upon further expansion and rearrangement,

$$\ln \frac{K_o}{K_1} = \ln \frac{i_o}{i_1} + \frac{f'(V)}{f(V)} \left(i_o - i_1\right) R \qquad (47)$$

or since

$$\beta = \frac{f'(V)}{f(V)} \; iR \qquad (48)$$

the true optical density, O. D., is given by

$$O.\ D. = \log \frac{i_o}{i_1} + \frac{\beta}{2.30} \frac{i_o - i_1}{i} \qquad (49).$$

Since $\frac{\beta}{2.30\ i}$ is a constant,

$$\frac{\beta}{2.30\ i} = \frac{f'(V)}{f(V)} \frac{R}{2.30} \qquad (50),$$

equation (49) can be written

$$O.D. = \log \frac{i_o}{i_1} + 0.006\,(i_o - i_1) \qquad (51)$$

where 0.006 is the average value of this constant for several experimentally determined values of β. Now the true optical density of a reaction cell can be computed for operation of the steady light lamp at 8v. Corrected optical densities are listed in Table 5. The correction accounts for about half the difference in optical densities for 6 and 8v lamp operation. The other half is apparently due to the change in the energy distribution curve of the steady light.

When the steady light lamp is operating at 8 instead of 6v, there is a shift of the peak of the energy distribution curve toward the shorter wavelengths. If J is the light transmitted in the wavelength range λ_1 to λ_2; $J_o(\lambda)$, the intensity of the incident light, a function of the wavelength; $\epsilon(\lambda)$, the extinction coefficient of I_2 in the solution, also a function of the wavelength; c, the I_2 concentration; and l, the distance the light travels through the solution, then for a particular wavelength Beer's law may be expressed as

$$J(\lambda) = J_o(\lambda)\exp(-\epsilon(\lambda)\,cl) \qquad (52)$$

and

$$J = \int_{\lambda_1}^{\lambda_2} J(\lambda)\,d\lambda = \int_{\lambda_1}^{\lambda_2} J_o(\lambda)\exp(-\epsilon(\lambda)\,cl)\,d\lambda \qquad (53).$$

For small absorption

$$J = \int_{\lambda_1}^{\lambda_2} J_o(\lambda)\left[1 - \epsilon(\lambda)\,cl\right]\,d\lambda \qquad (54)$$

and the amount absorbed is

$$\Delta J = \int_{\lambda_1}^{\lambda_2} J_o(\lambda) \epsilon(\lambda) \, c\,l\,d\lambda \qquad (55).$$

Now $\underline{J_o}(\underline{\lambda})$ is a product of three functions of the wavelength; one, the energy distribution with wavelength of the steady light, $\underline{L}(\underline{\lambda})$, another, the filter transmission, $\underline{F}(\underline{\lambda})$, and the other, the photoelectric cell sensitivity, $\underline{P}(\underline{\lambda})$; i.e.,

$$J_o(\lambda) = L(\lambda) \quad F(\lambda) \quad P(\lambda) \qquad (56).$$

Now equation (55) becomes

$$\Delta J = \int_{\lambda_1}^{\lambda_2} L(\lambda) \quad F(\lambda) \quad P(\lambda) \epsilon(\lambda) \, c\,l\,d\lambda \qquad (57)$$

and the amount absorbed is affected by changes in the emission curve of the steady light lamp (the $\underline{L}(\underline{\lambda})$ term). The peak of the energy distribution curve for the steady light is in the near infrared and as the peak shifts toward the shorter wavelengths the fractional amount of light absorbed at shorter wavelengths is expected to increase because $\underline{L}(\underline{\lambda})$ increases.

Tabular Presentation of the Data

In Table 5 are given the date of each experiment with I_2 in CCl_4 solutions, the oscilloscope sweep setting, the writing rate of the oscilloscope sweep (in millisec/$\underline{s}$ - unit), the oscilloscope gain setting, the gain ($\underline{g}$) of the amplifier-oscilloscope combination (in $\underline{s}$ - units deflection/ μamp), the gain correction term

Table 5

Summary of Data From I_2 in CCl_4 Solutions

Date of Experiment	Sweep Setting	Writing Rate $\left(\frac{\text{millisec}}{\text{s - unit}}\right)$	Gain Setting	$\left[\frac{\text{g}}{(\text{s-units})10^{-3}}{\mu\text{amp}}\right]$	β	Cell	i_o and i_1 (μamps)	O. D.	$[I_2]$ (mole/liter)10^{+5}	Picture No.
6/12/53	250-1250 v 70	0.0317	10 v 100	3.33 (6/11/53)	0.06	I_2 in CCl_4	3.87	0.098**		17
						air	4.82			18
						I_2 in CCl_4	3.74	0.112**		19
						air	4.81			22
						I_2 in CCl_4	3.74	0.112**		23
						air	4.81			24
								0.107± 0.006	0.72	
6/23/53	250-1250 v 70	0.0333	10 v 100	3.34	---	I_2 in CCl_4	2.56	0.243		9
						H_2O	4.37			12
						I_2 in CCl_4	2.55	0.246		13
						H_2O	4.38			14
						I_2 in CCl_4	2.50	0.254		16*
						H_2O	4.38			17*
								0.248±0.004	1.68	18*

* Flash lamp light unfiltered.

** Calculated correction for air blank included.

Table 5 (continued)

Date of Experiment	Sweep Setting	Writing Rate $\left(\frac{\text{millisec}}{\underline{s}\text{ - unit}}\right)$	Gain Setting	$\left[\frac{\underline{g}}{\frac{(\underline{s}\text{-units})10^{-3}}{\mu\text{amp}}}\right]$	β	Cell	i_o and i_1 (μamps)	O. D.	$[I_2]$ [(mole/liter)10^{+5}]	Picture No.
7/1/53	250-1250 v 70	0.0334	10 v 100	3.38	0.025	I_2 in CCl_4	3.45	0.080		28
						H_2O	4.12			29
						I_2 in CCl_4	3.16	0.110		30
						H_2O	4.02			31
						I_2 in CCl_4	3.42 / 3.14 (3.28)	0.105		36 / 37
						H_2O	4.14			38
						I_2 in CCl_4	3.21			
								0.098 ± 0.012	0.66	
7/16/53	250-1250 v 70	0.0321	10 v 100	2.98	0.098	I_2 in CCl_4	4.36	0.024		1
						H_2O	4.60			3
						I_2 in CCl_4	4.18	0.041		8
						H_2O	4.58			9
						I_2 in CCl_4	4.32	0.029		
						H_2O	4.61			
								0.031 ± 0.006	0.21	

Table 5 (continued)

Date of Experiment	Picture No.	Slope $\left[\frac{(\text{s-units})}{\text{sec}}^{-1}\right]$	i (μamps)	$\frac{1}{S_o}$ $[(\text{s-units})^{-1}]$	Flash Lamp Energy $[(\text{joules})10^{-2}]$	$[I]_o$ $\left[\left(\frac{\text{mole}}{\text{liter}}\right)10^{7}\right]$	$\frac{[I]_o}{2\Pi_2^2}$ (%)	ϕ	$t_{\frac{1}{2}}$ (millisec)	k $\left[\frac{(\text{mole}^{-1}\text{liter})10^{-10}}{\text{sec}}\right]$
6/12/53	17	61	3.56	0.032	2.0	1.6	1.1	0.17(±9%)	0.51	0.58
	18	73	3.56	0.036	2.0	1.5	1.0	0.16(±9%)	0.48	0.70
	19	72	3.56	0.034	2.0	1.5	1.0	0.16(±10%)	0.46	0.68
	22	84	3.54	0.029	4.2	1.8	1.2	0.11(±21%)	0.34	0.80
	23	74	3.54*	0.023	4.2	2.3	1.6	0.14(±27%)	0.30	0.70
	24	85	3.54*	0.021	4.2	2.5	1.7	0.15(±27%)	0.27	0.80
6/23/53	9	122	2.53	0.019	2.0	3.6	1.1	0.17(±3%)	0.15	0.90
	12	111	2.58	0.012	4.2	5.5	1.6	0.14(±51%)	0.11	0.84
	13	111	2.58	0.012	4.2	5.5	1.6	0.14(±49%)	0.11	0.84
	14	129	2.58	0.009	4.2	7.3	2.2	0.19(±82%)	0.07	0.97
	16**	94	2.58	0.014	2.0	4.8	1.4	0.22(±59%)	0.15	0.71
	17**	120	2.58	0.002	2.0	33	9.8	1.53(±456%)	0.02	0.91
	18**	109	2.58	0.004	2.0	16	4.8	0.75(±228%)	0.04	0.82

* Pictures taken in succession; steady light current read only for no. 23.

** Flash lamp light unfiltered.

Table 5 (continued)

Date of Experiment	Picture No.	Slope $\left[\frac{(\text{s-units})^{-1}}{\text{sec}}\right]$	i (μamps)	$\frac{1}{S_o}$ $[(\text{s-units})^{-1}]$	Flash Lamp Energy $[(\text{joules})10^{-2}]$	$\left[\frac{[I]_o}{\text{mole/liter}}\right]10^7$	$\frac{[I]_o}{2[I_2]}$ (%)	Φ	$t_{\frac{1}{2}}$ (millisec)	k $\left[\frac{(\text{mole}^{-1}\text{liter})10^{-10}}{\text{sec}}\right]$
7/1/53	28	59	3.28	0.035	2.0	1.5	1.1	0.17(±7%)	0.49	0.54
	29	60	3.39	0.030	2.0	1.7	1.3	0.20(±6%)	0.59	0.57
	30	67	3.42	0.038	2.0	1.4	1.1	0.17(±6%)	0.58	0.64
	31	68	3.23	0.047	2.0	1.2	0.9	0.14(±6%)	0.68	0.62
	36	72	3.28	0.016	4.2	3.4	2.6	0.23(±27%)	0.29$_5$	0.67
	37	63	3.24	0.020	4.2	2.7	2.0	0.18(±25%)	0.31	0.58
	38	62	3.24	0.023	4.2	2.4	1.8	0.16(±17%)	0.37	0.55
7/16/53	1	64	4.36	0.042	2.0	1.2	2.9	0.45(±26%)	0.65	0.65
	3	60	4.36	0.046	2.0	1.1	2.6	0.40(±26%)	0.75	0.60
	8	78	4.45	0.055	2.0	0.9	2.1	0.33(±26%)	0.70$_5$	0.80
	9	76	4.45	0.042	2.0	1.2	2.9	0.45(±28%)	0.55$_5$	0.78
								Average values and mean deviations 0.19 ± 0.05	0.72	± 0.11

(β), the steady light current readings (i_o and i_1) (in μamps), for the various solutions and cell blanks interposed in the steady light path, the corrected optical densities, the iodine concentration (in mole/liter), the phenomenon picture numbers, the slopes of the reciprocal signal-height versus time plots (in (s-units)$^{-1}$/sec), the steady light current (in μamps), the intercept ($1/S_o$) of each plot at t = o (in (s-units)$^{-1}$), the energy discharged through the flash lamp (in joules), the initial iodine atom concentration (in mole/liter), the percent of initial dissociation, the primary quantum yield (ϕ), the mean lifetime of the iodine atoms (in millisec), and the rate constant (k) for the recombination (in mole^{-1} liter/sec).

Estimation of the Primary Quantum Yield

The primary quantum yield in the gas phase for the dissociation of iodine molecules has been demonstrated to be essentially unity in the banded region of the absorption spectrum by Rabinowitch and Wood (4). The initial iodine atom concentrations for a reaction cell containing I_2 in argon at 2.0 x 10^2 and 4.2 x 10^2 joules flash lamp discharges were found to be 3.5 ($\pm$ 0.4 mean deviation) x 10^{-7} and 6.2 ($\pm$ 0.5) x 10^{-7} mole/liter, respectively. The optical density of this cell was essentially the same as that of a 10 cm length cell with the same components whose iodine concentration was 1.1 x 10^{-5} mole/liter so the concentration of the longer cell was (10/32.9 x 1.1) x 10^{-5} mole/liter. With this value

the fraction dissociated has been computed to be 5.3% for a 2.0×10^2 joules flash lamp discharge and 9.4% for a 4.2×10^2 joules flash lamp discharge. The maximum extinction coefficient for iodine in argon is nearly 20% lower than the maximum extinction coefficient in either CCl_4 or $\underline{n}$-C_7H_{16} and with this factor the values 6.5 and 12.0% have been selected for the fractional dissociation in the gases assuming unity primary quantum yield. These estimated maximum fractional dissociations corresponding to the two flash lamp energies were divided into the observed fractional dissociations in order to obtain the primary quantum yield in the liquids (cf values in Table 5). Tests with I_2 in argon systems, with the modified flash photolysis apparatus used in these experiments with liquids, produced recombination constants which were slightly higher than those reported in Part I of this thesis. The values of the fractional dissociation in the gas cells are slightly greater than they should be. On the other hand the light entering the gas-system cell is less than that for the liquid-system cells because in the former case there is reflection from two gas-glass boundaries instead of one gas-glass and one glass-liquid boundary. The reflection loss and the error in the fractional dissociations in the gas system nearly cancel each other.

The errors for the values of $\underline{\phi}$ in Table 5 are determined from Table 2 and equation (43) and in addition the

extremely low optical density solution for the experiment on 7/16/53 led to an uncertain iodine molecule concentration whose error (± 20%) has been included in the error values for the four pictures of this experiment. The average value and mean deviation at room temperature for $\underline{\phi}$, 0.19±0.05, represents the average of all values of $\underline{\phi}$ weighted inversely with the error associated with each value. The mean deviation is the average of the weighted deviations and there is presumably an additional possible error of at least 15% associated with iodine concentrations and assumptions in the fractional dissociation values.

Iodine solutions at four different optical densities were studied (cf Table 5). Essentially the same results were obtained from all of these solutions except for an approximately 60% increase in the initial iodine atom concentration upon doubling the energy of the flash lamp discharge. Figs. 16a and 16b illustrate the variation of $[I]_o$ with optical density (essentially iodine concentration) and with flash lamp energy.

Incidental Observations

When the Corning no. 3486 filters were removed, reaction cells with CCl_4 alone showed a large long-lived increase in optical density. The decay time of the negative signal was greater than or equal to 0.12 sec, the decay time for an ac signal with the amplifier-oscilloscope combination. This was observed with Eastman Kodak spectrophotometer grade CCl_4 and in some earlier experiments with cp CCl_4. However, the earlier

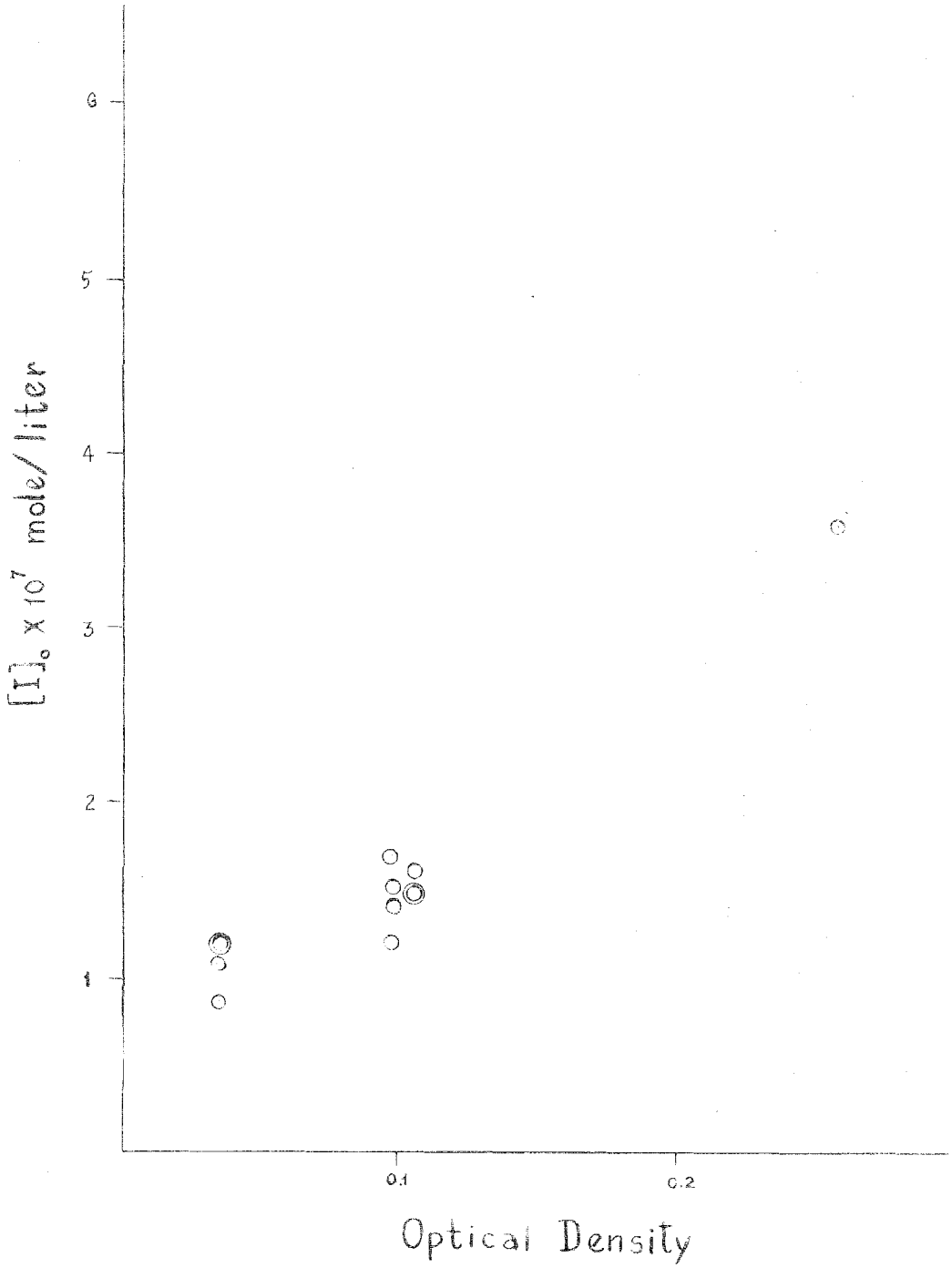

Fig. 16a Initial iodine atom concentration versus optical density of CCl_4 solutions for flash lamp discharges of 2.0×10^2 joules.

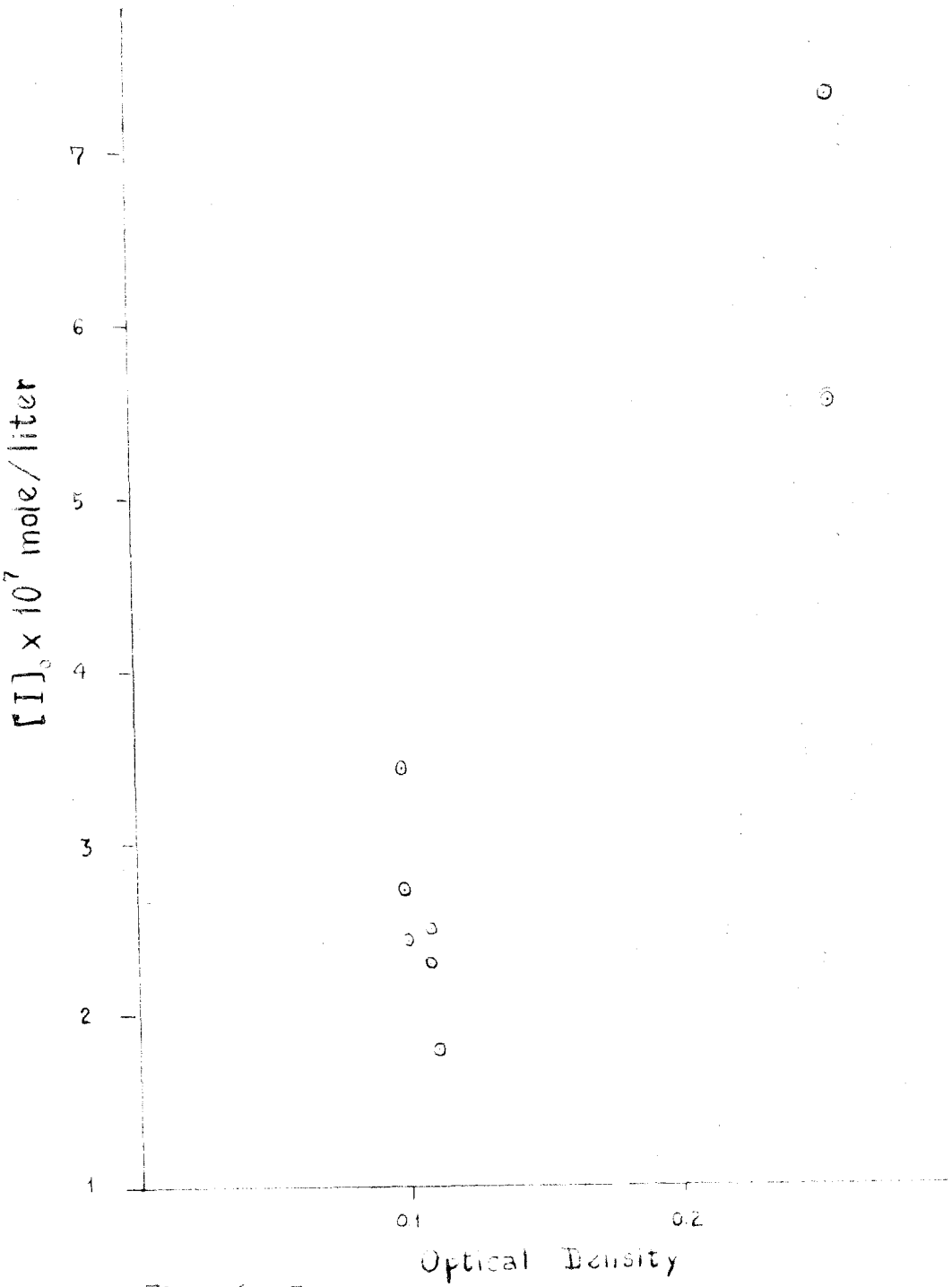

Fig. 16b Initial iodine atom concentration versus optical density of CCl_4 solutions for flash lamp discharges of 4.2×10^2 joules.

experiments also indicated that the cp CCl_4 is less satisfactory than spectrophotometer grade CCl_4 as a medium in which to observe the recombination of iodine atoms. The positive signals obtained decayed at about one-third the rate for the signals with I_2 in the spectrophotometer grade CCl_4. In Fig. 17 are shown the optical density versus wavelength plots for two samples of CCl_4, one cp material and the other spectrophotometer grade, for the region 260 through 410 mμ. The absorption peak in the cp material may be related to the impurity causing the slow signal decay when I_2 is present. If iodine atoms were removed by reaction and the product were less absorbing than I_2 in the region being studied spectrophotometrically, then a net positive signal would be superimposed upon the decay due to recombination.

An interesting observation (but presumably only coincidentally resembling the above negative-signal phenomenon) is that when S_8 dissolved in CCl_4 is flash photolyzed, a long-lived increase in the optical density of the cell occurs. This photochemical effect has already been investigated (5); S_8 goes to a colloidal form upon illumination and light is scattered.

This large negative signal was observed in the most dilute I_2 in CCl_4 solution (optical density = 0.031) while in the most dense solution (optical density = 0.248) normal-appearing positive signals were obtained which when compared against the flash alone furnished consistent rate constants and

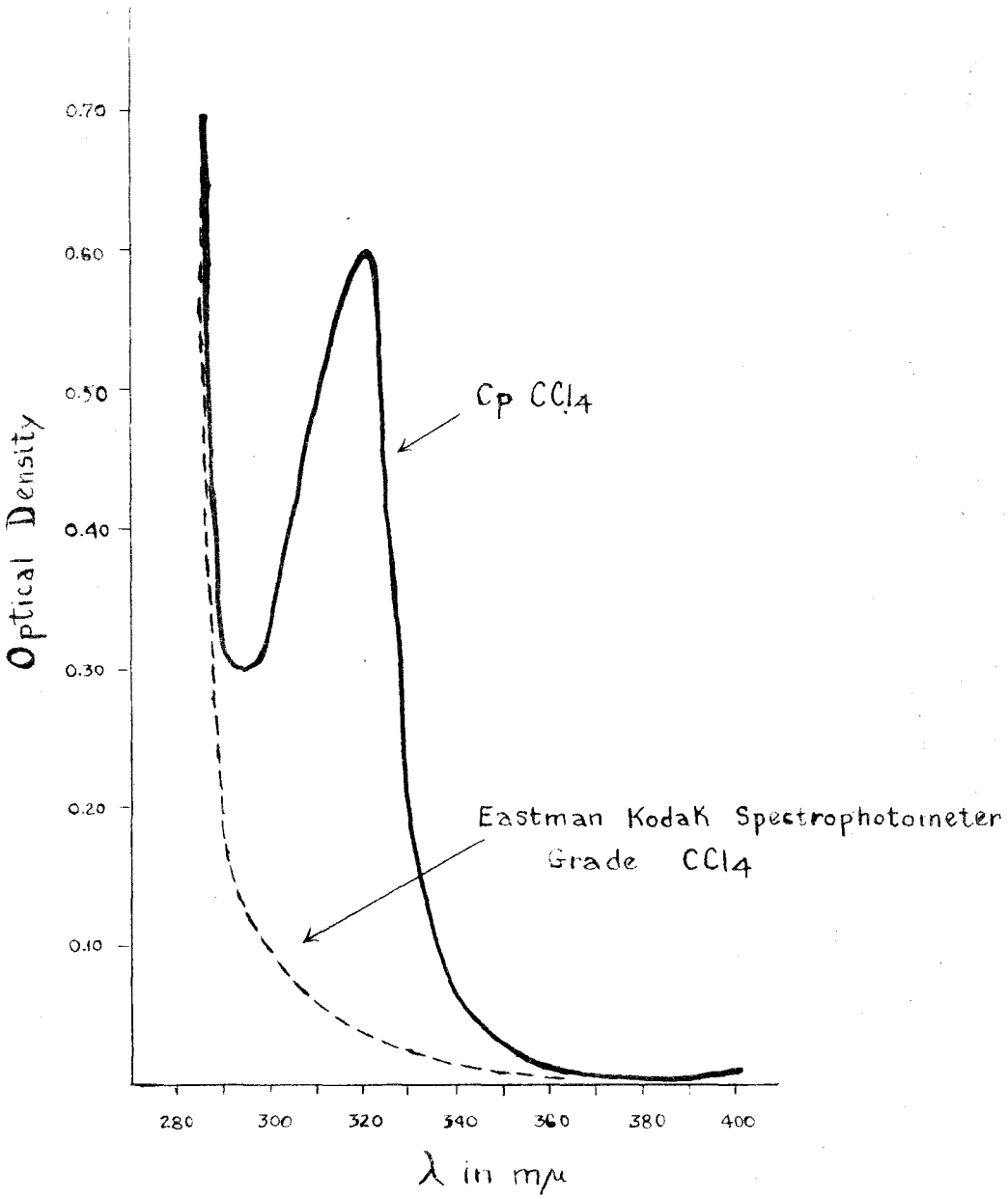

Fig. 17 Optical density versus wavelength for two samples of carbon tetrachloride measured against water in 10 cm long quartz cell.

only the intercepts (and, therefore, $[I]_o$) for two of the three pictures seem abnormal (cf pictures 16, 17, and 18 of the experiment on 6/23/53, Table 5).

As already mentioned, the long pyrex flash lamp and the Corning number 3486 filters were used in a series of experiments with I_2-in-argon gas cells. The ratio of 0.82 for the average value of the recombination constant for iodine atoms in argon from a large series of experiments* to the average value obtained with the apparatus in the present investigation is attributed to an asymmetrical distribution of light from the flash lamp. The rate constant in the latter experiments is apparently too high by a factor of 1/0.82, in all probability due to the non-uniform production of iodine atoms. The recombination constants in Table 5 would have a small correction compared to the gas system for comparable asymmetrical distribution of iodine atoms since the periods of observation are so different in terms of the half-times of the two kinds of reactions. However, the apparent increase in the rate of decay of the signal toward the end of the sweep is not due to a non-homogeneous concentration of iodine atoms.

The Rate Constant

The average value and the mean deviation for the recombination constant of iodine atoms in CCl_4 at room temperature is $(0.72 \pm 0.11) \times 10^{10}$ mole^{-1}liter sec^{-1}. A sense of the physical

---

* Cf Part I of this thesis.

meaning of this figure as characterizing the kinetics of the reaction can be obtained from the pictures of the oscilloscope trace during recombination as shown in Figs. 18 and 19.

b. I_2 in $\underline{n}$-C_7H_{16} Solutions

The Recombination Signals

The pure grade $\underline{n}$-C_7H_{16} obtained from Phillips Petroleum Company showed no change in optical density upon flash lamp illumination in a millisecond following the flash. Toward the end of a 30 millisecond sweep there was a small signal corresponding to a slight increase in optical density. Pure grade $\underline{n}$-C_7H_{16} without purification and I_2 furnished persistent positive signals (decrease in optical density) with a minimum in the signal just after the flash.

After purification of the $\underline{n}$-C_7H_{16}, normal appearing, rapidly decaying, positive signals were obtained with I_2 solutions with optical densities less than 0.2. On slow sweeps (ca 17 times as long as the period in which the recombination data were collected) the signal returned quickly to the zero signal state and remained on this base line. Above optical densities of 0.2, the signals were inconsistent. The non-uniform creation of iodine atoms can explain only number 2 of the following observations:

1. The generally observed (even in the gas phase experiments) apparent increase in the recombination rate toward the end of the sweep (small signal side).

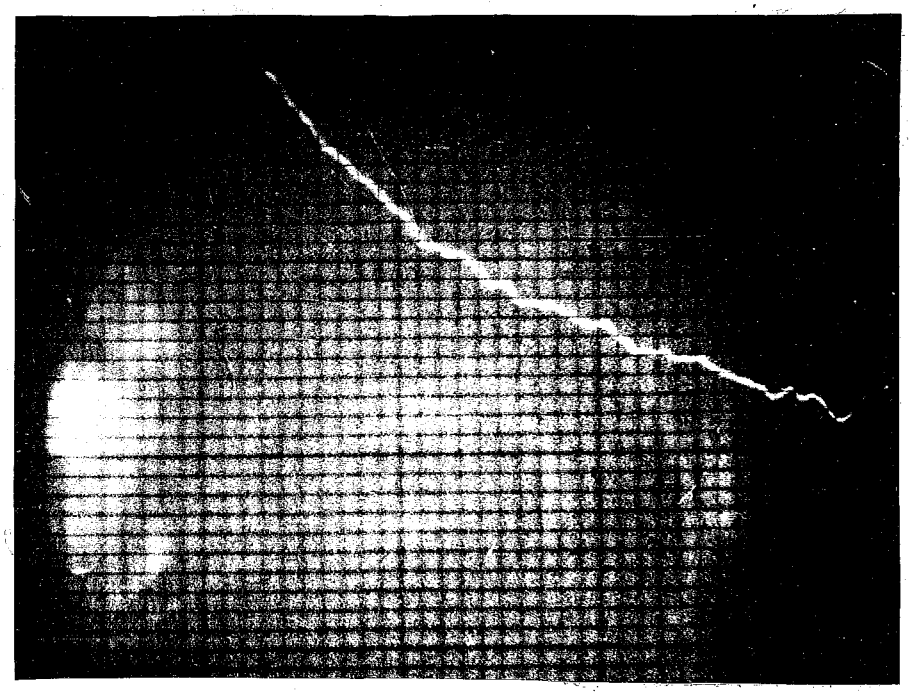

Fig. 18 Oscilloscope trace during the recombination of iodine atoms in CCl_4 (picture no. 12, 6/23/53, cf Table 5).

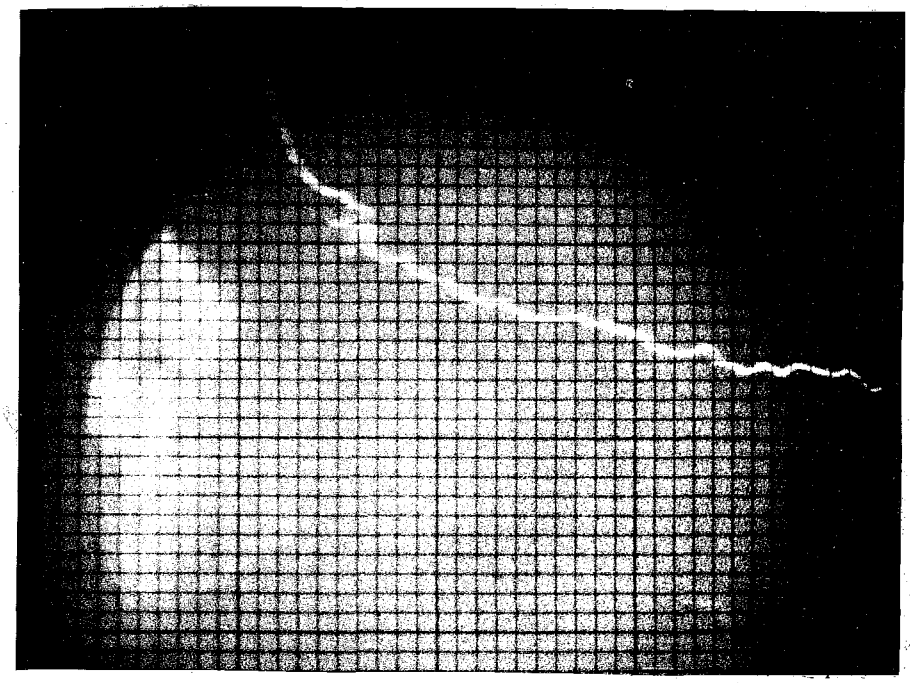

Fig. 19 Oscilloscope trace during the recombination of iodine atoms in CCl_4 (picture no. 9, 7/16/53, cf Table 5).

2. The difference between the gas cell recombination constants with different flash lamps.

3. The still smaller (than predicted from the steady light current reduction) signal in high optical density, I_2 in $\underline{n}$-C_7H_{16} solutions.

4. The erratic values in high optical density solutions; values that range from that consistent in the lower optical density experiments to 3 and 4 times this value.

Determination of the Effective Extinction Coefficient

Extinction coefficients found for I_2 in $\underline{n}$-C_7H_{16} experimentally using the reported (3) value of 910 for the extinction coefficient at 520 mμ were 372 (for a solution of optical density 0.213) and 379 (for a solution of optical density 0.216) (cf Table 6). The value of 3.7×10^2 was used to calculate the recombination constants in Table 7.

The Recombination Data

Data obtained for I_2 in $\underline{n}$-C_7H_{16} solutions are listed in Table 7, identical in arrangement to Table 5. The average recombination rate constant and its mean deviation for iodine atoms in $\underline{n}$-C_7H_{16} are $2.2(\pm 0.4) \times 10^{10}$ mole^{-1}liter sec^{-1} at room temperature.

Initial Iodine Atom Concentrations

There is more energy absorbed in the reaction cell when the flash lamp energy is doubled as clearly shown by the initial iodine atom concentrations in the gas phase. In the liquid phase

Table 6

Optical Density Data Used in Calculating the Extinction Coefficient for I_2 in $\underline{n}$-C_7H_{16} Under Conditions of the Recombination Experiments

A. First determination

1. Reaction cell (32.9 cm long) in steady light path

Cell	Steady light current (μamps)	Optical density (log i_o/i)	Corrected O. D.
I_2 in $\underline{n}$-C_7H_{16}	2.37	0.217	0.226
$\underline{n}$-C_7H_{16}	3.92		
I_2 in $\underline{n}$-C_7H_{16}	2.42	0.207	0.216
$\underline{n}$-C_7H_{16}	3.88		
I_2 in $\underline{n}$-C_7H_{16}	2.42	0.215	0.224
$\underline{n}$-C_7H_{16}	3.96		
I_2 in $\underline{n}$-C_7H_{16}	2.42	0.196	0.204
$\underline{n}$-C_7H_{16}	3.80		
I_2 in $\underline{n}$-C_7H_{16}	2.42	0.215	0.224
$\underline{n}$-C_7H_{16}	3.98		
I_2 in $\underline{n}$-C_7H_{16}	2.42	0.204	0.213
$\underline{n}$-C_7H_{16}	3.87		
I_2 in $\underline{n}$-C_7H_{16}	2.38	0.204	0.213
$\underline{n}$-C_7H_{16}	3.81		
I_2 in $\underline{n}$-C_7H_{16}	2.39	0.204	0.213
$\underline{n}$-C_7H_{16}	3.83		
I_2 in $\underline{n}$-C_7H_{16}	2.38	0.204	0.213
$\underline{n}$-C_7H_{16}	3.82		
	Average and mean deviation		0.216 ± 0.006

2. Same solution in 10 cm cell in Beckman model DU spectrophotometer

Optical density of solution against water at 520 mμ	$[I_2]$ (mole/liter)	ϵ $[(\text{mole/liter})^{-1}\text{cm}^{-1}]$
0.158	1.74×10^{-5}	379

Table 6 (continued)

B. Second determination (same solution as above)

1. Reaction cell (32.9 cm long) in steady light path

Cell	Steady light current (μamps)	Optical density (log i_o/i)	Corrected O. D.
I_2 in $\underline{n}$-C_7H_{16} / H_2O	2.31 / 3.77	0.213	0.222
I_2 in $\underline{n}$-C_7H_{16} / H_2O	2.35 / 3.73	0.200	0.208
I_2 in $\underline{n}$-C_7H_{16} / H_2O	2.35 / 3.73	0.200	0.208
I_2 in $\underline{n}$-C_7H_{16} / H_2O	2.31 / 3.70	0.204	0.212
I_2 in $\underline{n}$-C_7H_{16} / H_2O	2.28 / 3.69	0.208	0.216
	Average and mean deviation		0.213 ± 0.005

2. Same solution in 10 cm cell in Beckman model DU spectrophotometer

Optical density of solution against water at 520 mμ	$[I_2]$ (mole/liter)	ϵ $[(\text{mole/liter})^{-1}\text{cm}^{-1}]$
0.158	1.74×10^{-5}	372

C. Average value for $\epsilon = (3.7 \pm 0.2) \times 10^2$

Table 7

Summary of Data for I_2 in $\underline{n}$-C_7H_{16} Solutions

Date of Experiment	Sweep Setting	Writing Rate $\left(\frac{\text{millisec}}{\underline{s}\text{ - units}}\right)$	Gain Setting	$\left[\frac{\underline{g}}{\frac{(\underline{s}\text{-units})10^{-3}}{\mu\text{amp}}}\right]$	β	Cell	$\underline{i_o}$ and i $(\mu\text{amps})^{-1}$	O. D.	$\left[\frac{[I_2]}{(\text{mole/liter})10^{5}}\right]$	Picture No.
3/23/53	250-1250 v 70	0.0463	10 v 100	3.26	---	I_2 in $\underline{n}$-C_7H_{16}	3.05	0.068		2A
						H_2O	3.55			3A
						I_2 in $\underline{n}$-C_7H_{16}	3.06	0.068		4A
						H_2O	3.55			5B
						I_2 in $\underline{n}$-C_7H_{16}	3.04			6B
						H_2O	3.57	0.069		7B
						I_2 in $\underline{n}$-C_7H_{16}	3.05			
						I_2 in $\underline{n}$-C_7H_{16}	2.84	0.061		
						H_2O	3.26			
						I_2 in $\underline{n}$-C_7H_{16}	2.76	0.079		
						H_2O	3.30			
						I_2 in $\underline{n}$-C_7H_{16}	2.76	0.079		
						H_2O	3.30			
							0.071± 0.006		0.58	
4/1/53	250-1250 v 60	0.0484	10 v 100	3.48	---	H_2O	3.24	0.017		12A
						I_2 in $\underline{n}$-C_7H_{16}	3.12	0.030		13A
						$\underline{n}$-C_7H_{16}	3.35			16A
						H_2O	3.28	0.017		2B
						I_2 in $\underline{n}$-C_7H_{16}	3.16	0.032		3B
						$\underline{n}$-C_7H_{16}	3.41			8B

Table 7 (continued)

Date of Experiment	Sweep Setting	Writing Rate $\left(\frac{\text{millisec}}{\underline{s}\text{ - unit}}\right)$	Gain Setting	$\left[\frac{g}{(\underline{s}\text{-units})10^{-3}}{\mu\text{amp}}\right]^{\beta}$	Cell	i_o and i_{-1} $(\mu\text{amps})^{-1}$	O. D.	$[I_2]$ $[(\text{mole/liter})10^{5}]$	Picture No.
4/1/53 (continued)					H_2O	3.26	0.015		
					I_2 in $\underline{n}$-C_7H_{16}	3.16	0.037		
					$\underline{n}$-C_7H_{16}	3.43			
					H_2O	3.31	0.021		
					I_2 in $\underline{n}$-C_7H_{16}	3.15	0.036		
					$\underline{n}$-C_7H_{16}	3.41			
						0.026±	0.008	0.21	
5/20/53	250-1250 v 70	0.0359*	10 v 100	3.26*	I_2 in $\underline{n}$-C_7H_{16}	2.72	0.216		5
					$\underline{n}$-C_7H_{16}	4.38			6
					I_2 in $\underline{n}$-C_7H_{16}	2.69	0.227		7
					$\underline{n}$-C_7H_{16}	4.44			8
						0.221	±0.006	1.82	16
									19

* Determined 4/28/53.

Table 7 (contined)

Date of Experiment	Sweep Setting	Writing Rate $\left(\frac{\text{millisec}}{\underline{s}\text{ - unit}}\right)$	Gain Setting	g $\left[\frac{(\underline{s}\text{-units})10^{-3}}{\mu\text{amp}}\right]$	β	Cell	i_o and i $(\mu\text{amps})^{-1}$	O. D.	$[I_2]$ $[(\text{mole/liter})10^5]$	Picture No.
6/29/53	250-1250 v 70	0.0338	10 v 100	3.39	0.06	I_2 in $\underline{n}$-C_7H_{16}	3.51	0.047		8
						H_2O	3.89			9
						I_2 in $\underline{n}$-C_7H_{16}	3.42	0.054		10
						H_2O	3.85			13
						I_2 in $\underline{n}$-C_7H_{16}	3.47	0.047		14
						H_2O	3.86			18
							0.049 ±	0.003	0.40	19
										20
7/1/53	250-1250 v 70	0.0334	10 v 100	3.38	0.025	I_2 in $\underline{n}$-C_7H_{16}	2.89	0.168		1
						H_2O	4.18			2
						I_2 in $\underline{n}$-C_7H_{16}	2.91	0.175		3
						H_2O	4.27			6
						I_2 in $\underline{n}$-C_7H_{16}	2.88	0.171		7
						H_2O	4.19			13
							0.171 ±	0.003	1.41	
						I_2 in $\underline{n}$-C_7H_{16}	3.23	0.112		41
						H_2O	4.13			42
						I_2 in $\underline{n}$-C_7H_{16}	3.10	0.116		43
						H_2O	4.01			44
						I_2 in $\underline{n}$-C_7H_{16}	3.09	0.112		45
						H_2O	3.96			50
							0.113 ±	0.002	0.93	51

Table 7 (continued)

Date of Experiment	Picture No.	Slope $\left[\frac{(\underline{s}\text{-units})^{-1}}{\text{sec}}\right]$	$\underline{i}$ (μamps)	$\frac{1}{S_o}$ $[(\underline{s}\text{-units})^{-1}]$	Flash Lamp Energy $[(\text{joules})10^{-2}]$	$[I]_o$ $\left[\left(\frac{\text{mole}}{\text{liter}}\right)10^{7}\right]$	$\frac{[I]_o}{2[I_2]}$ (%)	$\underline{\phi}$	$t_{\frac{1}{2}}$ (millisec)	$\underline{k}$ $\left[\frac{(\text{mole}^{-1}\text{liter})10^{-10}}{\text{sec}}\right]$
3/23/53	2A	304	2.89	0.020	2.4	3.8	3.3		0.070	2.0
	3A	282	2.87	0.007	2.4	10.9	9.4		0.040	1.8
	4A	422	2.86	0.010	2.4	7.7	6.6		0.030	2.8
	5B	306	2.90	0.020	2.4	3.8	3.3		0.060	2.1
	6B	451	2.92	0.030	2.4	2.5	2.2		0.075	3.0
	7B	322	2.92*	0.025	2.4	3.0	2.6		0.080	2.1
4/1/53	12A	250	3.02	0.010	2.0	6.8	16	2.50(±192%)	0.04	1.8
	13A	293	3.02	0.040	2.0	1.7	4.0	0.62(± 76%)	0.14	2.2
	16A	294	2.97	0.048	2.0	1.4	3.3	0.52(± 68%)	0.17	2.1
	2B	288	2.89	0.037	4.2	1.9	4.5	0.40(± 76%)	0.14	2.0
	3B	292	2.88	0.040	4.2	1.8	4.3	0.38(± 70%)	0.16	2.0
	8B	262	2.89	0.030	4.2	2.4	5.7	0.50(± 95%)	0.10	1.8
5/20/53	5	338	2.74	0.034	2.9	2.3	0.6		0.13	2.1
	6	350	2.68	0.031	2.9	2.6	0.7		0.08	2.2
	7	403	2.68	-0.015	2.9					2.5
	8	711	2.70	-0.020	2.9					4.4
	16	525	2.70	0.070	2.9	1.2	0.3		0.13	3.2
	19	322	2.67	0.036	2.9	2.3	0.6		0.10	2.0

* 7B taken just after 6B, steady light current assumed same.

Table 7 (continued)

Date of Experiment	Picture No.	Slope $\left[\frac{(\text{s-units})^{-1}}{\text{sec}}\right]$	i (μamps)	$\frac{1}{S_o}$ $[(\text{s-units})^{-1}]$	Flash Lamp Energy $[(\text{joules})10^{-2}]$	$[I]_o$ $\left[\frac{\text{mole}}{\text{liter}}\right] 10^7$	$\frac{[I]_o}{2[I_2]}$ (%)	ϕ	$t_{\frac{1}{2}}$ (millisec)	$\left[\frac{k}{(\text{mole}^{-1}\text{liter})10^{10}}\right]$
6/29/53	8	238	3.42	0.029	2.0	2.2	2.8	0.44(±27%)	0.12	1.8
	9	240	3.42	0.020	2.0	3.3	4.1	0.64(±36%)	0.088	1.8
	10	232	3.42	0.011	2.0	5.9	7.4	1.15(±65%)	0.056	1.8
	13	206	3.45	0.020	2.0	3.2	4.0	0.63(±36%)	0.096	1.6
	14	222	3.40	0.020	2.0	3.3	4.1	0.64(±40%)	0.090	1.7
	18	211	3.45	0.013	4.2	5.0	6.2	0.55(±76%)	0.060	1.6
	19	250	3.40	0.002	4.2	33	41.3	3.66(±380%)	0.010	1.9
	20	230	3.38	0.007	4.2	9.4	11.7	1.04(±152%)	0.030	1.7
7/1/53	1	385	2.84	0.040	2.0	1.9	0.7	0.11(±30%)	0.11	2.5
	2	392	2.81	0.010	2.0	7.7	2.7	0.42(±144%)	0.025	2.5
	3	345	2.79	0.037	2.0	1.9	0.7	0.11(±34%)	0.10	2.2
	6	538	2.85	0.017	2.0	4.5	1.6	0.25(±87%)	0.035	3.5
	7	382	2.80	0.004	2.0	19	6.7	1.05(±323%)	0.010	2.5
	13	371	2.80	-0.040	4.2					2.4
	41	278	3.29	0.037	2.0	1.8	1.0	0.16(±23%)	0.16	2.1
	42	265	3.24	0.030	2.0	2.2	1.2	0.19(±29%)	0.13	2.0
	43	228	3.18	0.032	2.0	2.1	1.1	0.17(±30%)	0.14	1.7
	44	303	3.15	0.035	2.0	2.0	1.1	0.17(±32%)	0.12	2.2
	45	281	3.15	0.013	2.0	5.3	2.8	0.44(±63%)	0.060	2.0
	50	217	3.18	0.022	4.2	3.1	1.7	0.15(±40%)	0.10	1.6
	51	275	3.10	0.010	4.2	7.0	3.8	0.34(±108%)	0.035	2.0
								0.41±0.26		2.2±0.4

Average values and mean deviations

the intercept value, and therefore $[I]_o$, is much less reliable. Nevertheless, if the high values of $[I]_o$ (Table 7) for a few pictures are disregarded, there is the suggestion of a moderate change consistent with the interpretation of the data in terms of iodine atom production and recombination. This change is also indicated in Fig. 20 where the values of $[I]_o$ versus optical density show a trend in the case of 2.0×10^2 and 4.2×10^2 joule flash lamp discharges as well as with $[I_2]$ for a given flash lamp energy.

It is interesting to note that the semilogarithmic plots for the I_2 in $\underline{n}$-C_7H_{16} solutions are not linear (cf Figs. 21a and 21b). Fig. 22 is a typical reciprocal signal height versus time plot for an I_2 in $\underline{n}$-C_7H_{16} solution. Pictures showing the oscilloscope trace during recombination are shown in Figs. 23, 24, 25, and 26.

Estimation of the Primary Quantum Yield

The values for the primary quantum yield have been determined according to the procedure discussed in the preceding section on CCl_4 solutions. In the case of the $\underline{n}$-C_7H_{16} solutions there is greater uncertainty in the intercept values and, hence, the primary quantum yield. This is evident in the mean weighted deviation of $\pm$ 0.26 associated with the weighted mean value of 0.41 for $\underline{\phi}$ for the filtered flash light ($\lambda > 510$ mμ) at room temperature.

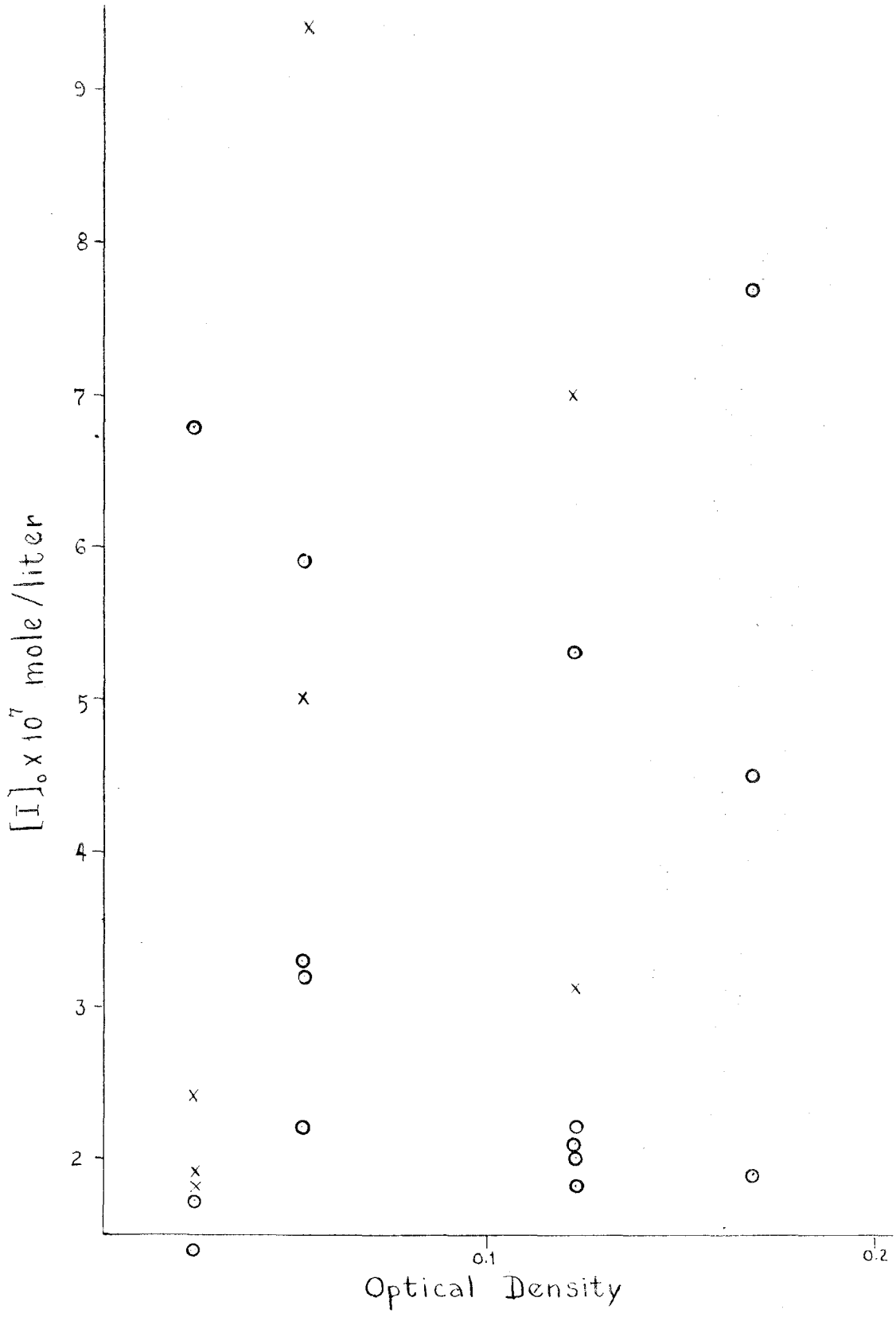

Fig. 20 Initial iodine atom concentration versus optical density of $\underline{n}$-C_7H_{16} solutions, circles are for 2.0×10^2 joule flash lamp discharges, crosses are for 4.2×10^2 joule discharges.

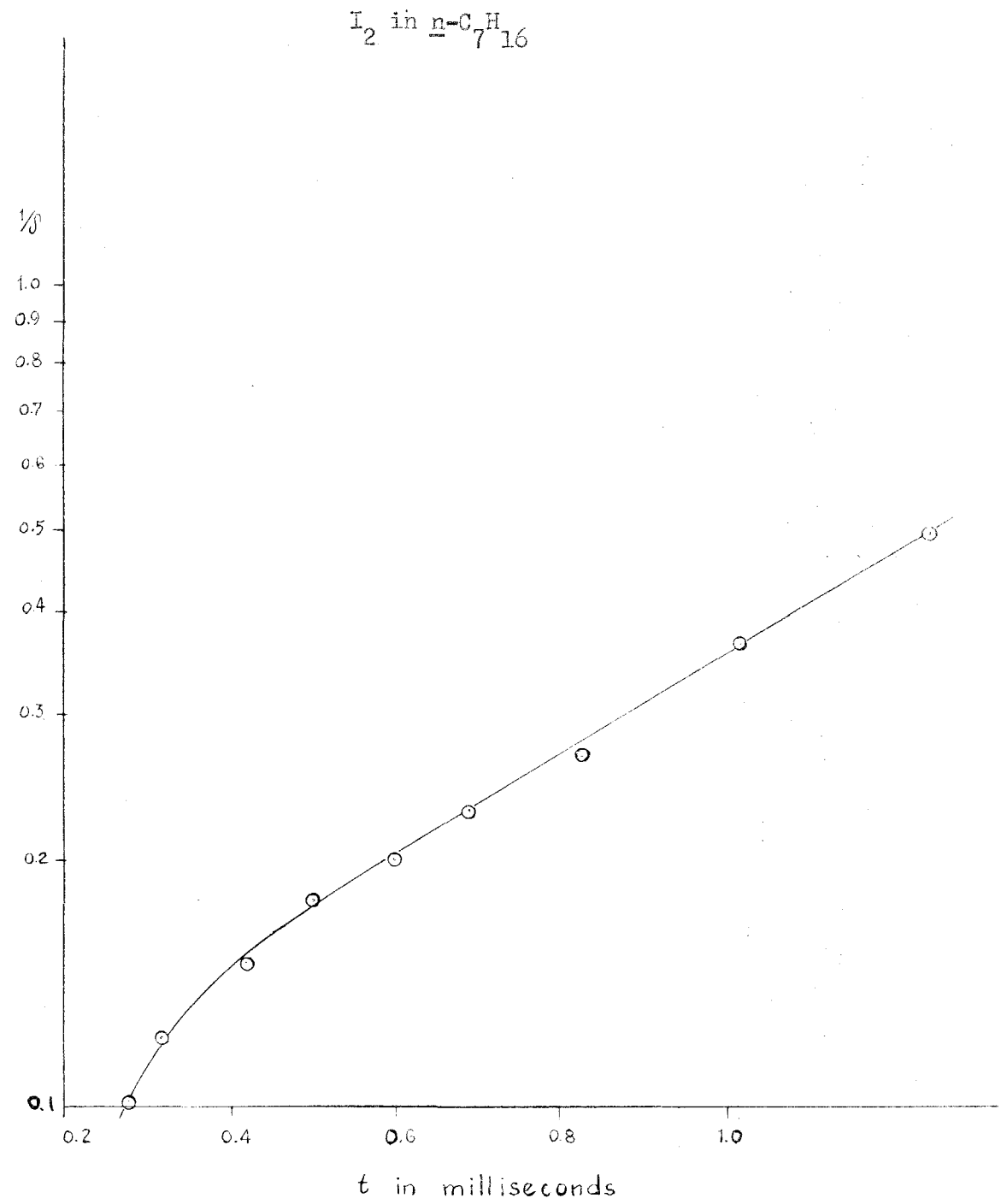

Fig. 21a Logarithm of reciprocal signal deflection versus time (picture no. 2A, 3/23/53).

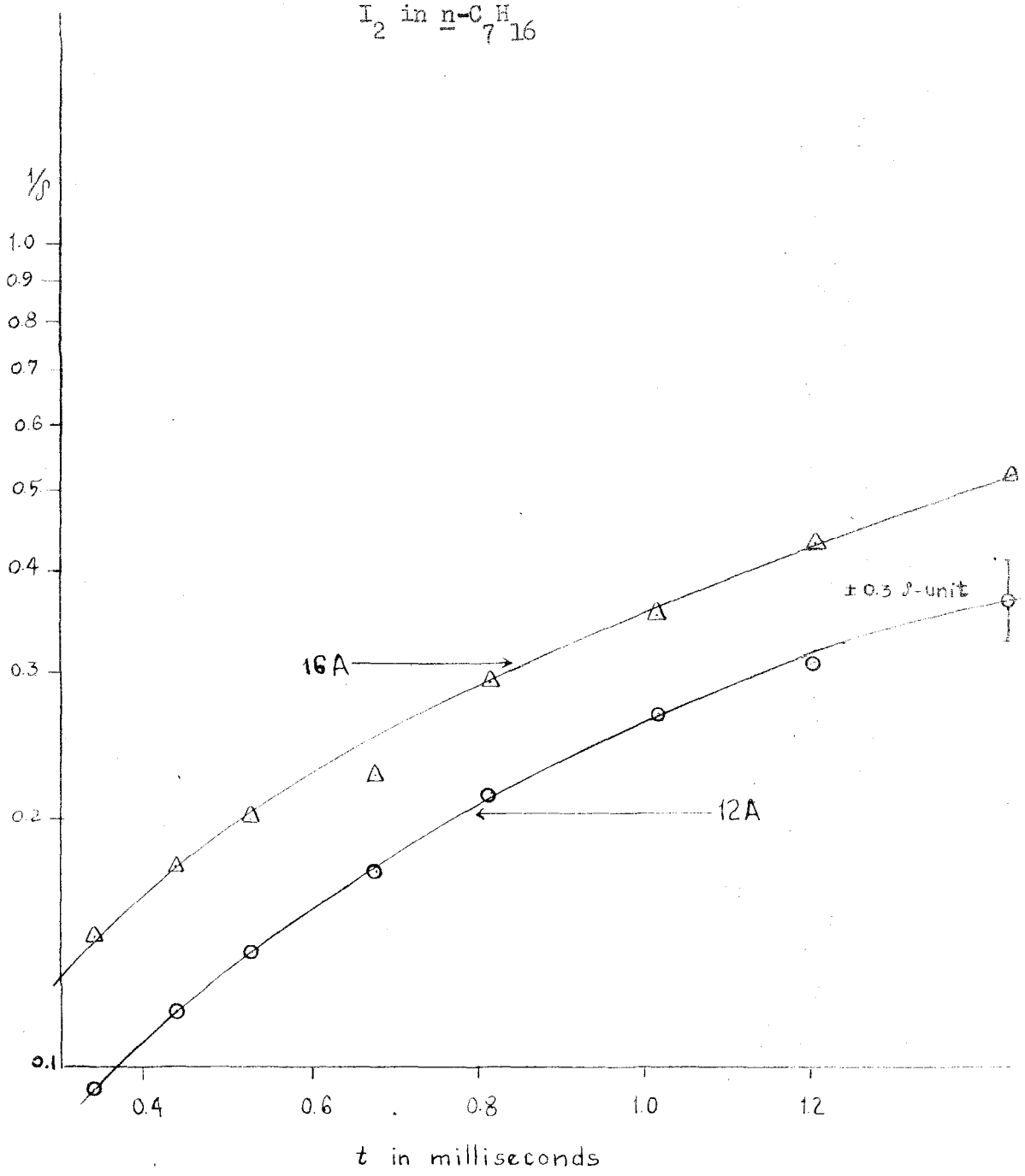

Fig. 21b Logarithm of reciprocal signal deflection versus time (pictures no. 12A and no. 16A, 4/1/53).

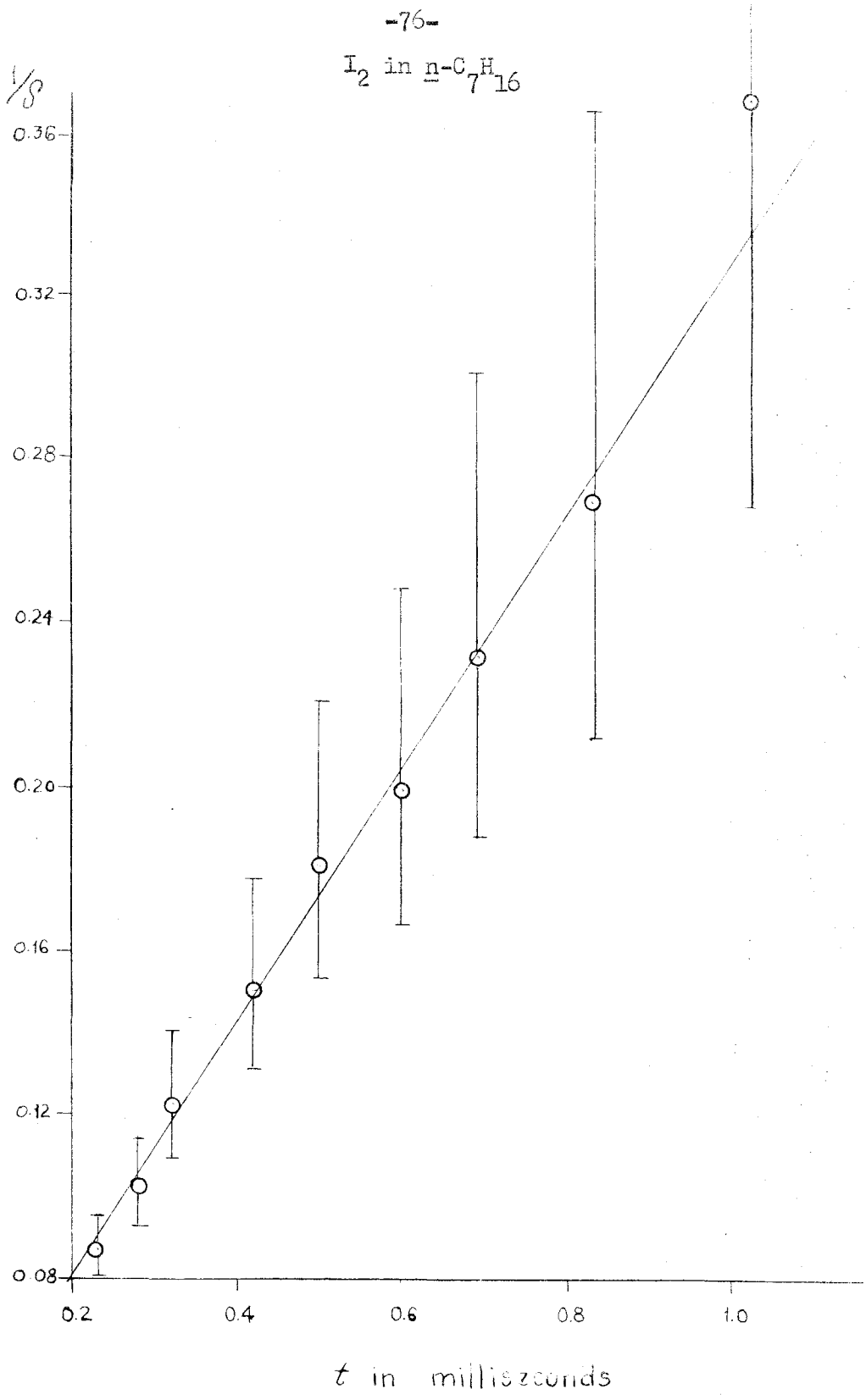

Fig. 22 Reciprocal signal deflection versus time (picture no. 2A, 3/23/53, error is ± 1 s-unit).

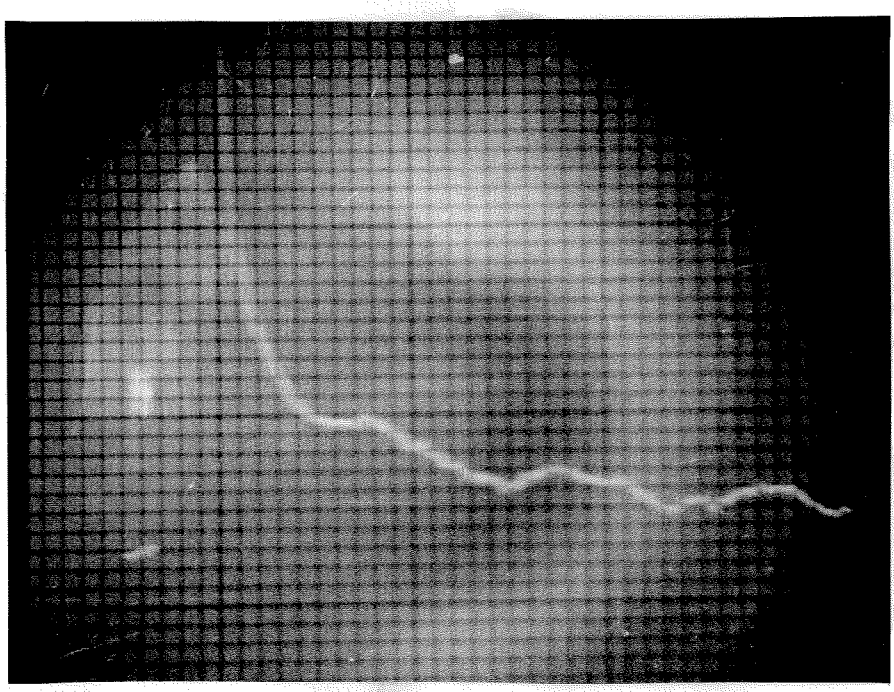

Fig. 23 Oscilloscope trace during the recombination of iodine atoms in $\underline{n}$-C_7H_{16} (picture no. 6B, 3/23/53, cf Table 7).

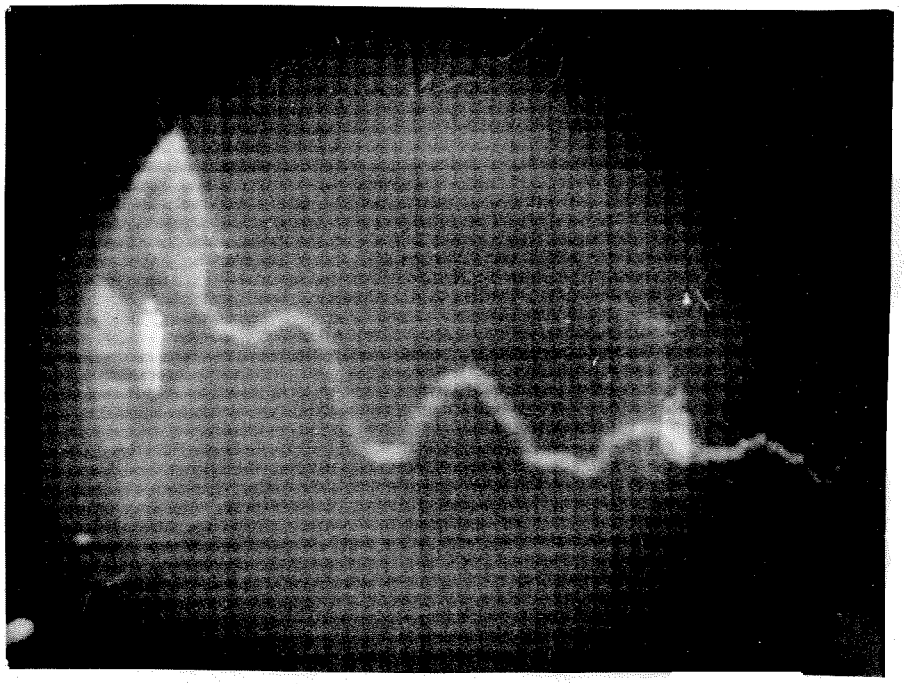

Fig. 24 Oscilloscope trace during the recombination of iodine atoms in $\underline{n}$-C_7H_{16} (picture no. 3B, 4/1/53, cf Table 7).

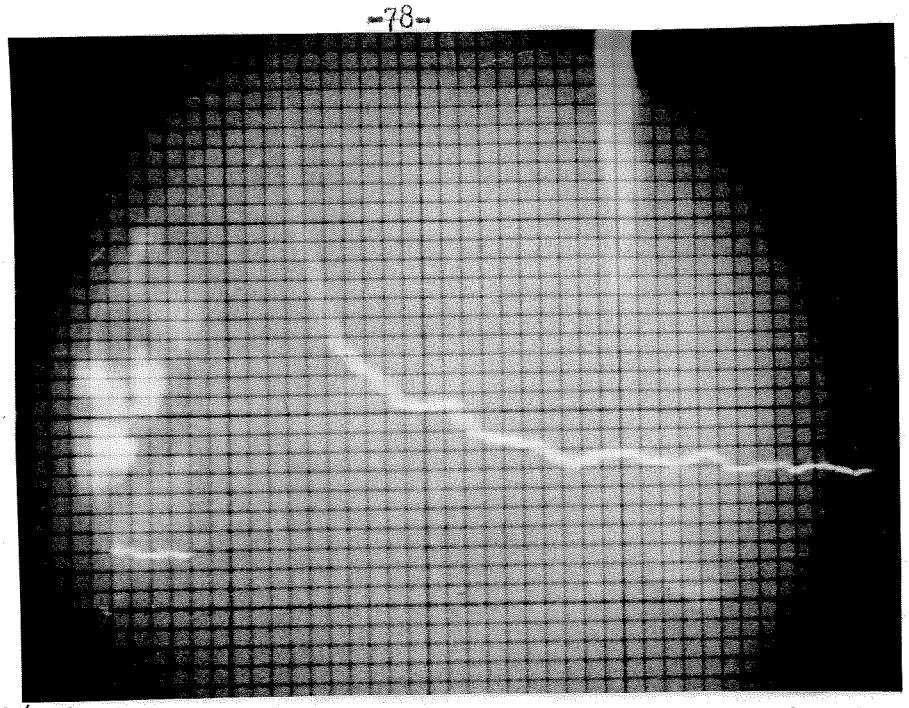

Fig. 25 Oscilloscope trace during the recombination of iodine atoms in $\underline{n}$-C_7H_{16} (picture no. 6, 5/20/53, *cf* Table 7).

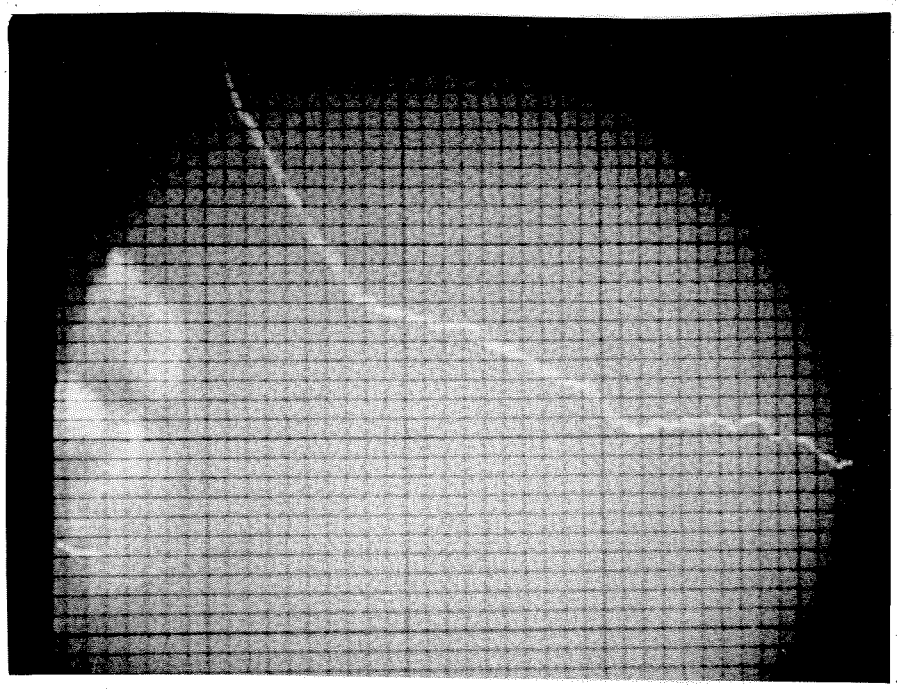

Fig. 26 Oscilloscope trace during the recombination of iodine atoms in $\underline{n}$-C_7H_{16} (picture no. 19, 6/29/53, *cf* Table 7).

5. Discussion

a. Recombination and the Quantum Yield

When iodine dissolved in inert solvents absorbs light, molecules can dissociate. However, each absorbed quantum leading to dissociation must have an energy at least that of 1.5422 ev, the dissociation energy, (6). The subsequent recombination of the iodine atoms is faciliated by the very high rate of collision of an iodine atom with solvent molecules. The numerous collisions may be considered effective in two ways:

1. If neither iodine atom from a photolyzed iodine molecule can penetrate the surrounding sheath of solvent molecules, recombination of these original partners can occur within a period of a few orders of magnitude of that of a molecular vibration. This primary recombination, discussed by Franck and Rabinowitsch (7), occurs in a time short of the minimum instrumentally-resolvable period obtainable at the present.

2. Individual iodine atoms homogeneously distributed throughout the solvent will combine whenever two of them meet while diffusing since a three-body collision is inevitable.

Although other mechanisms for the dissipation of the energy of excited molecules in solution have been suggested (7), primary recombination seems to be the only significant process accounting for the fractional quantum yields observed in these experiments (0.41 in $\underline{n}$-C_7H_{16} and 0.19 in CCl_4). As an example of one

of these discounted mechanisms, consider the reaction of an iodine atom with the solvent according to either of the equations

$$I + C_7H_{16} \rightarrow C_7H_{15}I + H \qquad (44a)$$

$$I + C_7H_{16} \rightarrow C_7H_{15} + HI \qquad (44b).$$

Reaction (44b) is the more likely of the two but it is just energetically possible at the shortest wavelength entering the reaction cell assuming the minimum activation energy to be the difference between bond energies. In the case of the equations

$$I + CCl_4 \rightarrow CCl_3I + Cl \qquad (45a)$$

$$I + CCl_4 \rightarrow CCl_3 + ICl \qquad (45b),$$

reaction (45a) is the more likely of the two although even it requires a more energetic iodine atom than can be furnished by the shortest wavelength used in these experiments. In addition, Rollefson and Libby (8) selected a system of CCl_4 and radioactive Cl_2 to irradiate. They wished to determine to what extent the reaction

$$Cl^* + CCl_4 \rightarrow CCl_3Cl^* + Cl \qquad (46)$$

occurred since this reaction should have a lower activation energy than that of reaction (45a). However, there was no detectable exchanges. Chemical interaction of the atoms with the solvent molecules in the recombination studies is unlikely on energetic grounds. The

results of the experiment cited just above suggest that only atoms with energies of at least several electron volts might form products with the solvent molecules (with a lifetime dependent on the rate of the reverse reaction).

The wavelengths absorbed by iodine molecules in these flash photolysis experiments are on the long wavelength side of the continuum. The iodine molecules are thus raised to an excited state and they dissociate in a very short time through collision with the solvent molecules. Presumably all the excited iodine molecules dissociate and the quantum yields less than unity are due solely to primary recombination. This conclusion is based on the experiments of Rabinowitch and Wood (4) who found for mixtures of I_2 vapor in several hundred mm pressures of gases quantum yields of unity in both the continuum and the band region. They also observed that dissociation generally occurs at the first collision except in the case of the very light body He where 10 or more collisions are necessary.

The diffusion coefficients x 10^5 for iodine molecules in $\underline{n}$-C_7H_{16} and CCl_4 at 25° C are 3.42 and 1.50 cm^2/sec, respectively (9). The ratio of 2.3 for these diffusion coefficients is nearly the same as the corresponding one for the values of the quantum yield. This suggests that a rough correlation may be made between the quantum yield and the ability of the atom to diffuse through the surrounding sheath of solvent particles, at least for photolysis at

long wavelengths where the kinetic energy of the atom is not significantly greater than thermal energies.

Rabinowitch and Wood (10) have discussed collisions in solutions. They concluded that collisions occur in sets in closely-packed media. A set consists of a number of collisions in a short time between two solute particles with a considerably longer interval between the occurrence of another collision-set when the solute particles separate from the first set. A pair of atoms which have just dissociated have the probability of $1/\bar{n}$ of escaping recombination with each other where $\bar{n}$ is the average number of collisions in a set (recombination is assumed to occur on the first collision in liquids because of the numerous collisions with solvent molecules). Rabinowitch and Wood (10) thought that $\bar{n}$ was approximately 2 for CCl_4. Their calculation was based on the density of CCl_4, and for C_7H_{16} with half the density, $\bar{n}$ would be approximately 1. The ratio of these probabilities of escape of primary recombination agrees with that for the quantum yields. However, as Rabinowitch and Wood (10) point out, with excess kinetic energy the dissociated particle can penetrate the surrounding sheath of solvent particles providing it is heavier than the solvent molecules. The conservation of momentum requires that the dissociated particle be reflected by the solvent molecules no matter how high the kinetic energy of the particle may be as long as the solvent

molecule has the greater mass. Thus, the quantum yield in CCl_4 is not expected to vary with wavelength* while that in C_7H_{16} (or C_6H_{14}) should. A difference of nearly 40% in the quantum yields at 436 mμ and 578 mμ for I_2 in C_6H_{14} have been reported by Zimmerman and Noyes (2). Their values are 0.59 and 0.37, respectively, at 25° C. The latter value is in good agreement with that found in the present experiments. In a more recent paper Lampe and Noyes (11) find the quantum yields at 436 mμ for iodine in C_6H_{14} and CCl_4 at 25° C to be 0.66 ± 0.04 and 0.14 ± 0.01, respectively. With this more precise value for the C_6H_{14} solutions and the ratio of 0.62 for the quantum yield at 578 mμ to the quantum yield at 436 mμ in the same solvent found by Zimmerman and Noyes (2) who measured stationary rate constants with the same solutions at different wavelengths, the calculated value of the quantum yield at 578 mμ is 0.41. This value is precisely the weighted average value obtained in the present studies. However, this close agreement is purely fortuitous in view of the assumptions involved in the calculation of the value in these studies. In qualitative agreement with expectations and the preceding experimental work are the results of Tamblyn and Forbes (12). They found the ratio of quantum yields at 4358Å, 5461Å, and 5780Å to be 1:0.29: 0.27 during the photo-iodination of diiodoacetylene in hexane at 0° C. In contrast, smaller differences between the quantum yields at long and short wavelengths were found by Dickinson (13) for iodine during the iodine

---

* This is assuming no chemical reactions between the dissociated particles and the solvent.

sensitized decomposition of ethylene iodide in CCl_4 at 76.6° C. His ratios for the quantum yields at 4358Å, 5461Å, and 5780Å were 1:0.87:0.75.

Furthermore, the stationary concentration of atoms in an irradiated solution is given by the rate of their production times their average life. Since the rate of production is proportional to $1/\bar{n}$ and the average life, to $\bar{n}$, the concentration is independent of the primary recombination and the photostationary state experiments cannot furnish any information about this process. The rough quantum yield data obtained in the present recombination studies do , however, illustrate the flexibility of the flash photolysis technique, and refinement of the experiments should permit extensive and precise studies in the photochemistry of solutions.

b. The Rate Constants

The data obtained in this study have been consistently interpreted with the second order rate equation for the recombination of iodine atoms (cf equation (4)). The non-linear semi-logarithmic plots of the reciprocal signal heights versus time for the $\underline{n}$-C_7H_{16} solutions (21a and 21b) suggest the inapplicability of a first order rate expression. However, the same representation of the data from the CCl_4 solutions (Figs. 13, 14, and 15) provides linear plots, as previously mentioned. In these solutions the rate of disappearance of iodine atoms could be considered simply proportional to their concentration. A second order expression, however, is more appropriate for the analysis of the data than is the first order for the following

reasons:

1. The values of the initial iodine atom concentrations as determined by extrapolation to $\underline{t} = o$ on the plots of reciprocal signal heights versus time are clearly proportional to the energy of the flash lamp discharge (cf Figs. 10 and 11). The intercept values on the semi-logarithmic plots do not indicate this relation.

2. Figs. 16a, 16b, and 20 based on values obtained with the second order rate expression illustrate the direct variation of the initial iodine atom concentration with the molecular iodine concentration. This relation is not demonstrable with the intercepts of the semi-logarithmic plots.

3. The ratio of 2.3 previously mentioned for the diffusion coefficients for iodine in n-heptane and CCl_4 may be compared to the ratio of 3.1 for the second order rate constants for recombination in these respective solvents since the recombination process is presumably diffusion controlled. The approximate agreement may be considered as an argument in favor of the second order rate constant since the ratio of the first order rate constants is essentially unity.

The coincidental fit of the data for CCl_4 solutions to semi-logarithmic plots is not too surprising since, according to the second order rate expression, the slope of the logarithm of the reciprocal signal height versus time curve should change by a factor of about 5 during the observational period in the case of $\underline{n}\text{-}C_7H_{16}$ solution while the change in slope over the same time interval in the case of CCl_4 solution with its much larger signals should be less than 2.

When the values of $[I]_s / q_a^{\frac{1}{2}}$ (in the range 400-580 mμ) determined by Rabinowitch and Wood (1) are averaged, one obtains

$1.6\ (\pm\ 0.6) \times 10^5$ and $1.0(\pm\ 0.2)10^5$ $(\text{sec atom/ml})^{\frac{1}{2}}$ for iodine in C_6H_{14} and CCl_4, respectively. The error is the mean deviation. When these values are combined with the present quantum yields (cf equation (5)), the rate constants for recombination are 0.96×10^{10} and 1.1×10^{10} in mole^{-1} liter sec^{-1}, respectively. The values obtained by Lampe and Noyes (11) using their quantum yields and the corresponding $[I]_s / q_a^{\frac{1}{2}}$ averages given above were 1.6×10^{10} and 0.84×10^{10} mole^{-1} liter sec^{-1} at 25° C. The value calculated by Zimmerman and Noyes (2) for the rate constant for recombination in hexane combining their data and those of Rabinowitch and Wood (1) was 1.1×10^{10} mole^{-1} liter sec.^{-1}

The rate constant for n-C_7H_{16} reported in the present experiments, 2.2×10^{10} mole^{-1} liter sec^{-1}, may be too large by 10-20% in view of the tendency for the higher optical density n-C_7H_{16} solutions to always furnish higher (and more erratic) rate constants. However, in view of the difficulty, inherent in all of these various experimental techniques, in obtaining precise measurements, the agreement among the various values of the rate constants (including the value 0.72×10^{10} mole^{-1} liter sec^{-1} for iodine in CCl_4 at room temperature obtained in the present studies) is considered to be good.

6. References

1. E. Rabinowitch and W. C. Wood, Trans. Faraday Soc. 32, 547 (1936).

2. J. Zimmerman and R. M. Noyes, J. Chem. Phys. 18, 658 (1950).

3. H. A. Benesi and J. H. Hildebrand, J. Amer. Chem. Soc. 71, 2703 (1949).

4. E. Rabinowitch and W. C. Wood, J. Chem. Phys. 4, 358 (1936).

5. A. Wigand, Z. Phys. Chem. 77, 423 (1911).

6. A. G. Gaydon, "Dissociation Energies and Spectra of Diatomic Molecules," Dover Publications, Inc., N. Y., 1950, p. 65.

7. J. Franck and E. Rabinowitsch, Trans. Faraday Soc. 30, 120 (1934).

8. G. K. Rollefson and W. F. Libby, J. Chem. Phys. 5, 569 (1937).

9. R. H. Stokes, P. T. Dunlop, and J. R. Hall, Trans. Faraday Soc. 49, 886 (1953).

10. E. Rabinowitch and W. C. Wood, Trans. Faraday Soc. 32, 1381 (1936).

11. F. W. Lampe and R. M. Noyes, J. Amer. Chem. Soc. 76, 2140 (1954).

12. J. W. Tamblyn and G. S. Forbes, J. Amer. Chem. Soc. 62, 99 (1940).

13. R. G. Dickinson, Chem. Rev. 17, 413 (1935); R. G. Dickinson and N. P. Nies, J. Amer. Chem. Soc. 57, 2382 (1935).

PART II

Some Studies of the Trace Quantities of Lead, Uranium, and Thorium in Marine Carbonate Skeletons

1. Introduction

The association of small quantities of elements with a particular matrix or host substance may reveal information concerning the tolerance of the matrix toward these elements, the environment in which the matrix formed, and the subsequent history of the system. From this point of view the calcium carbonate skeletons deposited by marine animals may be geochemically significant. They are a major source of the carbonate deposits of the earth and are present throughout a span of the sedimentary record which represents more than a tenth of the age of the earth. The extensive distribution in time and space of the marine carbonate skeletons suggests the suitability of this phase for investigations of coprecipitated elements. An example of a geochemically significant study of this type has been recently provided by Lowenstam (1) who found an indirect correlation of the strontium content of shells with their precipitation temperatures. This content increases with increasing aragonite percentage which is temperature dependent in the group of shells. While elements similar to calcium such as magnesium and strontium may be incorporated in the calcium carbonate lattices in percent quantities, the significance of elements present in amounts of the order of a thousand times smaller should not be neglected. Trace amounts of the heavy metals lead, uranium, and thorium can be isolated and studied

through recently developed techniques (2,3,4,5). These elements have been selected for study in connection with carbonate skeletons because analyses for these trace elements in shells can furnish the following information:

1. The concentrations of these trace elements.

2. The ratios of these concentrations as an approximation to the relative amounts of the elements present in sea water.

3. The isotopic composition of the lead in the ocean.

The third factor in the preceding outline deserves special emphasis. Important questions concerning the distribution of lead in the ocean may be answered by isotopic analyses of appropriately selected samples. This type of investigation has been initiated by Patterson, Goldberg, and Inghram (6) who examined three Pacific Ocean sediments. The isotopic ratios of one of these samples, the Lomita marl which formed near shore, deviate somewhat from those for the two deep ocean samples. This discrepancy may be due to acid leaching of a mineral in the Lomita marl with a nonrepresentative lead since the isotope ratios for the other two specimens, red clay and a manganese nodule collected hundreds of miles apart, are essentially the same and suggest a widespread uniformity in the isotopic composition of lead in ocean water.

A uniform isotopic composition for the lead in the ocean implies that circulation of ocean water is extensive and thoroughly mixes the water. If this has been the case throughout the existence of the ocean, lead in the geochemical cycle which has been withdrawn

from the ocean and "fossilized" in marine precipitates should vary in isotopic composition with the age of the precipitate. The lead in the older samples, excluding that produced in the samples through its radioactive progenitors, should have less lead of radiogenic origin than the lead in recent precipitates since the lead weathering out of the rocks and entering the ocean continuously increases with time in the end products of the radioactive decay of uranium and thorium. The variation in isotopic composition with time may eventually be demonstrated in marine calcium carbonate. However, the selection of representative samples still poses a problem as the present studies reveal.

A procedure which is described in the following section has been developed for the isolation of microgram quantities of lead, uranium, and thorium for colorimetric and mass spectrometric analyses from a single 200 gm sample of shell. Following this outline are some data obtained through these techniques. Oceanic lead analyses are extended to the Atlantic Ocean and the data are discussed in reference to the three previously outlined geochemical factors.

2. Isolation of the Trace Elements

a. Minimization of Contamination

The isolation of a trace element whose concentration in a substance is in the neighborhood of 1 ppm requires that every precaution be exercised to reduce contamination. Comtamination from

the air, apparatus, and reagents is a serious problem.

The laboratory in which the work described below was performed was specially designed for the analyses of trace amounts of lead. The use of lead and its compounds was avoided in the preparation of the laboratory. The washed and electrostatically filtered air of the laboratory is kept at a slightly higher pressure than the air outside.

All the glassware (Pyrex) is carefully washed in KOH and HNO_3 and finally rinsed with quadruply distilled water. Parafilm, a self-sealing sheet plastic, is used to cover the glassware and solutions. Evaporations in the stainless steel hoods are performed in glass containers in which a positive pressure of dry nitrogen gas is maintained. Therefore, the eddies in the hood draft are unlikely to introduce dust raised in the laboratory into either the solution in the beaker or its surrounding glass evaporation unit. These procedures to insure the purity of the sample during chemical manipulation have also been discussed by Tilton et al (5).

Reagents such as HCl, NH_4OH, and $(NH_4)_2CO_3$ have been prepared by bubbling the gas from tanks of the liquid or gas through glass filter frits and Tygon and glass tubing into quadruply distilled water. Cp HNO_3 and triply distilled water were redistilled in quartz. Organic solvents such as hexone* and $CHCl_3$ were extracted three times with equal volumes of 2N HCl, each acid extraction being followed by a sufficient number of rinsings with water to remove traces of the acid.

---

* 4-Methyl-2-pentanone

b. Treatment of the Sample

Recent shell material has been used to develop the procedure described below for the isolation of the trace constituents lead, uranium, and thorium. The steps in this analysis are discussed in the following outline.

A. Preparation of the sample for the isolation of individual elements.

1. To minimize the inclusion in the analysis of extraneous substances associated with the shell, the surfaces are ground off with silicon carbide wheels (made by Mizzy, Inc., N. Y.).

2. A 220 gm sample is washed with 2N HCl three times with three water rinsings after each acid washing and dried at 110° C.

3. The sample weighing ca 200 gms is weighed out and baked in a muffle furnace at about 400° C for at least 48 hrs. This step is to carbonize the organic material in recent shells. When the sample has not been heated long enough, dissolution is hindered by the formation of a slowly collapsing foam.

4. The sample is dissolved in 6N HCl and spike solutions are added. Typical spikes and their purposes are as follows:

(a) About 45 mg of Fe^{+3} in solution is added as a carrier to bring down the trace amounts of lead, uranium and thorium.

(b) A Pb^{210} solution with about 7000 counts/min is added to determine lead yield.

(c) Approximately 30 micrograms of Pb^{206} in solution is added to determine the lead concentration by isotope dilution.

(d) Approximately 5 micrograms of Th^{230} in solution is added to determine the thorium (Th^{232}) concentration by isotope dilution.

(e) Approximately 6 micrograms of U^{235} in solution is added to determine the uranium concentration by isotope dilution.

5. The solution, black from suspended carbon, is filtered through small wads of glass wool.

6. The solution is heated on a hot plate and ammonia gas is bubbled in until a pH between 7 and 8 is reached. Organic material and the concentrated calcium solution may inhibit the iron hydroxide precipitation at this stage and account for the low yields observed as well as the slowness of precipitation with smaller amounts of Fe^{+3}.

7. The supernatant is discarded after the precipitate is centrifuged down. It is washed twice with water with tests to insure that the pH is no less than 7 and redissolved in a ml or so of HNO_3 and a few ml of water.

B. Separation of the uranium.

1. 5M $(NH_4)_2CO_3$ solution is carefully added until a precipitate forms. Two or three drops of carbonate solution are added in excess (a large excess should be avoided otherwise some of the iron may be carried over with the extracted uranium).

2. After centrifuging, the uranium-containing super-

natant is evaporated down and heated to destroy $(NH_4)_2CO_3$. The precipitate from the centrifugation is retained for thorium and lead extractions.

3. The solids are dissolved in a small amount of HNO_3 and 10-15 ml of a saturated NH_4NO_3 solution are then added. The pH is adjusted to 2 or slightly greater with HNO_3 and ammonia and this solution is extracted with three 15 ml. portions of hexone.

4. The combined portions of hexone are extracted with three 15 ml. portions of 1-2% HNO_3.

5. The combined nitric acid solutions containing the extracted uranium are evaporated down and heated to eliminate NH_4NO_3. If the residue is not negligible (indicating carry-over of contaminants such as iron), the above hexone and HNO_3 extractions are repeated. The uranium is transferred with a few ml of concentrated HNO_3 to a 5 ml beaker and this solution evaporated to dryness. The sample is now ready for mass spectrometric analysis.

C. Extraction of thorium.

1. The precipitate from step B2 is dissolved in 1 ml of conc. HNO_3 and 10-15 ml of saturated NH_4NO_3 solution are added. This solution is extracted with three 15 ml portions of hexone and reserved for the isolation of lead. The combined portions of hexone are in turn extracted with three 15 ml portions of 1-2% HNO_3.

2. The combined nitric acid solutions containing the thorium are evaporated down and heated to eliminate NH_4NO_3. If the residue does not indicate that another extraction is necessary because of iron carry-over, the thorium is transferred with a few ml of conc. HCl* to a 5 ml beaker. This solution is evaporated down and then a few ml of HNO_3 are added. A final evaporation furnishes the sample for mass spectrometric analysis.

D. Extraction of lead.

1. Conc. NH_4OH is added to the solution from which the thorium is extracted in step C-1 until a pH between 7 and 8 is obtained. The resulting iron hydroxide precipitate containing the lead is centrifuged. After the supernatant is discarded the precipitate is dissolved in a few drops of HNO_3 and 20 ml of 25% ammonium citrate solution are added.

2. This solution is made basic (pH 8) with NH_4OH and is immediately extracted with a few milligrams of dithizone in 40-50 ml $CHCl_3$.

3. The dithizone phase is extracted with 25 ml 1-2% HNO_3.

4. To the lead-containing nitric acid solution is added 5 ml of a 2% KCN, 20% conc. NH_4OH solution and then 2.5 ml portions of a solution of $CHCl_3$ containing 6 mg of dithizone/liter

---

* Conc. HCl is recommended here since in the preparation of the Th^{230} spike solution, the ThO_2 furnished by the Oak Ridge National Laboratory was found to be unaffected by hot conc. HNO_3 while dissolution was rapid in hot conc. HCl.

are used to extract the lead. Each portion is equivalent to approximately 5 micrograms of lead. An estimate of the amount of lead present can be made by means of the color change, green dithizone solution to pink lead dithizonate solution. Bismuth and thallium can interfere; however, their contribution in these analyses is considered negligible.

5. The lead dithizonate solution is evaporated down in a 5 ml beaker. A ml of conc. HNO_3 and one of conc. $HClO_4$ are added and this solution evaporated to complete dryness. The sample is now ready for mass spectrometric analysis.

In this way a single 200 gm sample of marine carbonate may be analyzed for trace amounts of uranium, thorium, and lead. The initial carbonizing and filtering step is not necessary for sufficiently ancient specimens such as the Mississippian Spirifer from New Mexico.

The carbon filtered out can be oxidized with hot conc. HNO_3. The solution is a red-brown color suggesting that not all of the organic material has been carbonized. However, organic compounds that might contain or might be able to complex the heavy metals are most likely absent after this pyrolysis and any absorption effects on carbon particles should be of no concern because of equilibration between them and the spiked acid solution. Yields seem to be around 25% for lead and probably are about the same for uranium and thorium.

3. Data

Table 1 summarizes the descriptions of the three carbonate samples selected for analysis. Several shells of Strombus gigas, each weighing 1-2 kgm, were kindly donated for these experiments by Dr. Heinz Lowenstam of the Geology Department. He collected these large present-day gastropods in Castle Harbor, Bermuda. The belemnites were furnished by Dr. H. C. Urey, University of Chicago. The Spirifers generally have 2-3 gms of shell per specimen . They were collected by the writer with the assistance of Dr. L. C. Pray, of the Geology Department, in New Mexico.

The extraction of lead from a 10gm sample of each of the three specimens listed in Table 1 indicated in visual colorimetric comparison less than 1 ppm in each case. If a yield of 25% is assumed for these extractions the lead content for these shells is less than 0.4 ppm. The lead from a 120.7 gm sample of Strombus gigas was extracted and a precise comparison was made in the Beckman model DU spectrophotometer at 510 mμ between this lead solution and the lead in 2 and 4 microgram standard solutions according to the dithizone colorimetric procedure used by Patterson (4). Linear interpolation between the optical densities for the standard solutions and the observed density of the Strombus lead solution indicated 3.3_5 micrograms of lead.* The yield in this

---

* See paragraph D-4 in the preceding section concerning chemical procedure.

Table 1

Description of Shells Studied

Species or Genus	Locality	Formation	Age	Shell Material
Strombus gigas (a gastropod)	At Castle Roads just inside Castle Harbor (by the eastern outlet of the harbor), Bermuda.	Grassy, carbonate-sand, ocean bottoms, 18 ± 3 feet deep.	Recent	Aragonite
Cylindroteuthis puzosiana (a belemnite cephalopod)	Fletton, near Peterborough, Northamptonshire, England.	Oxford clay	Upper Jurassic	Calcite*
Spirifer (a brachiopod)	S. E. flank of Almo Peak, SE¼ sec. 25, T.16S., R.10E., Otera Co., New Mexico.	Uppermost Dona Ana member of the Lake Valley.	Uppermost lower Mississippian	Calcite**

* Oxygen isotope data indicate little if any exchange with fresh water.

** Oxygen isotope data indicate only a little exchange with fresh water although in thin section the calcite is coarsely recrystallized.

extraction was 15%; therefore, the lead concentration is 0.19 ppm in the Strombus gigas. The accuracy of this determination is considered to be within ± 20%. Some error occurs because of changes in lead concentration due to $CHCl_3$ evaporation. Error of the order of a few percent can be introduced by the yield factor.

The sample of lead isolated from the Strombus gigas as well as the uranium samples discussed in the following paragraph were analyzed mass spectrometrically. The atomic ratios for the lead are the following:

$$\frac{Pb^{206}}{Pb^{204}} = 18.02 \qquad \frac{Pb^{207}}{Pb^{204}} = 15.37 \qquad \frac{Pb^{208}}{Pb^{204}} = 37.17$$

Uranium was isolated from both the Strombus gigas sample and a control solution. The control received essentially the same treatment as the Strombus gigas in respect to the amount and purity of reagents and chemical processing. Both the sample and the control had been spiked with U^{235}. The few tenths of a microgram of uranium isolated from the Strombus gigas was found to have by mass spectrometric analysis the atomic ratio $U^{235}/U^{238} = 0.736 \pm 0.010$; the uranium extracted from the control, $U^{235}/U^{238} = 220 \pm 10$. The difference between these two ratios is attributed to dilution of the added U^{235} by the uranium present in the 215 gm sample of shell material. The concentration of uranium calculated from these data is 0.036 ppm. This value is believed to be accurate to within ±0.002 ppm.

Table 2 summarizes the analytical data discussed above.

Table 2

Summary of Analytical Data

Specimen	Lead Concentration (ppm)	Lead Isotopic Composition $\frac{Pb^{206}}{Pb^{204}}$	$\frac{Pb^{207}}{Pb^{204}}$	$\frac{Pb^{208}}{Pb^{204}}$	Uranium Concentration (ppm)
Strombus gigas	0.19 ± 0.04	18.02	15.37	37.17	0.036 ± 0.002
Cylindroteuthis puzosiana	<1	----------			----------
Spirifer	<1	----------			----------

4. Discussion

The concentrations of lead and uranium, 0.19 and 0.036 ppm, respectively, found in the Strombus gigas shell are, in general, low compared to the amounts believed present in other marine sediments (6, 7, 8, and 9). For example, Patterson (see reference 8) found an average lead concentration of 1.2 ppm with a mean deviation of ± 0.5 ppm in the acid soluble portion of 6 Paleozoic and pre-Cambrian carbonate rocks and an average uranium content of 1.3± 0.7 ppm has been reported (9) for 4 carbonate rocks. Besides the larger concentrations given for these rocks, the ratio of lead to uranium appears to be near unity instead of over 5 as in the Strombus shell. These rocks contain mineral phases other than calcium carbonate* which may provide acid-soluble lead and uranium. For example, 5% of such phases (a typical value for the insoluble residue of these rocks) would need to average only 20 ppm of acid-soluble lead and 25 ppm of uranium to account for these differences in concentrations. Also lead and uranium may have been gradually added to these rocks from ground water. In view of the low concentrations for lead and uranium in the Strombus shell and the 0.31 ppm of lead reported (6) for the Lomita marl, marine calcium carbonate evidently contributes very little of these heavy metals to sediments.

---

* The lead concentration in the calcitic brachiopod as well as the belemnite cannot be significantly greater than that for the aragonite phase.

In ocean water the mass ratio of lead to uranium seems to be approximately 3 (10)* and this is in reasonable agreement with the ratio of 5 found in the aragonite. The apparent strontium to lead ratio of 3×10^3 for ocean water (10) is also in good agreement with the value of 5×10^3 from 0.09% strontium (spectroscopically determined) in the Strombus shell and the observed lead content. However, the comparison between quantities present at low level concentrations and those present in per cent quantities must be critically viewed. For example, mass action effects may well become negligible compared to discrimination by the crystal structure for solutes whose concentrations are within an order of magnitude or two of that of the host as is evidently the case for strontium and magnesium in the calcite and aragonite structures. In ocean water magnesium is about 100 times more abundant than strontium (10). Yet in aragonite magnesium (12) is nearly at the same concentration level as strontium (1). In the case of calcite, however, the magnesium is favored; its concentration (as $MgCO_3$) may rise to 10-15% (12) and the strontium carbonate drops to a few tenths of a per cent (13).** Nevertheless, the interesting fact

---

* A ratio of about 2 is obtained using the average value of 2.49 ppm of U found in Pacific Ocean samples by Stewart and Bentley (11).

** Odum (14) has found higher values.

remains that the ratios of the amounts of calcium*, strontium, lead, and uranium in ocean water are approximately the same as the ratios for these elements in aragonite.

The isotopic ratios observed for the lead of the Strombus gigas appear unique. All the ratios are lower than those for the Pacific Ocean sediments (6). This difference indicates less admixing of radiogenic lead and primeval lead. There is a formal similarity to the Strombus lead isotope ratios and those of a galena sample from the Argentine mines, San Juan Co., Colo. The values found for this lead ore by Stieff, Stern, and Milkey (16) are the following:

$$\frac{Pb^{206}}{Pb^{204}} = 18.06, \quad \frac{Pb^{207}}{Pb^{204}} = 15.34, \quad \frac{Pb^{208}}{Pb^{204}} = 37.03$$

The isotopic composition of lead in the Atlantic Ocean may differ significantly from that for lead in the Pacific Ocean in view of the degree of isolation of these two major ocean bodies and the difference in the major portion of the rocks bounding these two oceans. The Pacific Ocean is ringed with late volcanic rocks while much of the drainage into the Atlantic Ocean is through Paleozoic and pre-Cambrian terrain. However, isotope data from the Essonville granite (5) and Paleozoic and pre-Cambrian carbonate

---

* Lowenstam (15) cites the range of 0.0129 to 0.0138 for the values of the strontium-calcium ratio for ocean water around reefs at the Bermuda Islands and Guam. These are apparently atomic ratios.

rocks (8) may be averaged and considered representative of lead of eastern North America. The average ratios and mean deviations are the following:

$$\frac{Pb^{206}}{Pb^{204}} = 20.6 \pm 1.2, \quad \frac{Pb^{207}}{Pb^{204}} = 15.7 \pm 0.3, \quad \frac{Pb^{208}}{Pb^{204}} = 39.7 \pm 2.8$$

Although admittedly derived from a small number of examples, these data suggest that the Strombus lead should have a greater radiogenic component than it has in order to be representative of Atlantic Ocean lead.

The Strombus lead is most likely a non-representative oceanic lead.

The Castle Harbor water in which the Strombus grew may have been contaminated by non-indigenous lead. A large American army airfield lines the north border of the harbor. This boundary was formed by interconnecting a number of small islands by dredging fill down to a depth of 50 feet into Tertiary formations along the northern half of Castle Harbor. Oil and gasoline from storage tanks along the shore seep into the harbor (17). The presence of many foreign substances may have modified the isotopic composition of the lead in the water. The platform beneath the Bermuda Islands is composed of volcanic rock which probably formed during late Tertiary (18). During the dredging operations mentioned above altered volcanic debris was encountered. Lead-bearing particles

of the volcanic rock may have been included in the shell of the Strombus.

The inclusion of particles with acid-soluble lead and uranium invalidates the comparision of lead to uranium ratios in the shell and the ocean water as discussed above. However, lead incorporated in the shell may have been selected from lead dissolved in the water. If the harbor water with a small amount of lead of typical oceanic composition were exposed through the dredging operations to labile lead in the weathered volcanic fragments, the composition of the lead in solution would become through exchange essentially that of the volcanic lead since the ratio of lead concentrations in these two respective phases is generally of the order of 10^{-3} (10 and 5). A plateau basalt from the Shoshone lava field, Lincoln County, Idaho, analyzed by Patterson (19) coincidentally resembles in isotopic composition the lead from the Strombus shell. The atomic ratios for this basalt are

$$\frac{Pb^{206}}{Pb^{204}} = 18.12, \quad \frac{Pb^{207}}{Pb^{204}} = 15.45, \quad \frac{Pb^{208}}{Pb^{206}} = 38.08.$$

The agreement with the Strombus lead in this case is not as good as with the lead ore cited above since the basalt has more thorium end product, Pb^{208}.

The exchange between the small amount of lead in the ocean water and the relatively large amount in weathering volcanic rocks

may require millions of years before the composition in the weathering rock becomes typical of ocean lead. In this case the dredging in the harbor-home of the Strombus would be incidental. Thus, carbonate samples selected in the vicinity of volcanic islands may not contain representative oceanic lead but may have lead from the volcanic rocks.

5. References

1. H. A. Lowenstam, Proc. Nat. Acad. Sci. 40, 39 (1954).

2. R. J. Hayden, J. H. Reynolds, and M. G. Inghram, Phys. Rev. 75, 1500 (1949).

3. G. R. Tilton, "The Distribution of Trace Quantities of Uranium in Nature," PhD dissertation, Department of Chemistry, University of Chicago (1951).

4. C. Patterson, "The Isotopic Composition of Trace Quantities of Lead and Calcium," PhD dissertation, Department of Chemistry, University of Chicago.

5. G. R. Tilton, C. Patterson, H. Brown, M. Inghram, R. Hayden, D. Hess, and E. Larsen Jr., "The Isotopic Composition and Distribution of Lead, Uranium, and Thorium in a Pre-Cambrian Granite," unpublished manuscript.

6. C. C. Patterson, E. D. Goldberg, and M. G. Inghram, Bull. G S A 64, 1387 (1953).

7. W. D. Urry, Amer. J. Sci. 239, 191 (1941).

8. H. S. Brown, Progress Rep. to Sept. 1, 1953, U. S. A. E. C. Contract No. AT (11-1)-208.

9. R. D. Evans and C. Goodman, Bull. G S A 52, 459 (1941).

10. H. U. Sverdrup, M. W. Johnson, and R. H. Fleming, "The Oceans," Prentice-Hall, Inc., N. Y. (1942), pp. 176-7.

11. D. C. Stewart and W. C. Bentley, Sci. n. s. 120, 50 (1954).

12. K. E. Chave, J. Geol. 62, 266 (1954).

13. Mr. Arthur Chodos, California Institute of Technology (private communication).

14. H. T. Odum, Sci. n. s. 114, 407 (1951).

15. H. A. Lowenstam, J. Geol. 62, 284 (1954).

16. L. R. Stieff, T. W. Stern, and R. G. Milkey, U. S. Geol. Sur. Circ. 271 (1953).

17. Dr. H. A. Lowenstam, California Institute of Technology (private communication).

18. H. B. Moore and D. M. Moore, Bull. G S A 57, 207 (1946).

19. Dr. C. C. Patterson, California Institute of Technology (private communication).

Propositions

1. Recent data (1) on the U and Th content of bentonites suggest a new method for estimating geologic ages. As volcanic ash alters throughout geologic time, the relative sorption strength for Th and U in this ion-exchange bed is assumed not to change although its exchange capacity does. Ions of charge less than 4 such as UO_2^{+2} are, compared to Th^{+4}, easily desorbed from ion exchange resins (2), and this fact suggests that Th may be concentrated in respect to U in such natural formations as bentonites. The high Th/U ratios obtained by Osmond (1) in Cretaceous and Ordovician bentonites are in agreement with this viewpoint. The averages for 14 recent ash samples, 19 Cretaceous bentonite samples, and 7 Ordovician bentonite samples furnish three points. The straight line through these points plotted against time indicates that the system accumulates another atom of Th for every one of U every 10 M yrs.

References

1. J. K. Osmond, Final Report, "Radioactivity of Bentonites", U. S. A. E. C. Contract No. AT (11-1)-178, 1954.

2. D. Dyrssen, Sartyck ur Svensk Kemisk Tidskrift 62, 153 (1950).

2. Thermoluminescent peaks occur at successively higher temperatures for blue, green, and violet fluorite (1). These thermolabile colors occur naturally and can also be obtained through irradiation. The temperatures indicate successively deeper electron traps. In addition

radioactive fluorite is usually (only 1 exception out of 18 cases) dark-violet to black (2). In view of these observation the proposal is made that the violet color of fluorite is related to an impurity ion of charge +4 or higher.

References

1. F. Daniels and D. F. Saunders, Final Report, "The Thermoluminescence of Crystals," U. S. A. E. C. Contract No. AT (11-1)-27, 1950.

2. V. R. Wilmarth, H. L. Bauer, Jr., M. H. Staatz, and D. G. Wyant, "Uranium in Fluorite Deposits" in U. S. Geol. Sur. Circ. 220, 1952, p. 13.

3. Because of the great duration of geologic time, Przibram (1) has suggested that differences between the natural colors of certain minerals and the colors of the thermally bleached specimens after irradiation may be due to the gradual accumulation of an excess of the more stable color centers over the less stable centers. A simple, quantitative discussion is now proposed in order to develop this idea. Since the electrons in the metastable positions have a mean lifetime

$$\tau = 10^{-13} \exp E/kT \qquad (1)$$

where τ is in seconds (2), electrons trapped in shallow wells may be thermally ionized in a few years at room temperature while the

probable release time for other metastable electrons may be thousands and even millions of years. For a naturally colored mineral with N_{io} concentration of the i th type of trapping center and N_i concentration of color centers in this trap where these color centers have a mean lifetime of τ_i, the following direct proportionality can be shown from the assumption of steady-state conditions:

$$N_i \propto N_{io} \tau_i \qquad (2).$$

References

1. K. Przibram, Endeavour 13, 37 (1954).

2. R. Casler, P. Pringsheim, and P. Yuster, J. Chem. Phys. 18, 887 (1950).

4. The common structure for carbonates of the divalent ions with ionic radii smaller than that of Ca^{+2} is the calcite structure. The larger cations prefer the aragonite structure. The distribution of trace elements in shells reflects this discrimination by the structure. Although the absolute concentrations of these elements, apparently in solid solution, in aragonite and calcite structures depend upon the type of animal producing the shell and the temperature at which the shell was formed (1), the concentration of, for example, Sr in aragonite is 2 to 3 times that in calcite in shells precipitated by closely related animals (2). This suggests that the concentrations of the larger cations in calcite are depressed by a

factor of approximately 2 from what the concentrations would be in comparable aragonite. Since the Sr/Pb ratio in marine aragonite (3) seems to be essentially the same as in ocean water, the lead content of calcite shells may be similarly depressed. The proposal is made that the same Sr/Pb ratio exists in calcite shells as in aragonite shells. Furthermore, the lead content of calcite shells from animals phylogenetically comparable to Strombus gigas should be only 1 ppm or less. The U content of such shells may be similarly depressed to values of about 0.02 ppm or less.

References

1. K. E. Chave, J. Geol. 62, 266 (1954).

2. Mr. Arthur Chodos, California Institute of Technology (private communication).

3. This thesis, Part II.

5. A change in the transmission of quartz occurs within a few weeks after irradiation. The absorption spectrum initially has several well-defined absorption peaks in the range from about 300 mμ to 700 mμ, but after 5 weeks, the peaks are much smaller and light transmission shows a continuous decrease as wavelength decreases (1). The latter spectrum is also characteristic of naturally occurring smoky quartz. The term transmission has been deliberately applied above, since the curve not only resembles the transmission curve for a system of submicroscopic light-scattering particles, but the scattered light from naturally occurring smoky quartz was noted some

time ago (2). The proposal is made that irradiation-induced lattice defects migrate throughout the crystal until combination occurs with a second kind of defect, presumably either an impurity or a structural defect. The combination is considered to lead to a light-scattering center. The migrating unit may well be the positive hole associated with an O^- ion. With a value for the activation energy of diffusion of a vacancy found through studies of several ionic crystals (3), an estimate of the lifetime of the migrating unit has been calculated which agrees with the available experimental data.

References

1. N. Mohler, Amer. Mineral. 21, 258 (1936).

2. R. J. Strutt, Proc. Roy. Soc., London 95A, 476 (1919).

3. R. G. Breckenridge in "Imperfections in Nearly Perfect Crystals," John Wiley and Sons, Inc., N. Y., 1952, p. 242.

6. Glass is a metastable phase. Its transformation to the crystalline phase at low temperatures is evidently a sluggish change since a volcanic glass is known from the Permian (about 200 M yrs old), and although pre-Tertiary natural glasses are rare, the many examples in the Tertiary with ages up to 60 M yrs further substantiate the stability of this phase. However, on surfaces irregular, diffusely birefringent films are observed. Perlites are volcanic glasses characterized by extensive internal fracturing and

relatively high (3-4%) water content and apparently occur through rapid chilling of a magma. The thicknesses of devitrified films in these rocks show a trend with age and the proposal is made that the devitrification may be in some cases a characteristic of the age of the rocks. The rate of devitrification at room temperature is believed to be of the order of 3 μ/100 M yrs.

7. The proposal is made that the upper limit for the diffusion constant of water into glass is 10^{-22} cm^2/sec at room temperature. This estimate is based on a proposed mechanism for the surface devitrification of glass. This phase change is, following Buerger's discussion (1), a reconstructive type and in view of the energy required to break the Si-O linkage, expected to be extremely sluggish. In fact, since the rate depends on a factor of the form $e^{-E/kT}$, if a minimum estimate of the activation energy, E, is the energy required to break the Si-O bond, then the very small factor of 10^{-67} is obtained suggesting that the rate of this process may be insignificant even in respect to geological time. If water diffuses into the glass and forms -OH groups, the breaking of the cross-linking, necessarily precursive to transformation, may require a considerably smaller activation energy.

Reference

1. "Phase Transformations in Solids," John Wiley and Sons, Inc., N. Y. (1951), p. 190.

8. Sulfur-bearing proteins are suggested as the source of sufficient $SO_4^{=}$ to bring about precipitation of Ba and Sr from sea water in Xenophyophora (1) and Radiolaria (2), both of the protozoan class Sarcodina. Although Sr^{+2} ions are 500 times more prevalent in ocean water than Ba^{+2} ions (3), because of the difference between their solubility products, only slight differences in their concentrations should be required to bring about Ba^{+2} precipitation in one area and Sr^{+2} precipitation in another.

References

1. F. E. Schulze and H. Thierfelder, Ber. Gesell. Naturforsch. Freunde Ber. 1, 2 (1905).

2. H. T. Odum, Sci. n. s. 114, 211 (1951).

3. H. U. Sverdrup, M. W. Johnson, and R. H. Fleming, "The Oceans," Prentice-Hall Inc., N. Y. (1942), p. 176.

9. Benioff (1) has shown that aftershock sequences may be interpreted in terms of relaxation stresses in the rock. The principal shock, initiating the series of subsequent shocks which are called aftershocks, is considered to be the elastic strain energy stored in the rock masses of a fault. The aftershocks represent elastic after-working of the rock, each shock being a creep strain recovery increment. The accumulated value of these increments represents at any particular time a fraction of the recovery. To represent the aftershock data Benioff used certain

empirical expressions previously obtained in laboratory experiments. However, the proposal is made that an equally satisfactory (and perhaps better) representation of the data can be obtained with the sigmoid equation,

$$S/S_{\infty} = 1 - \exp(-At^{B}) \qquad (1)$$

where S is the accumulated creep strain recovery (times a constant k) at time t, S_{∞} represents the complete recovery, and A and B are constants. Several aftershock sequences have been represented by this type of equation.

Reference

1. H. Benioff, Bull. Seis. Soc. Amer. 41, 31 (1951).

10. The expansibility qualities of high water content natural glasses apparently depends on the nature of the distribution of the water, whether monomerically scattered, hydrogen-bonded, or concentrated in bubbles. Water content is generally reported as loss on ignition. These analyses do not furnish any information on how the water is held. Recently (1) the infrared absorption spectrum of a perlite has been studied in this regard. However, the proposal is made that investigation of this problem is possible through nuclear magnetic resonance techniques. Data concerning the extent of aggregate water can supplement spectra studies and combined with expansibility characteristics of the same perlites, may furnish criteria on which the perlite

industry can base its selection of raw material.

Reference

1. W. D. Keller and E. E. Pickett, Amer. J. Sci. 252, 87 (1954).